TECHNISCHE UNIVERSITÄT MÜNCHEN

TUM School of Life Sciences

Analysis of the precision of digital technologies for recording the spatial variability of yield and nitrogen uptake in winter wheat as a basis for site-specific fertilization

Matthias Johannes Stettmer

Vollständiger Abdruck der von der TUM School of Life Sciences der Technischen Universität München zur Erlangung des akademischen Grades eines

Doktors der Agrarwissenschaften (Dr. agr.)

genehmigten Dissertation.

Vorsitz: Prof. Dr. Gerd Patrick Bienert

Prüfer*innen der Dissertation: 1. Prof. Dr. Heinz Bernhardt
2. Prof. Dr. Kurt-Jürgen Hülsbergen

Die Dissertation wurde am 27.03.2023 bei der Technischen Universität München eingereicht und durch die TUM School of Life Sciences am 12.10.2023 angenommen.

Table of Contents

Table of Contents

Danksagung

Die Erstellung dieser Dissertation wäre ohne die zahlreiche Hilfe vieler Menschen nicht möglich gewesen. Für die stets entgegengebrachte Unterstützung bin ich sehr dankbar und möchte mich dafür bei allen sehr herzlich bedanken. Besonders danke ich meinem Betreuer und Erstgutachter Prof. Dr. Heinz Bernhardt für die Bereitstellung der Promotionsmöglichkeit, die Betreuung und Unterstützung während meiner Tätigkeit als wissenschaftlicher Mitarbeiter. Für die weitere Begutachtung und Bewertung dieser Dissertation möchte ich Prof. Dr. Kurt-Jürgen Hülsbergen und Prof. Dr. Gerd Patrick Bienert meinen Dank aussprechen. Bei Dr. Franz-Xaver Maidl bedanke ich mich für die stets professionelle und fachliche Unterstützung in allen Fragen rund um diese Dissertation.

Die Zeit am Lehrstuhl für Agrarsystemtechnik und am Lehrstuhl für Ökologischen Landbau und Pflanzenbausysteme habe ich sehr geschätzt. Besonders die Zusammenarbeit und die regen fachlichen Diskussionen mit allen Kollegen haben mich sehr gefördert. Weiterer großer Dank gilt dem gesamten Team der Versuchsstation Dürnast und des Labors. Stellvertretend für alle Beteiligten bedanke ich mich bei Andreas Kern und Ingo Brauer von der Versuchsstation und den Laborleitern Dr. Ludwig Nätscher und Robert Kahle.

Stellvertretend für die gesamte Farmtastic Consulting GmbH, bedanke ich mich bei der Geschäftsführung und den Gesellschaftern Jürgen Schwarzensteiner und Dominik Freiherr von Poschinger-Bray für die Koordination und Organisation der Finanzierung meiner Forschungsarbeit sowie die großzügige Unterstützung bei der Anfertigung dieser Dissertation. In Vertretung aller Helfer bei den Versuchsarbeiten am Gut Makofen bedanke ich mich besonders bei Jakob Berg. Weiterer großer Dank gilt der Poschinger Bray´schen Güterverwaltung, die in diesem Projekt als Versuchsbetrieb fungiert hat.

Zu guter Letzt danke ich von ganzem Herzen meiner Familie und meinen Freunden für die unermüdliche Unterstützung und das große Verständnis, insbesondere während der Abfassung dieser Dissertation. Vielen Dank, dass ihr meinen Weg und meine Entscheidungen stets mit Rat und Tat unterstützt. Ohne Eure Hilfe wäre diese Promotion nicht möglich gewesen!

List of Figures

List of Tables

List of Abbreviations

a	Year
cm	Centimeter
DM	Dry matter
EU	European Union
ha	Hectare
hl	Hectoliter
kg	Kilogram
l	Liter
$LU\ ha^{-1}$	Livestock unit per hectare
m	Meter
mg	Milligram
mm	Millimeter
nm	Nanometer
N	Nitrogen
t	Ton

Summary

Wheat is the second most produced grain in the world after corn. In the EU and especially in Germany, winter wheat is the most important crop in arable farming, and it is produced on half of the German cereal acreage. However, the constantly growing world population in combination with climate change, increasing scarcity of land, and serious environmental pollution bring new challenges to the production systems. In particular, the groundwater pollution with nitrate from agricultural fertilizers is a major problem. A promising approach in precision agriculture to solve this problem is site-specific nitrogen fertilization.

The literature shows that this approach helps to (a) increase N-efficiency, (b) lower N-balances, and (c) achieve precise fertilizer application according to crop nitrogen requirements. In this way, nitrogen overfertilization and losses can be avoided in low-yield zones, and the yield and quality potential can be realized in high-yield zones without exhausting the nitrogen content in the soil. In this context, various methods for site-specific nitrogen fertilization were developed and tested. These approaches can be divided into three categories: "mapping", "online", and "mapping + online". Based on various scientific studies, fertilization systems based on the mapping + online approach, which uses sensor or satellite data, have been established for site-specific nitrogen fertilization of winter wheat. The basic prerequisite for the successful use of these fertilizer systems is the correct delineation of yield zones and the exact recording of nitrogen uptake at characteristic growth stages during the vegetation period. Yield potential maps and the current nitrogen uptake represent the two basic data sources of modern site-specific fertilizer systems.

Various digital methods are available to generate yield potential maps and measure the nitrogen uptake. In this work, the precision of state-of-the-art methods for yield mapping (combine harvester, sensor, satellite) and for estimating the nitrogen uptake (sensor, satellite) in winter wheat was investigated. The aim of the analyses was to assess (a) the recording of the spatial variability and (b) the estimations of the absolute level of yield and nitrogen uptake of the digital methods. Plot combine harvester data and biomass samples were used as ground truth data. For this purpose, various field trials were conducted on two research farms (Dürnast, Makofen) in southern Germany in the years 2018-2021. The Dürnast site was chosen because it has been extensively studied over many years, specifically for site-specific nitrogen fertilization of winter wheat. The Makofen site was selected to evaluate the precision of the tested digital methods at a supposedly homogeneous high-yield site. In

addition, the Makofen site has hardly been researched regarding site-specific nitrogen fertilization. The accuracy of the tested methods was evaluated using statistical indicators (mean, median, minimum, maximum, and standard deviation) and correlation analyses between the estimates of the respective method and the ground truth data.

The results show that the tested methods can provide very accurate data and underline the great potential of site-specific agricultural technology. Thus, absolute yield potential maps can be generated with sensor and combine harvester data ($R^2 = 0.69$–0.75), with combine harvester data being prone to outliers ($R^2 = 0.30$). Good relative zone maps can be generated based on satellite data ($R^2 = 0.53$–0.68), but the satellite data-based plant growth model PROMET reveals problems in modeling the absolute yield height when weather extremes occur. Therefore, further investigations are urgently required, on the one hand, to better evaluate the reliability of combine harvester data across manufacturers and, on the other hand, to better characterize the background for the large absolute deviations in the PROMET model. This would useful as more and more applications for modern combine harvesters with yield sensors and equipment, as well as freely available satellite data, are being found on farms, which is why good validation of such applications is of great importance. Furthermore, the tested digital methods for yield recording can not only function as a database for site-specific fertilization but are also very interesting for other areas of application. For example, for the creation of tree strips, flower strips, or agroforestry systems, long-term low-yield areas can be identified, or soil investigations can be planned based on this. This area of application is very interesting for both conventional and organic farms. As the results of these investigations show ($R^2 = 0.57$–0.83), the recording of the current nitrogen uptake is possible with both the sensor-based and the satellite data-based approach. The occurrence of significant deviations can be explained by external influences at the time of the measurements. Both approaches have advantages and disadvantages, which must be weighted differently depending on the size and concept of the farm. Further investigations should deal with a higher spatial resolution of new satellite systems and the further development of vegetation indices. In addition to winter wheat, evaluations should also take place in other important arable crops.

Ultimately, this study shows the great potential of site-specific agricultural technology and underlines that these applications can make a major contribution to reducing nitrogen losses in the production of winter wheat. To utilize the advantages of site-specific land management

to the fullest in practice, additional investigations into the further development and improvement of digital technologies as well as other possible application areas are required.

Zusammenfassung

Weizen ist nach Körnermais das am zweithäufigsten produzierte Getreide der Welt. In der EU und in Deutschland ist Winterweizen die wichtigste Kultur im Ackerbau und wird auf der Hälfte der deutschen Getreideanbauflächen produziert. Die stetig wachsende Weltbevölkerung in Kombination mit dem Klimawandel, zunehmende Flächenknappheit und ernstzunehmende Umweltbelastungen bringen jedoch neue Herausforderungen an die Produktionssysteme mit sich. Besonders die Grundwasserbelastung mit Nitratüberschüssen aus der landwirtschaftlichen Düngung ist hierbei ein großes Problem. Ein vielversprechender Ansatz der Präzisionslandwirtschaft, um dieses Problem zu lösen, ist die teilflächenspezifische Stickstoffdüngung.

Die Literatur zeigt, dass dieser Ansatz dazu beiträgt, (a) die N-Effizienz zu erhöhen, (b) die N-Salden zu senken, und (c) eine präzise Düngerausbringung gemäß dem Stickstoffbedarf der Pflanzen zu erreichen. Dadurch können in ertragsschwachen Zonen Stickstoffüberdüngung und -verluste vermieden und in ertragsstarken Zonen das Ertrags- und Qualitätspotential realisiert werden, ohne den Stickstoffgehalt im Boden zu erschöpfen. In diesem Zusammenhang wurden verschiedene Verfahren zur teilflächenspezifischen Stickstoffdüngung entwickelt und erprobt. Diese Ansätze lassen sich in drei Kategorien einteilen: „Mapping", „Online" und „Mapping + Online". Auf Basis verschiedener wissenschaftlicher Untersuchungen haben sich bei der teilflächenspezifischen Stickstoffdüngung von Winterweizen vor allem Düngesysteme basierend auf dem Mapping + Online-Ansatz, der Sensor- oder Satellitendaten nutzt, etabliert. Grundlegende Voraussetzung für den erfolgreichen Einsatz dieser Düngesysteme ist die korrekte Abgrenzung von Ertragszonen und die exakte Erfassung der Stickstoffaufnahme zu charakteristischen Wachstumsstadien während der Vegetationsphase. So stellen Ertragspotentialkarten und die aktuelle Stickstoffaufnahme die zwei grundlegenden Datenquellen moderner teilflächenspezifischer Düngesysteme dar.

Um Ertragspotentialkarten zu generieren und die Stickstoffaufnahme zu messen, stehen verschiedene digitale Methoden zur Verfügung. In dieser Arbeit wurde die Präzision der State of the Art Methoden zur Ertragserfassung (Mähdrescher, Sensor, Satellit) und zur Schätzung der Stickstoffaufnahme (Sensor, Satellit) in Winterweizen untersucht. Ziel der Analysen war es (a) die Erfassung der räumlichen Variabilität sowie (b) die Schätzung der absoluten Höhe von Ertrag und Stickstoffaufnahme mit den digitalen Methoden zu bewerten.

Als Ground Truth Daten wurden Parzellenmähdrescherdaten und Biomasse-Handschnitte verwendet. Dazu wurden in den Jahren 2018-2021 verschiedene Feldversuche auf zwei Versuchsbetrieben (Dürnast, Makofen) in Süddeutschland durchgeführt. Der Standort Dürnast wurde gewählt, weil er im Bereich der teilflächenspezifischen Stickstoffdüngung von Winterweizen langjährig gut untersucht ist. Der Standort Makofen wurde ausgewählt, um die Präzision der erprobten digitalen Methoden an einem vermeintlich homogenen Hochertragsstandort zu evaluieren. Darüber hinaus ist der Standort Makofen in der Thematik der teilflächenspezifischen Stickstoffdüngung kaum erforscht. Die Genauigkeit der getesteten Methoden wurde anhand statistischer Indikatoren (Mittelwert, Median, Minimum, Maximum und Standardabweichung) und Korrelationsanalysen zwischen den Schätzwerten der jeweiligen Methode und der Ground Truth Daten ausgewertet.

Die Ergebnisse zeigen, dass die getesteten Methoden sehr genaue Daten liefern können und untermauern das große Potential der teilflächenspezifischen Landtechnik. So lassen sich absolute Ertragspotentialkarten gut mit Sensor- und Mähdrescherdaten ($R^2 = 0.69$–0.75) erzeugen, wobei Mähdrescherdaten anfällig für Ausreißer ($R^2 = 0.30$) sind. Auf Basis von Satellitendaten lassen sich gute relative Zonenkarten generieren ($R^2 = 0.53$–0.68), jedoch offenbart das satellitendatenbasierte Pflanzenwachstumsmodell PROMET Probleme bei der Modellierung der absoluten Ertragshöhe, wenn Wetterextreme auftreten. Daher sind weitere Untersuchungen dringend erforderlich, um einerseits die Verlässlichkeit von Mähdrescherdaten herstellerübergreifend besser zu evaluieren und andererseits die Hintergründe für die großen absoluten Abweichungen bei PROMET besser zu charakterisieren. Dies wäre sehr wichtig, da moderne Mähdrescher mit Ertragssensor und entsprechender Ausstattung sowie kostenlos verfügbare Satellitendaten immer mehr Anwendung auf landwirtschaftlichen Praxisbetrieben finden, weshalb eine gute Validierung solcher Anwendungen von großer Bedeutung ist. Weiterhin können die getesteten digitalen Methoden zur Ertragserfassung nicht nur als Datenbasis für die teilflächenspezifische Düngung fungieren, sondern sind auch für andere Anwendungsbereiche sehr interessant. So können zum Beispiel für die Anlage von Baumstreifen, Blühstreifen oder Agroforstsystemen langjährig ertragsschwache Stellen ausfindig gemacht werden oder Bodenuntersuchungen danach geplant werden. Dieser Anwendungsbereich ist sowohl für konventionell als auch ökologisch wirtschaftende Betriebe sehr interessant. Die Erfassung der aktuellen Stickstoffaufnahme ist sowohl mit dem sensor- als auch dem satellitendatenbasierten Ansatz gut möglich, wie die Ergebnisse dieser Untersuchungen zeigen ($R^2 = 0.57$–0.83).

Zusammenfassung

Aufgetretene deutliche Abweichungen lassen sich durch äußere Einflüsse zum Zeitpunkt der Messungen erklären. Beide Ansätze haben Vor- und Nachteile, welche je nach Betriebsgröße und -konzept unterschiedlich zu gewichten sind. Weiterführende Untersuchungen sollten sich mit einer höheren räumlichen Auflösung neuer Satellitensysteme und der Weiterentwicklung von Vegetationsindices befassen. Außerdem sollten neben Winterweizen auch Evaluierungen in anderen wichtigen Ackerkulturen stattfinden.

Letztendlich zeigen diese Untersuchungen das große Potential der teilflächenspezifischen Landtechnik und untermauern, dass diese Anwendungen einen großen Beitrag zur Reduktion der Stickstoffverluste bei der Produktion von Winterweizen leisten können. Um die Vorteile der teilflächenspezifischen Landbewirtschaftung in vollen Zügen in der Praxis nutzen zu können, bedarf es weiterer Untersuchungen zur Weiterentwicklung und Verbesserung der digitalen Technologien sowie weiterer möglicher Anwendungsbereiche.

1 General introduction

1.1 Importance of wheat cultivation

With a global production of 775 million tons from a cultivated area of 221 million hectares in 2021, wheat is the second most produced grain in the world after corn (USDA FOREIGN AGRICULTURAL SERVICE 2022a; USDA FOREIGN AGRICULTURAL SERVICE 2022b). In the European Union (EU) and especially Germany, winter wheat is the most important crop with a production of 139 million tons (EU) and 21 million tons (Germany) in 2021 (BOOGAARD ET AL. 2013; SVOBODA ET AL. 2015; BUNDESMINISTERIUM FÜR ERNÄHRUNG UND LANDWIRTSCHAFT 2021). With a cultivation area of around 2.9 million hectares, winter wheat is cultivated on around 51% of the entire German grain cultivation area (STATISTISCHES BUNDESAMT 2022). Due to suitable climatic conditions and the high yield potential of the soil in many regions, winter wheat cultivation is of enormous economic importance for German farmers (MACHOLDT AND HONERMEIER 2017). Conventional wheat production in Germany takes place at a high to very high level of intensity and yield. This requires intensive nitrogen fertilization, crop management, and high precision, considering the actual yield potential (spatial variability). In the last 20 years, the acreage for winter wheat in Germany was constant at around 3 million hectares (Figure 1).
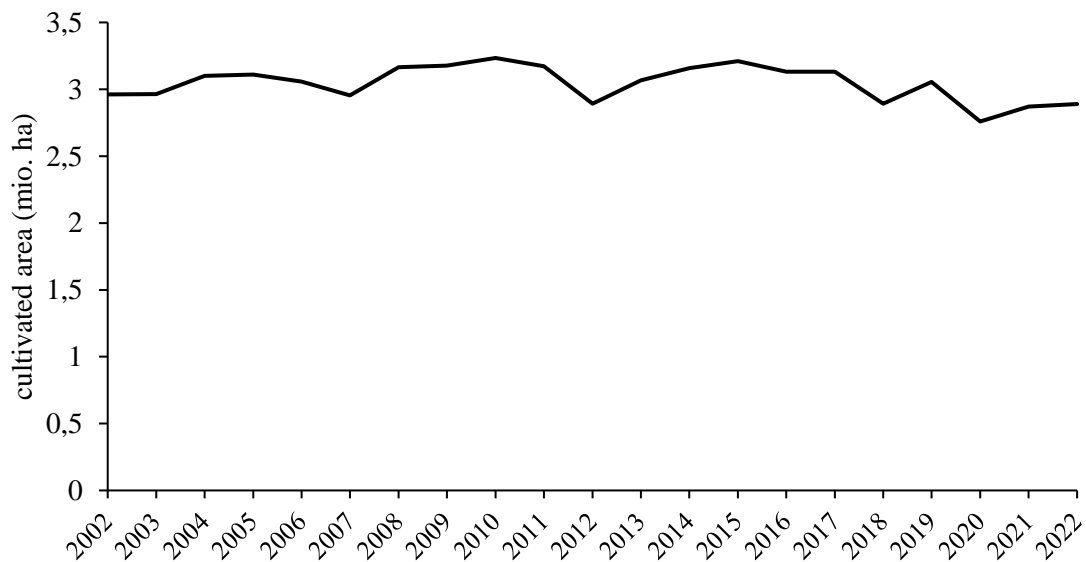
Figure 1: Cultivated area of winter wheat in Germany between 2002 and 2022 (STATISTISCHES BUNDESAMT 2022)

With peak yields of up to 12 t ha^{-1} and an average yield of 7.4 t ha^{-1}, Germany achieves the highest wheat yields of the most prominent wheat exporters worldwide (Figure 2) (ZIMMER

2016). As the most important crop in Germany, winter wheat is essential for feeding the world population (SVOBODA ET AL. 2015; IGREJAS AND BRANLARD 2020).
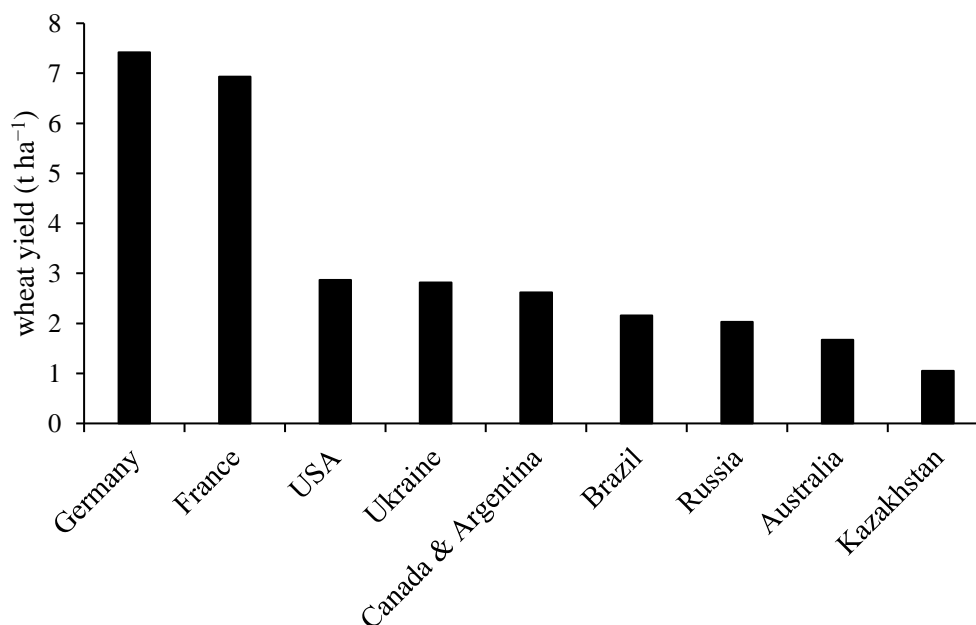
Figure 2: Wheat yields (t ha^{-1}) of the world's major wheat exporters (ZIMMER 2016)

In addition to non-food uses for animal feed, energy, and industry, around 65% of the wheat produced is used for human nutrition (GABRIEL ET AL. 2017). Depending on the intended use, there are different quality classes for winter wheat in Germany (Table 1).

Table 1: Quality classes of winter wheat in Germany (PFLEGER 2015; BUNDESSORTENAMT 2022)

Quality class	Falling number [a]	Protein content [a,b]	Sedimentation value [a]	Utilization
E (premium quality)	≥ 6	≥ 6	≥ 7	Human nutrition
A (good quality)	≥ 5	≥ 4	≥ 5	Human nutrition
B (standard quality)	≥ 4	≥ 2	≥ 3	Human nutrition
C (lowest quality)	-	-	-	Feed, energy, industry

[a] These numbers are a quantitative assessment of the parameters given in integers ranging from 1 to 9: 9 stands for very high values and 1 stands for very low values.

[b] Due to the comparatively high environmental impact, the protein content has been described in relation to the tested standard varieties since 2019.

The quality classes of winter wheat differ by various requirements for chemical, physical, and rheological properties (DOWELL ET AL. 2006; GABRIEL ET AL. 2017). Table 1 shows the most important characteristics of the quality classes when marketing winter wheat. While

the falling number is primarily influenced by the variety and the weather, the protein content is largely influenced by nitrogen fertilization. The sedimentation value correlates positively with the protein content and is also variety specific (BUNDESSORTENAMT 2022).

In the context of an increasing world population and the simultaneous loss of arable land due to the development of housing, industry, and infrastructure, the production of winter wheat will continue to be of particular importance in the future (DÖÖS 2002). It is necessary to produce more wheat on less land through more efficient production systems to ensure human nutrition (LIU ET AL. 2015). In addition to local conditions such as soil and climate, the yield and quality of winter wheat are significantly influenced by the choice of variety and crop management (EREKUL ET AL. 2005). Nitrogen fertilization is a central aspect of the cultivation of winter wheat (MAIDL ET AL. 1998). In addition to the supply of all other necessary nutrients, adapted nitrogen fertilization has the greatest influence on the yield and quality of wheat in a healthy wheat crop (SKUDRA AND LININA 2011; GAJ ET AL. 2013; HAWKESFORD 2014).

1.2 Importance of nitrogen fertilization in winter wheat cultivation

Nitrogen is an essential element in plants due to its key role in chlorophyll production, which is fundamental to the photosynthetic process (MUÑOZ-HUERTA ET AL. 2013). In addition, nitrogen is part of various enzymatic proteins that catalyze and regulate plant growth, as well as in the production of chemical components that protect the plant from pests and diseases (HOFFLAND ET AL. 2000; SINFIELD ET AL. 2010; MUÑOZ-HUERTA ET AL. 2013). Due to these functions, biomass and crop yields are significantly influenced by nitrogen fertilization (TREMBLAY ET AL. 2011). Early nitrogen fertilization up to growth stage 39 primarily promotes an increased yield, while late nitrogen application up to BBCH 65 primarily affects the grain quality (protein content) (MAIDL ET AL. 1998; MOHAMMED ET AL. 2013; DICK ET AL. 2016).

Concurrently, however, nitrogen fertilizers have a high loss potential and can cause significant environmental impacts (CUI ET AL. 2010; MEYER AND KOLBE 2021; MITTERMAYER ET AL. 2022). Particularly, nitrate leaching is one of the most important processes of nitrogen loss in agricultural ecosystems (HUANG ET AL. 2017). Leached nitrate can result in groundwater pollution and eutrophication of surface water, thus threatening human health (ZHANG ET AL. 2015). Intensively cultivated arable land is one of the most

important sources of leached nitrate (GU ET AL. 2013; QUEMADA ET AL. 2013; HUANG ET AL. 2017).

This creates a conflict of interest for farmers between the supply of nitrogen to crops and environmental protection (ZHANG ET AL. 2015; ZHANG 2017). On the one hand, high yields with the best possible quality are the goal of winter wheat cultivation; on the other hand, excess fertilizer and nitrogen not absorbed by the plants leads to losses and environmental pollution (KÜSTERMANN ET AL. 2010). Especially when producing wheat of the quality classes E and A, high nitrogen fertilization is necessary in the later growth stages to achieve the protein levels required for marketing (ZECEVIC ET AL. 2010; BUNDESSORTENAMT 2022). In the past, this situation has often led to overfertilization and nitrogen losses (STREBEL ET AL. 1989; THORBURN ET AL. 2003; WENDLAND ET AL. 2020). For example, the N balances in Germany, at 90 to 100 kg ha^{-1} a^{-1}, have been too high for years (HÜLSBERGEN ET AL. 2020). A study by HÜLSBERGEN ET AL. 2017 shows significant correlations between N balances and measured nitrate losses in 23 fields (measured using soil samples to a depth of 9 m and nitrate analyses). Exceeding the nitrate limit of 50 mg nitrate l^{-1} in groundwater in some areas of Germany is a consequence of this (WENDLAND ET AL. 2020). High nitrogen losses occur particularly in regions with intensive animal production (> 2 LU ha^{-1}) (HÜLSBERGEN ET AL. 2020). For this reason, the legal framework for the fertilization of agricultural land in Germany has been revised several times and recorded in the Fertilizer Ordinance (SCHRÖER ET AL. 2022). In the future, it will therefore be necessary to use modern fertilizer systems and algorithms to reduce the N balances and improve the N efficiencies to harmonize successful crop production with environmental protection.

1.3 Spatial variability of nitrogen uptake

Nitrogen-efficient fertilization is made more difficult by the spatial variability of nitrogen uptake in the field. Depending on numerous overlapping factors and their interactions (soil factors, climate factors, and agricultural management practices), the spatial variability of nitrogen uptake in the field can vary noticeably (KUCKE AND KLEEBERG 1997; TARKALSON ET AL. 2006; WANG ET AL. 2010; CAO ET AL. 2012; CAO ET AL. 2018; MITTERMAYER ET AL. 2021). Particularly, the influence of the weather in combination with soil properties, such as soil texture, available water capacity, humus content, nutrient content, and pH, varies very locally, resulting in varying crop nitrogen uptakes in the field (MAIDL ET AL. 1999; LOPEZ-LOZANO ET AL. 2010; FARID ET AL. 2016; SERVADIO ET AL. 2017; STETTMER ET AL. 2022a).

This effect can be further intensified by the uniform fertilization that prevails on most German farms due to different nutrient removals in the high- and low-yield zones of a field (FROGBROOK AND OLIVER 2007; HÜLSBERGEN ET AL. 2017; STAMATIADIS ET AL. 2018; WANG ET AL. 2019; STETTMER ET AL. 2022a). Every uniform soil treatment (fertilization, liming, or irrigation) will lead to areas within a field that are either over- or under-treated (PATZOLD ET AL. 2008). This results in small-scale fluctuating nitrogen balances and stocks in soil, causing high emissions and nitrate losses in zones with low yield potential and overfertilization (DALGAARD ET AL. 2012; MITTERMAYER ET AL. 2021; STETTMER ET AL. 2022a; STETTMER ET AL. 2022b). Therefore, systems adapted to small-scale crop variations for winter wheat fertilization are required, which should consider the heterogeneity of fields and their different yield potentials to minimize the environmental impact through nitrate losses.

1.4 Site-specific nitrogen fertilization

Site-specific nitrogen fertilization is a promising approach to minimize the environmental impact of nitrogen losses in winter wheat production (MAIDL ET AL. 2004; DIACONO ET AL. 2013; MULLA 2013; LIU ET AL. 2018; PRÜCKLMAIER 2020). The literature shows that this method helps to (a) increase the N efficiency, (b) lower N balances, and (c) achieve precise fertilizer application according to the nitrogen needs of plants (PERALTA ET AL. 2015; VINZENT ET AL. 2017; ARGENTO ET AL. 2021; WECKESSER ET AL. 2021; SCHUSTER ET AL. 2022). In this way, nitrogen over-fertilization and losses can be avoided in low-yield zones, and the yield and quality potential can be realized in high-yield zones without exhausting the nitrogen content in the soil (WECKESSER ET AL. 2021). In this context, various methods for site-specific nitrogen fertilization were developed and tested. These approaches can be divided into three categories: "mapping", "online", and "mapping + online" (Table 2) (MAIDL ET AL. 2004; GANDORFER 2006; WECKESSER ET AL. 2021).

Table 2: Site-specific fertilization systems (MAIDL ET AL. 2004; WECKESSER ET AL. 2021)

Fertilization System	Principle	Data origin	Examples
Mapping-approach	Fertilization based on a historical yield potential map	Soil texture, electrical conductivity, elevation modelling, yield maps	N-Manager (FARMFACTS 2022a), Potential Map Method (CLAAS 2020)
Online-approach	Fertilization based on the current nitrogen uptake in the crop	Biomass and nitrogen uptake based on sensor and satellite data, vegetation indices, algorithms, plant growth models	Cropsat (DATAVÄXT 2022), GreenSeeker System (FARMFACTS 2022b), Atfarm (YARA 2022)
Mapping + Online-approach	Combination of mapping- and online-approach	Yield potential maps, current nitrogen uptake based on sensor or satellite data	ISARIA (FRITZMEIER 2021), TUMA (MAIDL 2016), N-Manager Pro (FARMFACTS 2022a)

With the mapping approach, fertilization is controlled using historical field information (AUERNHAMMER 2001; OSTERMEIER ET AL. 2007; HÜLSBERGEN ET AL. 2020). Yield potential maps are generated based on georeferenced soil parameters (e.g., soil texture, electrical conductivity, and elevation modeling) or yield mapping data (annual or multi-year) (SCHMIDHALTER ET AL. 2008; GUASTAFERRO ET AL. 2010; SALEH AND BELAL 2014; WECKESSER ET AL. 2021). In particular, the delineation of management zones based on yield maps is of central importance here (JIN ET AL. 2017; HUNT ET AL. 2019; BLASCH ET AL. 2020; ZHAO ET AL. 2020). Nitrogen fertilization is based on the level of yield potential in the individual management zones; the current plant development is not considered with this method (MAIDL ET AL. 2004). This can have an adverse effect if the yield zones of a field change at short notice because of external influences (e.g., weather, plant diseases, wildlife damage, etc.) (BLACKMORE ET AL. 2003; WELSH ET AL. 2003).

With the online approach, fertilization is controlled based on the current plant development (biomass, N uptake) (AUERNHAMMER 2001; OSTERMEIER ET AL. 2007; HÜLSBERGEN ET AL. 2020). Plant development at the time of fertilization is analyzed using non-contact

measurement methods, and a fertilization value is derived from this (MAIDL ET AL. 2004). Classically, reflection measurements are conducted with sensors or satellites and vegetation indices are calculated from them. Based on the vegetation indices used, the supply status of the plants can be determined, and the required amount of nitrogen fertilizer can be calculated (CAMMARANO ET AL. 2014; PREY AND SCHMIDHALTER 2019; WECKESSER ET AL. 2021; STETTMER ET AL. 2022a). In the case of tractor-mounted sensor systems, this calculation takes place in real time, so when the sensor is passed over, the fertilizer spreader is controlled accordingly, and the respective quantity is applied. For satellite systems, this process is divided into two steps. In the first step, an application map containing the fertilizer quantities to be applied is generated from current satellite data. In the second step, this application map is processed with the fertilizer spreader. With the online approach, annual effects that cause plant development in the individual yield zones to deviate from the multi-year average can be considered when fertilizing (BLACKMORE ET AL. 2003; DIACONO ET AL. 2012). At the same time, however, the same application curve is used for the entire field, which can lead to oversupply in low-yield areas and undersupply in high-yield areas (EBERTSEDER ET AL. 2003; SCHÄCHTL 2004; SPICKER 2016; HÜLSBERGEN ET AL. 2020).

The mapping + online approach is a combination of both. This method is based on two important data sources by considering both the current plant development (online approach) and historical yield potential maps (mapping approach) (AUERNHAMMER 2001; OSTERMEIER ET AL. 2007; HÜLSBERGEN ET AL. 2020). The yield potential is defined via the mapping approach; thus, the basis of the fertilizer amount is determined. The final amount of nitrogen to be applied is fine-tuned by determining the degree of nitrogen supply of the plants using reflection measurements (sensor, satellite) based on the online approach (MAIDL ET AL. 2004; HÜLSBERGEN ET AL. 2020; ARGENTO ET AL. 2021). By combining the two approaches, the disadvantages of the individual methods are mitigated, and the two approaches complement each other well (AUERNHAMMER 2001; EBERTSEDER ET AL. 2003). Various studies on this show the superiority of site-specific nitrogen fertilization according to the mapping + online approach in winter wheat (MAIDL ET AL. 2004; SCHMIDHALTER 2014; ARGENTO ET AL. 2021). The advantages of this method have also been shown in field trials in winter oilseed rape, winter barley, and maize (SPICKER 2016; VINZENT ET AL. 2017; PRÜCKLMAIER 2020). MAIDL ET AL. (2004) showed that fertilization using the mapping + online approach in winter wheat is significantly superior to fertilization using the mapping approach in terms of yield. Furthermore, the amount of nitrogen fertilizer applied was

reduced by an average of 6% compared to the online approach. ARGENTO ET AL. (2021) were able to reduce the amount of nitrogen fertilizer by up to 40% by using the mapping + online approach and improve the nitrogen efficiency by around 10% on average. For this reason, fertilization systems based on the mapping + online approach, which uses sensor or satellite data, have been established for site-specific fertilization of winter wheat (MAIDL ET AL. 2004; SCHMIDHALTER 2014; SPICKER 2016; VINZENT ET AL. 2017; SCHUSTER ET AL. 2022).

1.5 Aims and outlines

The aim of this work was to analyze the precision of different digital technologies for recording the spatial variability of the yield and nitrogen uptake in winter wheat as a basis for site-specific nitrogen fertilization. The precision of the input data is an essential prerequisite for the accuracy and further development of site-specific nitrogen fertilizer systems. On the one hand, there are data on the spatial variability of the yield (e.g., yield potential maps); on the other hand, there are data on the site-specific current nitrogen uptake of the plant population, which can be determined using different digital methods. Therefore, the focus of this work was to investigate the currently most important methods for recording the spatial variability of wheat yields and nitrogen uptake, especially the analysis of their precision.

For the analysis of the precision of digital technologies for recording the spatial variability of winter wheat yield, the following were examined:

- How exactly can the relative yield variation in the field be identified by the methods (sensor, satellite, combine harvester)?
- How exactly can the methods estimate the absolute yield level?
- Are the estimates of the methods examined suitable as a data basis for site-specific fertilization?

For the analysis of the precision of digital technologies for recording the spatial variability of nitrogen uptake at different growth stages in winter wheat, the following were examined:

- How exactly can the relative differences in nitrogen uptake in the field be identified by the methods (sensor, satellite)?
- How exactly can the methods estimate the absolute level of the nitrogen uptake?

- Are the estimates of the methods examined suitable as a data basis for site-specific fertilization?

The investigations were carried out on heterogeneous fields in different soil and climate regions of southern Germany. For this purpose, plot trials were set up to enable the comparison of the various digital methods. The spatially variable input data used for the method comparison were determined using various digital methods and technologies (combine harvester yield sensors, tractor-mounted multispectral sensors, satellite data, vegetation indices, and a plant growth model). Nitrogen fertilization was carried out uniformly on all study fields. To be able to validate the quality and precision of the digital systems, a comparison with ground truth data (biomass samples and plot harvester data) was carried out. The precision of the methods was examined by comparing the statistical indicators (mean, median, minimum, maximum and, standard deviation) and by analyzing correlative relationships.

The results should give new insights into the precision of modern fertilizer systems using the mapping + online approach. For this purpose, the currently most important digital methods for recording the spatial variability of nitrogen uptake and yield in winter wheat were examined in the Straubing region for the first time in parallel and in comparison with ground truth data using plot trials, with the goal to systematically evaluate the suitability, accuracy, and error susceptibility of the tested methods.

These investigations should contribute to the improvement and further development of the digital methods examined to be able to generate precise data for site-specific applications in agricultural practice in the future. Furthermore, the comparison of methods should create better awareness of the differences between different data sources and their effects.

This doctoral thesis is divided into five chapters:

- Chapter 1 (General introduction) introduces the research field in a broader context and contains the subject and aims of the thesis.
- Chapter 2 (Status of science and technology) provides an overview of the current state of knowledge and technology for site-specific yield mapping and determination of the nitrogen uptake.
- Chapter 3 (Methodological approach) presents the study sites, study fields, and digital methods used for the investigations.

- Chapter 4 (Publications) contains a short summary highlighting the author´s individual contributions to the following publications.

  - Analysis of Nitrogen Uptake in Winter Wheat Using Sensor and Satellite Data for Site-Specific Fertilization. Agronomy (2022) 12(6): 1455.

  - Three Methods of Site-Specific Yield Mapping as a Data Source for the Delineation of Management Zones in Winter Wheat. Agriculture (2022) 12(8): 1128.

- Chapter 5 (Discussion) discusses the methods used in these investigations and the results achieved in a broader context.

- The publications are listed in the appendix.

2 Status of science and technology

2.1 Methodological approaches and results of site-specific yield mapping

Site-specific yield recording has been around for more than 30 years. In the 1990s, for example, the first studies on yield recording in combine harvesters took place (PFEIFFER ET AL. 1993; PEREZ-MUNOZ AND COLVIN 1996; STRUBBE ET AL. 1996; DEMMEL 2013). Results with very different levels of precision were obtained (KORMANN ET AL. 1998). The reasons for these clear inaccuracies could not be clarified in the field tests.

Since the early 2000s, most manufacturers have offered yield recording systems in combine harvesters (NOACK 2007). In practice, however, these systems have not yet been fully established. This is due to measuring principles with different degrees of accuracy and their moderate further development by agricultural machinery manufacturers, and also due to the many influencing factors (calibration, environmental influences, and harvesting conditions) that make precise yield recording in the combine harvester difficult (STEINMAYR 2002; NOACK 2006; TOSCANO ET AL. 2019). Various studies on this still show significant inaccuracies in yield mapping using combine harvester yield recording systems (ARSLAN AND COLVIN 2002; SIMBAHAN ET AL. 2004; NOACK 2006; BACHMAIER 2007). Thus, HÜLSBERGEN ET AL. (2020) and MITTERMAYER ET AL. (2022) analyzed combine harvester data from several fields with ground truth data (plot combine harvester data and biomass hand cuts) and found very large variation in the precision of the combine harvester data. The combine harvester data correlated closely with the ground truth data on individual fields, while only weak correlations were found on other fields.

In addition to yield mapping using combine harvesters, new non-contact measuring methods have entered the market in recent years, which, based on reflection measurements and scientifically based algorithms, enable yield mapping even before harvesting (ÖTTL AND SIXT 2021). There is the possibility of using algorithms to create yield estimates based on sensor or satellite data (HANK ET AL. 2015; MAIDL ET AL. 2019). This development and the increasing importance of site-specific farming should also lead to the further development of yield recording in combine harvesters. The companies Claas and John Deere, two of the world's leading combine harvester manufacturers, have made a system change in recent years. The Claas company replaced the volume flow sensor with a mass flow sensor to reduce the calibration effort in the field (ÖTTL AND SIXT 2021). The John Deere brand, on

the other hand, will use the Active Yield system in the future to record yields without active calibration (JOHN DEERE 2019).

The following chapters provide an overview of the current state of knowledge and the technology of the various methods for site-specific yield recording of winter wheat.

2.1.1 Combine Harvester

To be able to map the yield with a combine harvester, other sensors and components are required in different areas of the combine harvester in addition to the actual sensor for measuring the yield. These can be divided into five areas and are shown schematically in Figure 3.
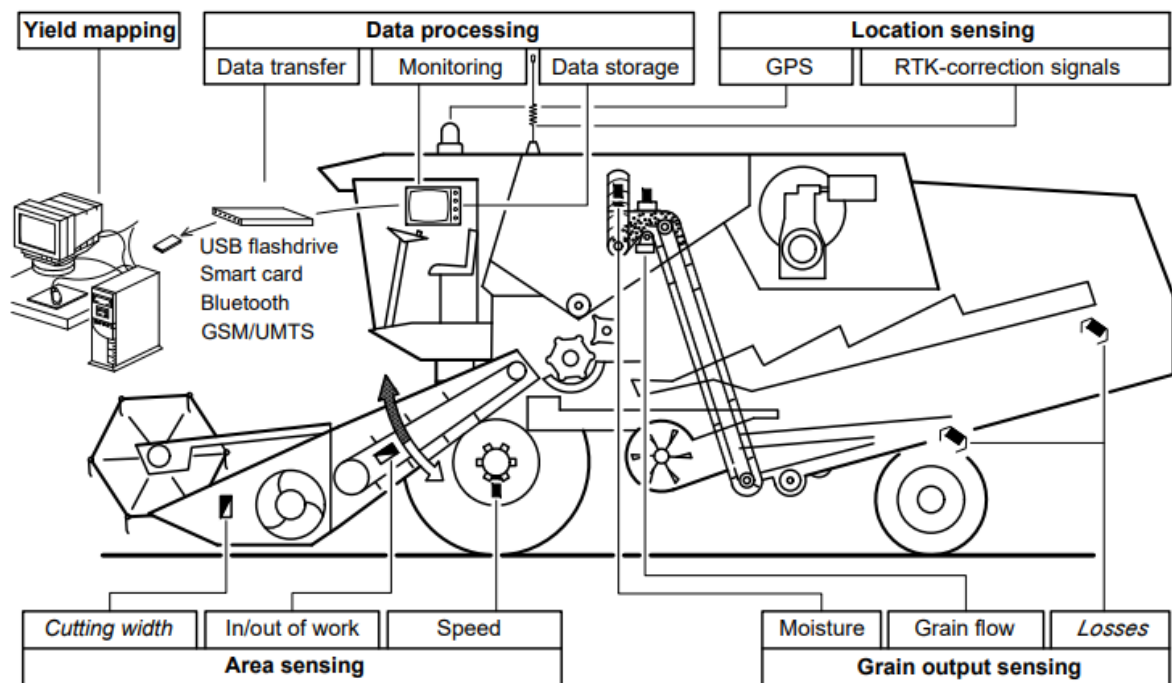
Figure 3: Components of a yield measurement system in a combine harvester (NOACK 2006)

For the calculation of the local yield, at least the throughput of the crop, the harvested area, and the vehicle position must be determined. The throughput of the crop is recorded with the yield sensor in the upper area of the grain elevator and corrected with the values of the moisture sensor and loss sensor (grain output sensing). To be able to determine the absolute amount of the yield, the yield value must be related to the harvested area. For this purpose, this is calculated via the detection of the cutting width and the speed of the combine harvester (area sensing). At the same time, the vehicle's position is recorded via GPS sensors so that the yield data can be georeferenced (location sensing). All these measurement data are

processed and saved in the yield monitor (data processing). After a field has been harvested, the data can be transferred from the yield monitor via various interfaces (USB flash drive, Bluetooth, mobile network) to the manufacturer's programs or other farm management systems, in which the measurement data are converted into a map (yield mapping) (DEMMEL 2001; NOACK 2006; CHUNG ET AL. 2016; FULTON ET AL. 2018).

Various yield sensors, which continuously record the throughput of the harvested crop, have been developed for yield measurement in combine harvesters. The available measuring systems are based on two basic measuring principles (DEMMEL 2001; NOACK 2006; REINKE ET AL. 2011; CHUNG ET AL. 2016; FULTON ET AL. 2018).

2.1.1.1 Volume flow sensors

With this principle, the throughput of the crop is determined volumetrically. The volume of the grain flow is recorded by the yield sensor and converted to the mass flow using the specific weight (hl weight). There are two types of volume flow sensors (Figure 4).
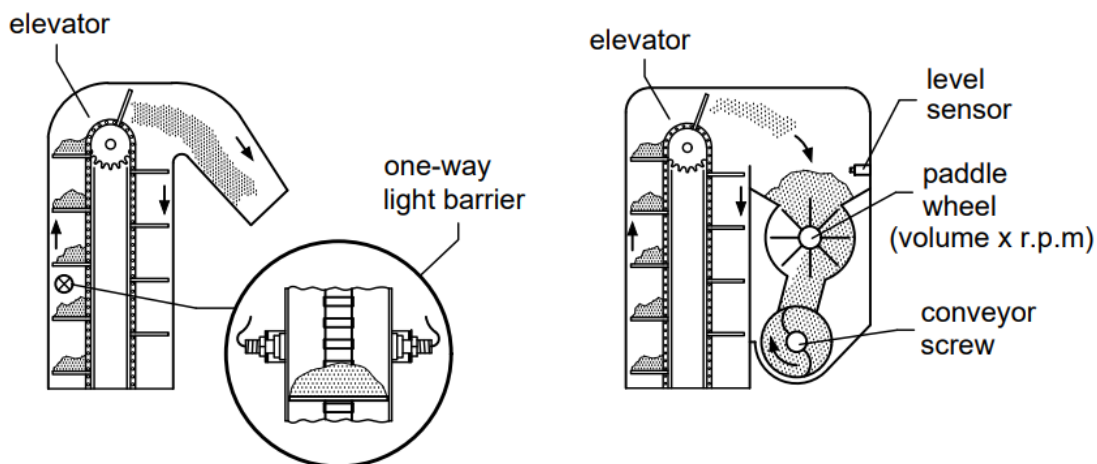
Figure 4: Functioning of an open volume flow sensor (left) and a closed volume flow sensor (right) (DEMMEL 2001).

Open volume flow measurement systems work with a light barrier in the upper area of the flow side of the grain elevator. The beam of light is interrupted by the conveyed grain on the elevator paddles. With the help of the calibration function, the volume of the conveyed grain can be calculated from the duration of the dark phase. Closed volume flow measurement systems work with a paddle wheel at the end of the grain elevator. Due to the closed design of the paddle wheel, the volume is known during one rotation. By determining the number

of rotations of the paddle wheel, the volume of grain conveyed can be calculated (KORMANN ET AL. 1998; DEMMEL 2001; NOACK 2006; CHUNG ET AL. 2016).

This measuring principle requires a lot of calibration. Since the bulk density (hl weight) of the individual varieties and crops differs significantly, this must be determined separately each time using a measuring cylinder and scales and entered into the yield monitor to ensure correct yield recording (DEMMEL 2001; ARSLAN AND COLVIN 2002; NOACK 2006).

2.1.1.2 Mass flow sensors

In contrast to volume flow sensors, mass flow sensors determine the mass flow directly. A distinction is made between radiometric measuring systems (indirect measurement) and impulse measuring systems (direct measurement) (Figure 5).
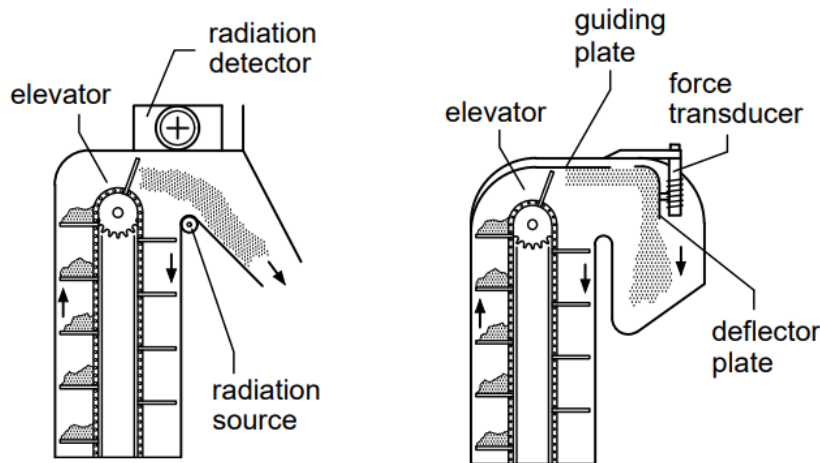
Figure 5: Functioning of a radiometric mass flow sensor (left) and a force/impetus mass flow sensor (right) (DEMMEL 2001).

Radiometric measuring systems record the mass flow by determining the absorption of gamma radiation. For this purpose, a radioactive radiation source is mounted on one side of the elevator shaft and a radiation detector is mounted on the other side. When grain is conveyed through the elevator, the grains pass between the radiation source and detector. In the process, radiation is absorbed. The mass flow of the harvested crop can be recorded using the radiation intensity measured on the detector and the calibration curve. Impulse measuring systems measure the force or the impulse that the grain kernels exert on measuring fingers or a deflector plate. These are attached to the elevator head and equipped with a force transducer (KORMANN ET AL. 1998; DEMMEL 2001; NOACK 2006; CHUNG ET AL. 2016; FULTON ET AL. 2018).

Mass flow sensors also need to be calibrated. This is usually achieved by weighing a bunker load on a vehicle scale and entering the corresponding weight into the yield monitor. A correction factor is calculated from this. In John Deere´s newly developed yield recording system, Active Yield, the mass flow sensor in the grain elevator is supplemented by three load cells in the grain tank (Figure 6).

Figure 6: Load cells in the grain tank (JOHN DEERE 2019)

These load cells calculate the change in weight of the grain as the grain tank is filled, allowing for continuous calibration of the mass flow sensor. As a result, errors can be minimized, and active calibration is no longer necessary (JOHN DEERE 2019).

2.1.2 Sensor data

Two different measuring principles are used for non-contact evaluation of crop stands. On the one hand, these are measurements of the laser-induced chlorophyll fluorescence and, on the other hand, these are reflection measurements. Vegetation indices can be calculated from the intensity of these measured variables. Based on the vegetation indices, scientific algorithms can be used to draw conclusions about the nutritional status of the plants or the yield (RECKLEBEN 2014). Absolute yield maps (t ha^{-1}) for winter wheat can be generated using the algorithms of MAIDL ET AL. (2019).

Laser-induced chlorophyll fluorescence is an active measurement method that is independent of sunlight. The chloroplasts inside the leaf are stimulated by a laser beam and the chlorophyll subsequently produces fluorescent light in the infrared (730 nm) and red (690 nm) range. The plant can reabsorb part of the red fluorescent light, while this is not possible in the infrared range. By measuring the fluorescent light of both ranges, these can

be brought into relation. A vegetation index can be calculated from the quotient between red and infrared light. The vegetation index is therefore dependent on the chlorophyll content of the leaves. However, there are some measurement difficulties, since the chlorophyll content is strongly dependent on the variety, the growth stage, and the leaf layer measured and can thus falsify the vegetation index (SCHÄCHTL ET AL. 2005; LIMBRUNNER AND MAIDL 2006; THOREN AND SCHMIDHALTER 2009; BERG 2020).

For this reason, reflection sensors are now predominantly used for non-contact determination of the nutritional status and yield of winter wheat. In the case of reflection measurements, a distinction must be made between active and passive sensors. Passive sensors do not have their own light source and rely on sunlight and can therefore only be used during the day. Active sensors are equipped with their own light source and are therefore ready for use regardless of sunlight. Reflectance sensors measure the reflected light in different wavelength ranges, both in the visible (< 670 nm) and in the near-infrared range (> 720 nm). Vegetation indices can be calculated from the reflection data of the individual measured wavelengths. The selection of suitable wavelengths for the calculation and development of vegetation indices is a major scientific challenge. Well-known vegetation indices are the NDVI (Normalized Difference Vegetation Index), SRI (Simple Ratio), SAVI (Soil Adjusted Vegetation Index), IR/G (Ratio Infrared/Green), REIP (Red Edge Inflection Point), and YARA_ALS (ERDLE ET AL. 2011; RECKLEBEN 2014; WESTERMEIER AND MAIDL 2019; HÜLSBERGEN ET AL. 2020). The vegetation index REIP, which MAIDL ET AL. (2019) also use in their algorithms, is particularly suitable for yield estimates of winter wheat.

2.1.3 Satellite data

The procedure for satellite-data-based yield mapping is very similar to that for sensor data. Vegetation indices are calculated from reflectance measurements. Based on these data, various parameters (yield, biomass, degree of nutrient supply) can be determined using scientific algorithms and models. Absolute yield maps (t ha^{-1}) for winter wheat based on satellite data can be created with the plant growth model PROMET (Process of Radiation, Mass, and Energy Transfer) (HANK ET AL. 2015; WEIS 2019).

The basic difference to the sensor data is that the reflection data do not come from a tractor-mounted multispectral sensor but are based on remote sensing. This means that, due to the large distance between the sensor and the target area, some corrections to the raw data are necessary; this is not required for measurements close to the plant. The remote sensing data

are influenced by the atmosphere (clouds, aerosols, and trace gases) and the adjacency effect. Atmospheric disturbances occur even in cloudless conditions, so atmospheric correction is arguably the most important part of satellite data preprocessing (VERHOEF AND BACH 2003; WU ET AL. 2005; HADJIMITSIS ET AL. 2010). In the field of agriculture, the MODTRAN Interrogation Technique is mainly used (HANK ET AL. 2015).

There are various satellites that are equipped with the appropriate sensors so that they can be used for agricultural remote sensing. These are mainly the Sentinel-2 satellites of the Copernicus program and the Landsat satellites of the US Aerospace Agency NASA. These satellites enable a spatial resolution of up to 10 x 10 m and deliver data every three to five days. Furthermore, their spectral sensors cover the range of visible light up to the infrared range, which is important for vegetation data. To be able to offer even more precise satellite data in the future, the current developments in agricultural satellites are moving towards even higher spatial resolution and shorter intervals between returns. The PlanetScope satellites from the US company Planet already enable a resolution of 3 x 3 m and deliver image data every one to two days (HANK ET AL. 2015; WEIS 2019; PLANET 2022).

2.1.4 Results of site-specific yield mapping

Tables 3 and 4 provide an overview of studies that have already dealt with the precision of digital methods for site-specific yield mapping.

Table 3:Methodological approaches and results of site-specific yield mapping

Method type	Trial type	Crop	Precision	Reference
Combine harvester with a volume flow sensor (light barrier)	[a]	Corn	Error: 3%	PFEIFFER ET AL. (1993)
Combine harvester with a volume flow sensor (light barrier)	Testing stand [c]	Corn, wheat	Error: 13%	STRUBBE ET AL. (1996)
Combine harvester with a mass flow sensor (force transducer)	Field trial [c]	Corn	R^2: 0.89	PEREZ-MUNOZ AND COLVIN (1996)
Combine harvester with a mass flow sensor (force transducer)	Testing stand [c]	Corn	R^2: 0.97	PEREZ-MUNOZ AND COLVIN (1996)
Combine harvester with a volume flow sensor (paddle wheel)	Testing stand [c]	Corn, wheat, barley	Error: 4%	KORMANN ET AL. (1998)
Combine harvester with a mass flow sensor (force transducer)	Testing stand [c]	Corn, wheat, barley	Error: 4%	KORMANN ET AL. (1998)
Combine harvester with a mass flow sensor (radiometric, X-ray)	Testing stand [c]	Corn	R^2: 0.98	ARSLAN ET AL. (2000)
Satellite data (NDVI)	Field trial [d]	Wheat	R^2: 0.57–0.63	REYNIERS ET AL. (2006)
Satellite data combined with a plant growth model	Field trial [e]	Wheat	R^2: 0.82	HANK ET AL. (2015)
Satellite data (NDVI)	Field trial [f]	Wheat	R^2: 0.54–0.74	TOSCANO ET AL. (2019)
Satellite data (NDVI)	Field trial [f]	Wheat	R^2: 0.65	WANG ET AL. (2019)
Satellite data combined with a prediction model	Field trial [f]	Wheat	R^2: 0.85	WANG ET AL. (2019)
UAV based hyperspectral sensor and a plant growth model	Field trial [e]	Wheat	R^2: 0.48	SONG ET AL. (2020)

[a] no information; [b] no further information on the yield sensor; [c] only the weight was checked using a scale; [d] spatial variability was checked using yield data from a plot harvester; [e] weight and spatial variability were checked using yield data from a combine harvester; [f] spatial variability was checked using yield data from a combine harvester; [g] weight and spatial variability were checked using yield data from a plot harvester and biomass samples

Table 4: Methodological approaches and results of site-specific yield mapping

Method type	Trial type	Crop	Precision	Reference
Satellite data combined with a plant growth model	Field trial [f]	Wheat	R^2: 0.76	ZHAO ET AL. (2020)
Combine harvester with a mass flow sensor (force transducer)	Field trial [g]	Wheat	R^2: 0.77	HAUSER ET AL. (2021)
Tractor mounted multispectral sensor and algorithm	Field trial [g]	Wheat	R^2: 0.70	HAUSER ET AL. (2021)
Satellite data combined with a plant growth model	Field trial [g]	Wheat	R^2: 0.56	MITTERMAYER ET AL. (2021)
Combine harvester with a volume flow sensor [b]	Field trial [g]	Wheat	R^2: 0.66	MITTERMAYER ET AL. (2021)
Tractor mounted multispectral sensor and algorithm	Field trial [g]	Wheat	R^2: 0.63	MITTERMAYER ET AL. (2021)

[a] no information; [b] no further information on the yield sensor; [c] only the weight was checked using a scale; [d] spatial variability was checked using yield data from a plot harvester; [e] weight and spatial variability were checked using yield data from a combine harvester; [f] spatial variability was checked using yield data from a combine harvester; [g] weight and spatial variability were checked using yield data from a plot harvester and biomass samples

The results in Tables 3 and 4 show that after the start of yield recording in combine harvesters in the 1990s, no significant progress (in terms of measurement methods, error analyses, evaluation attempts, etc.) was made for many years. Only due to the increasing importance of site-specific land management and the market entry of alternative options for yield mapping based on sensor or satellite data has research in this important area increased again in recent years. Apart from a few exceptions that examined individual systems (REYNIERS ET AL. 2006; SONG ET AL. 2020; HAUSER ET AL. 2021; MITTERMAYER ET AL. 2021), there are no evaluations in which the state-of-the-art methods for site-specific yield recording were checked with real ground truth data in plot trials. Further investigations are essential, especially for the creation of absolute yield maps, as an important data basis for site-specific fertilization.

2.2 Methodological approaches and results of site-specific analysis of nitrogen uptake

There have been sensor-based fertilizer systems on the market for around 20 years, which record the degree of nitrogen supply of winter wheat at different growth stages on a site-specific basis and can adjust the amount of nutrients to be applied in real time. At first, these were mechanical systems that measured the bending resistance with the help of a pendulum sensor. In addition to the nutritional status, this parameter is also significantly influenced by the stability of the variety and the use of growth regulators, and it is therefore not practicable (EHLERT ET AL. 2003; RECKLEBEN 2014). For this reason, reflection sensors are now predominantly used for non-contact determination of the nitrogen uptake of winter wheat. Two basic measuring principles can be distinguished with tractor-mounted and satellite-based multispectral sensors (SONG ET AL. 2009; DIACONO ET AL. 2013; RECKLEBEN 2014; HÜLSBERGEN ET AL. 2020).

The following chapters provide an overview of the current state of knowledge and technology for the various methods for site-specific determination of nitrogen uptake in winter wheat.

2.2.1 Sensor data

Laser-induced chlorophyll fluorescence and reflection measurements are available for non-contact determination of the nitrogen uptake in winter wheat using sensors close to the plant. As a result of the dependence on the chlorophyll content in the laser-induced chlorophyll fluorescence, as already explained in Section 2.1.2, reflection sensors are now predominantly used to record the nitrogen supply of winter wheat crops (RECKLEBEN 2014; BERG 2020; HÜLSBERGEN ET AL. 2020). The same principle applies to nitrogen uptake as to yield recording (see 2.1.2). With the help of other algorithms, the nutrient uptake can then be estimated from the vegetation index determined by reflection measurement. The absolute nitrogen uptake at different growth stages based on sensor data can be calculated using algorithms from MAIDL (2011). Various vegetation indices are available for this purpose. The literature shows that some vegetation indices are generally more or less suitable for determining the nitrogen uptake, depending on the crop type, while other vegetation indices are more or less suitable depending on the growth stage of the crop (LI ET AL. 2010; PREY AND SCHMIDHALTER 2019; WESTERMEIER AND MAIDL 2019). Studies on this show that the vegetation index REIP (Red Edge Inflection Point) can provide very robust and accurate data on the nitrogen uptake, especially in winter wheat (ERDLE ET AL. 2011; CAMMARANO

ET AL. 2014; CAO ET AL. 2018). MAIDL (2011) also uses the REIP in his algorithms for estimating absolute nitrogen uptake.

2.2.2 Satellite data

The procedure for recording the nitrogen uptake based on satellite data is also analogous to that for recording the yield (2.1.3). The MODTRAN Interrogation Technique is also used for atmospheric correction, and the same satellites are used as described in 2.1.3. However, the plant growth model PROMET is not used to calculate the absolute nitrogen uptake; instead, a radiative transfer model (soil leaf canopy) is used (VERHOEF AND BACH 2007; MIGDALL ET AL. 2009; HANK ET AL. 2015).

2.2.3 Results of site-specific analysis of nitrogen uptake

Table 5 provides an overview of studies that have already dealt with the precision of digital methods for site-specific analysis of the nitrogen uptake.

Table 5: Methodological approaches and results of site-specific analysis of nitrogen uptake

Method type	Trial type	Crop	Precision	Reference
Satellite data and vegetation indices	Field trial [b]	Wheat	R^2: 0.74	JIA ET AL. (2011)
Handheld multispectral sensor and vegetation indices	Field trial [b]	Wheat	R^2: 0.60–0.89	CAO ET AL. (2015)
Remote sensing data and vegetation indices [a]	Field trial [b]	Wheat	R^2: 0.86	CHEN (2015)
Handheld multispectral sensor and vegetation indices	Field trial [b]	Wheat	R^2: 0.62	PAVULURI ET AL. (2015)
Satellite data and vegetation indices	Field trial [b]	Wheat	R^2: 0.81	MAGNEY ET AL. (2017)
Handheld multispectral sensor and vegetation indices	Field trial [b]	Wheat	R^2: 0.61	CAO ET AL. (2018)
Handheld multispectral sensor and vegetation indices	Field trial [b]	Wheat	R^2: 0.59	PREY AND SCHMIDHALTER (2019)
Combine harvester with a mass flow sensor and a protein sensor	Field trial [c]	Wheat	R^2: 0.61	WANG ET AL. (2019)
Handheld multispectral sensor and algorithm	Field trial [b]	Wheat	R^2: 0.90	WESTERMEIER AND MAIDL (2019)
Tractor mounted multispectral sensor and algorithm	Field trial [d]	Wheat	R^2: 0.64	MITTERMAYER ET AL. (2021)

[a] no further information on the data type; [b] spatial variability was checked using data from biomass samples; [c] spatial variability was checked using data from a yield sensor and a protein sensor from a combine harvester; [d] absolute height (kg ha^{-1}) and spatial variability were checked using data from biomass samples

Table 5 shows that some studies were able to achieve good correlations with the nitrogen uptake using digital methods. However, most have dealt with relative estimates from vegetation indices or just determined the total nitrogen uptake at harvest. The absolute amount of nitrogen uptake at characteristic growth stages that are important for fertilization has not yet been investigated in detail. Only WESTERMEIER AND MAIDL (2019) compared the nitrogen uptake at characteristic growth stages with vegetation indices, and MITTERMAYER ET AL. (2021) dealt with the absolute level of nitrogen uptake at harvest; however, to date,

no evaluations have been carried out in which the state-of-the-art methods for recording the spatial variability of the absolute nitrogen uptake in plot trials with real ground truth data were checked. Further method comparisons are therefore urgently needed, especially for the evaluation of the precision and the further development of site-specific nitrogen fertilization.

3 Methodological approach

3.1 Site and weather conditions

The studies were conducted on three trial fields at two trial sites in southern Germany. In 2018, a field at the Dürnast Research Station (48°40'66" N 11°69'49" E), 3 km west of Freising (485 m a. s. l.), was selected, and in 2020 and 2021, investigations were conducted in two fields at the Makofen Research Farm (48°81'55" N 12°74'31" E), 15 km southeast of Straubing (320 m a. s. l.) (Figure 7).
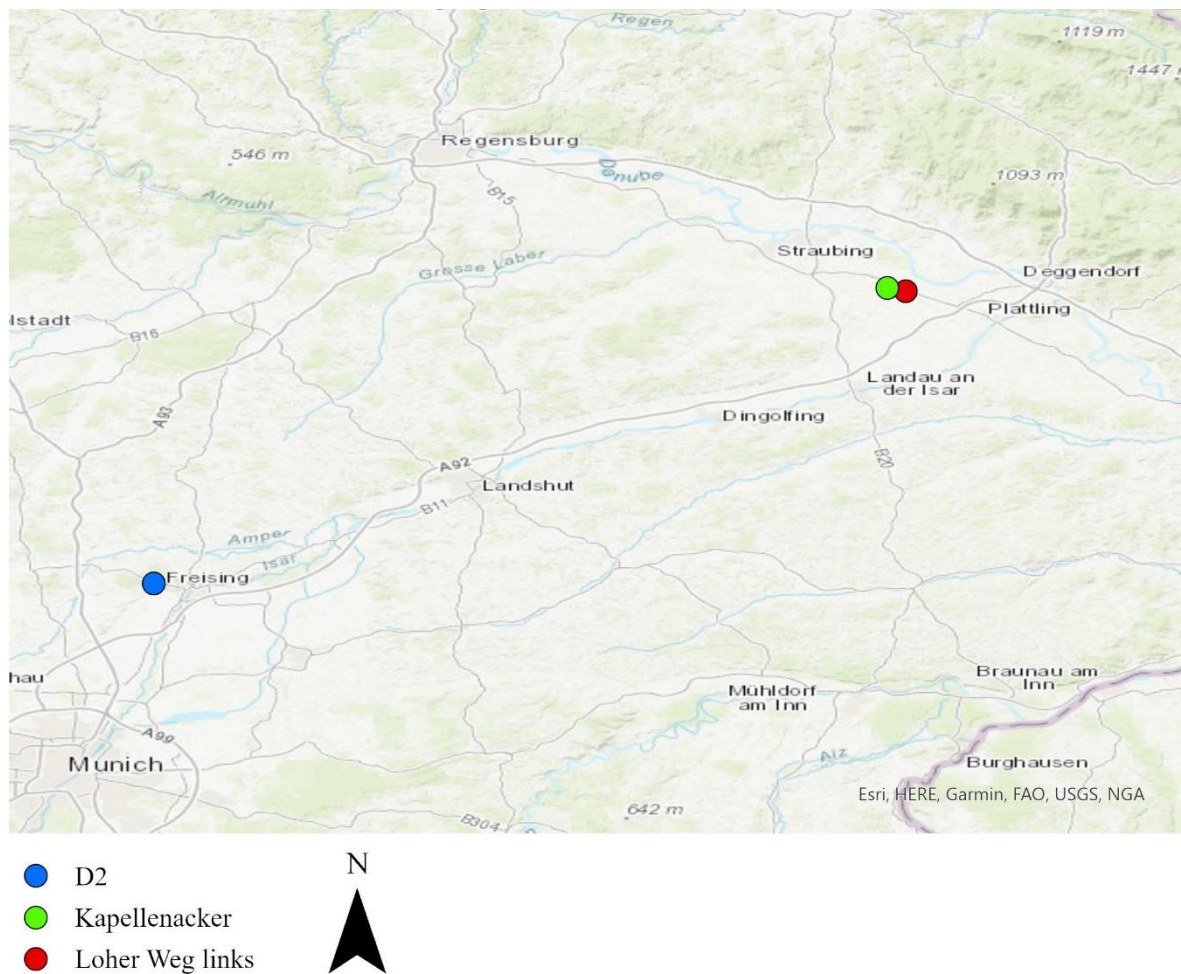
Figure 7: Study sites and fields

While the climatic conditions at both study sites are similar, the soils differ. Investigations were carried out in the Munich tertiary hill country, and in the Lower Bavarian Gäuboden, south of the Danube River and the Bavarian Forest. The trial field in Dürnast consists of medium-quality soil with hilly relief, while the trial fields in Makofen are flat and characterized by very fertile loess soil, which is typical for the Gäuboden region. This classification is based on the soil fertility index (LANDESAMT FÜR DIGITALISIERUNG,

BREITBAND UND VERMESSUNG 2022). The soil type at both locations is silty loam, but the contents of sand and silt differ. The Dürnast location was chosen because it has been well studied over many years, specifically on the topic of site-specific nitrogen fertilization. The Makofen location was chosen to evaluate the precision of the tested digital methods at a supposedly homogeneous high-yield location. Furthermore, the Makofen site has hardly been researched in the topic of site-specific nitrogen fertilization and can thus be related to long-term data from the Dürnast site. Overall, fields with a high level of soil heterogeneity were deliberately selected at both locations to ensure the best possible conditions for a method comparison on spatial variability. Table 6 shows the most important site and weather conditions of the experimental sites.

Table 6: Site and weather conditions of the experimental farms

Property	Dürnast	Makofen
Region	Upper Bavaria	Lower Bavaria
	30 km north of Munich	115 km northeast of Munich
District	Freising	Straubing-Bogen
Average height [m]	475	322
Soil classification	Cambisol	Cambisol
Soil type	silty loam	silty loam
Mean sand content (0–30 cm) [%]	40.5	6.5
Mean silt content (0–30 cm) [%]	39.5	69.7
Mean clay content (0–30 cm) [%]	20.0	23.8
Mean available water capacity (in 10 cm) [Vol.%]	17.0	23.6
Mean soil organic carbon content (0–30 cm) [% DM]	1.4	1.3
Mean total nitrogen content (0–30 cm) [% DM]	0.13	0.13
Mean pH-value (0–30 cm)	6.2	6.7
Mean plant available phosphorus content (0–30 cm) [mg $(100g)^{-1}$]	13.7	16.4
Mean plant available potassium content (0–30 cm) [mg $(100g)^{-1}$]	15.2	18.1
Mean annual temperature[a] [°C]	8.7	9.5
Mean annual precipitation[a] [mm]	789	781

[a] average of the last 20 years

In general, there are excellent conditions for arable farming at all trial sites, with sufficient precipitation (>780 mm a^{-1}) and high soil quality (silty loam). The study sites represent high-yield regions in Upper and Lower Bavaria, with intensive crop rotations and management (MITTERMAYER 2022). The three study fields range in size from 4.2 to 6.9 ha. The selection of the study fields was based on the following characteristics:

- Heterogeneity of the study fields (based on long-term biomass maps, soil properties, and the expertise of the farm managers);
- Uniform crop management;
- Representativeness of the study region.

Furthermore, different farming systems are typical in the two study regions. The trial field near Freising is managed in a mixed farm, while the fields in Makofen are managed in a cash crop system (long-term low or no organic fertilizer application), which is typical for the Gäuboden region. Therefore, the study fields differ in their nitrogen mineralization potential, even if the trials were exclusively mineral fertilized. Table 7 contains a characterization of the farming systems, investigation parameters, and methods.

3 Methodological approach

Table 7: Characterization of the farming systems, the investigation parameters, and methods

Field	D2	Kapellenacker	Loher Weg links
Size [ha]	4.2	5.0	6.9
Coordinates	48°24'18" N	48°48'57" N	48°48'55" N
	11°41'53" E	12°44'25" E	12°45'10" E
Soil fertility index[a]	55–60	75–85	70–80
Farm	Dürnast	Makofen	Makofen
Farming system	Mixed farming	Arable farming	Arable farming
Livestock unit [LU ha^{-1}]	1.0	0	0
Year of investigation	2018	2020/2021	2020/2021
N fertilization, total (org/min)	0/167	0/180	0/172
Investigation parameters	Yield	Yield, N uptake	Yield, N uptake
Digital methods	Combine harvester yield sensing system, Tractor mounted sensor and algorithm, Satellite data and model	Combine harvester yield sensing system, Tractor mounted/handheld sensor and algorithm, Satellite data and model	Combine harvester yield sensing system, Tractor mounted/handheld sensor and algorithm, Satellite data and model
Ground Truth data	Plot harvester data	Plot harvester data, Biomass hand sampling	Plot harvester data, Biomass hand sampling

[a] The soil fertility index is a quantitative assessment of soil fertility given in integers in a range of 0–100, with 100 representing the most fertile soil in Germany

3.2 Methods for determining yield and nitrogen uptake

In the present study, the yield and nitrogen uptake data were analyzed with a high spatial resolution using different digital technologies and methods. The following chapter characterizes the methods used. Plot harvester data and hand-cut biomass samples were used as ground truth data to validate the applied digital methods.

3.2.1 Methods for determining yield

The yield data were determined using the following methods:

- Plot harvester (ground truth data) (WINTERSTEIGER 2022);

- Combine harvester with yield mapping (mass flow sensor) (NOACK 2006);

- Process of Radiation, Mass, and Energy Transfer (PROMET) plant growth model based on satellite data (MAUSER AND BACH 2009);

- Algorithm based on reflection measurements using a tractor-mounted multispectral sensor (MAIDL ET AL. 2019; TEC5 2022).

Winter wheat yields were determined with the plot harvester and the combine harvester (mass flow sensor) on the harvest dates 27 July 2018, 30 July 2020, and 10 August 2021. A New Holland CX 8050 combine harvester was used in 2018, and a John Deere S780 was used in 2020 and 2021 to map yields. The PROMET yield data were made available by the developer Vista GmbH. Depending on the availability, the PROMET plant growth model used satellite data shortly before the harvest date to estimate the wheat yield (HANK ET AL. 2015). Based on satellite data, the PROMET plant growth model calculated the wheat yield considering further data (HANK ET AL. 2015; STETTMER ET AL. 2022b). The model requires four groups of input data that affect the spatial simulation of the crop yield:

- Agricultural management (sowing date, fertilization events, harvest date);
- Crop specifications (variety, photoperiod sensitivity, assimilation rate);
- Dynamic environmental driver variable (temperature, precipitation, radiation, wind);
- Static environmental parameters (location, terrain, soil properties) (HANK ET AL. 2015).

The reflection measurements for the algorithm by MAIDL ET AL. (2019) were carried out in the BBCH 65 growth stage. Based on these measurements, the REIP 700 vegetation index was calculated, and the algorithms used to estimate the spatial variability of wheat yield were based on this index (MAIDL ET AL. 2019).

3.2.2 Methods for determining nitrogen uptake

The nitrogen uptake data were determined using the following methods:

- Biomass samples (ground truth data) (SAINT-DENIS AND GOUPY 2004);

- An algorithm based on reflection measurements using a handheld multispectral sensor (MAIDL 2011; TEC5 2022);

- Radiative transfer model (soil–leaf–canopy) based on satellite data (VERHOEF AND BACH 2007; HANK ET AL. 2015).

Nitrogen uptake data were determined using the respective methods in the growth stages BBCH 31, BBCH 39, BBCH 55, and BBCH 65. Therefore, for the ground truth data, an area of 2.5 m² of plants was manually cut off in each plot. These samples were weighed, chopped, and dried at 105°C in the laboratory. This resulted in the above-ground biomass yield being obtained. The Dumas method was used to analyze the nitrogen content of each sample, and thus, the nitrogen uptake of each plot could be determined (SAINT-DENIS AND GOUPY 2004). The reflection measurements with the handheld multispectral sensor for the algorithm by MAIDL (2011) were conducted in the respective growth stages in the individual plots. The REIP 700 vegetation index was calculated based on these measurements, and the algorithms used to estimate the absolute nitrogen uptake of winter wheat were based on this index considering further data, such as the yield potential and variety properties (MAIDL 2011). Depending on the availability, the radiative transfer model used up-to-date satellite data to estimate the absolute nitrogen uptake of winter wheat. Based on the satellite data, the radiative transfer model calculated the absolute nitrogen uptake at the respective growth stages considering additional data, such as observational parameters, soil reflectance information, leaf optical properties, and canopy properties (VERHOEF AND BACH 2007; HANK ET AL. 2015; STETTMER ET AL. 2022a).

4 Publications

4.1 Analysis of nitrogen uptake in winter wheat using sensor and satellite data for site-specific fertilization

Matthias Stettmer, Franz-Xaver Maidl, Jürgen Schwarzensteiner, Kurt-Jürgen Hülsbergen, and Heinz Bernhardt

Abstract: Sensor- and satellite-based determination of nitrogen uptake provides critical data in site-specific fertilization algorithms. Therefore, two basic noncontact measurement methods (sensor and satellite) were investigated in winter wheat, and their precision was evaluated in this study. Nitrogen uptake at four characteristic growth stages (BBCH 31, BBCH 39, BBCH 55, and BBCH 65) was determined using algorithms based on sensor and satellite data. As a reference, nitrogen uptake was determined using biomass samples in the laboratory (ground truth data). The precision of the tested methods was evaluated using statistical indicators (mean, median, minimum, maximum, and standard deviation) and correlation analyses between the nitrogen uptake of the ground truth data and that of the respective method. The results showed moderate to strong correlations with the nitrogen uptake of the ground truth data for both methods ($R^2 = 0.57$–0.83). Both sensor and satellite data best represented nitrogen uptake in BBCH 39 and 55 ($R^2 = 0.63$–0.83). In sum, there were only slight deviations in the absolute amount of nitrogen uptake ($\leq\pm15\%$). Clear deviations can be explained by external influences during measurement. Overall, the investigations showed that the nitrogen uptake could be appropriately determined as a data basis for site-specific fertilization systems using sensor and satellite data.

Contributions of authors: Matthias Stettmer (75%), Franz-Xaver Maidl (10%), Jürgen Schwarzensteiner (5%), Kurt-Jürgen Hülsbergen (5%), and Heinz Bernhardt (5%)

4.2 Three methods of site-specific yield mapping as a data source for the delineation of management zones in winter wheat

Matthias Stettmer, Martin Mittermayer, Franz-Xaver Maidl, Jürgen Schwarzensteiner, Kurt-Jürgen Hülsbergen, and Heinz Bernhardt

Abstract: In this study, three digital, site-specific, yield-mapping methods for winter wheat were examined, and their precision was evaluated. The crop yields of heterogeneous fields at three locations were determined on a site-specific basis using a yield-recording system composed of a combine harvester and algorithms based on reflection measurements made via satellites, as well as a tractor-mounted sensor. As a reference, the yield was determined with a plot harvester (ground truth data). The precision of the three methods was evaluated via statistical indicators (mean, median, minimum, maximum, and standard deviation) and correlation analyses between the yield of the ground truth data and the respective method. The results show a yield variation of 4.5–10.9 t ha^{-1} in the trial fields. The yield of the plot harvester was strongly correlated with the yield estimate from the sensor data (R^2 = 0.71–0.75), it was moderately correlated with the yield estimate from the satellite data (R^2 = 0.53–0.68), and it ranged from strongly to weakly correlated with the yield map of the combine harvester (R^2 = 0.30–0.72). The absolute yield can be estimated using sensor data. Slight deviations (<10%) in the absolute yield are observed with the combine harvester, and there are clear deviations (±48%) when using the satellite data. The study shows differences in the precision and accuracy of the investigated methods. Further research and optimization are urgently needed to determine the exactness of the individual methods.

Contributions of authors: Matthias Stettmer (75%), Martin Mittermayer (5%), Franz-Xaver Maidl (5%), Jürgen Schwarzensteiner (5%), Kurt-Jürgen Hülsbergen (5%), and Heinz Bernhardt (5%)

5 Discussion

In this study, georeferenced yield and nitrogen uptake data were determined on heterogeneous arable fields using different digital methods and technologies. Ground truth data (plot harvester data and hand-cut biomass samples) were used to validate the applied digital methods. The precision was tested by comparing the statistical indicators (mean, median, minimum, maximum, and standard deviation) and examining correlative relationships. The aim was to assess the accuracy of the different digital methods. The investigations were carried out on two farms in southern Germany.

5.1 Discussion of methods

5.1.1 Site selection

The extent of the spatial variability of the examined parameters influences the method comparison. Just as site-specific land management makes particular sense on heterogeneous arable land, it also makes sense to investigate the precision of the underlying digital methods on heterogeneous arable land (ROßKOPF ET AL. 2015; WHELAN 2018). For this reason, fields that represent the heterogeneity of the study region were selected for the investigations. The greater the variation in nitrogen uptake and yield on the dates examined, the clearer the accuracy of the individual methods becomes. The heterogeneity of the test fields was recorded using soil analysis (soil type, usable field capacity, and nutrient contents), long-term biomass maps (satellite), and the experiences of the farm managers. The knowledge of farm managers is a particularly good starting point to assess the heterogeneity of arable land, as the studies by HEIJTING ET AL. (2011) show. Furthermore, small-scale heterogeneities in soil and plant stands in the Dürnast study region were already identified in previous studies (HEIL AND SCHMIDHALTER 2017; MITTERMAYER ET AL. 2021). The standard soil analysis conducted after the selection of the plot locations and the delineation of yield zones (high, medium, and low) on the trial fields clearly show the heterogeneity of the areas. The different yield zones result in different nutrient withdrawals; however, in the past, the trial fields were farmed uniformly, which led to the accumulation of nutrients (phosphorus, potassium, magnesium) in the low-yield zones (Table 8) (PATZOLD ET AL. 2008; DALGAARD ET AL. 2012; MITTERMAYER ET AL. 2021). This fact confirms the need for site-specific fertilization to be able to reduce nutrient losses and especially nitrate losses.

Table 8: Average soil properties in the yield zones

Property	High yield zone	Middle yield zone	Low yield zone
Mean pH value (0–30 cm)	6.3	6.6	7.2
Mean plant available phosphorus content (0–30 cm) [mg $(100g)^{-1}$]	13.3	11.2	21.5
Mean plant available potassium content (0–30 cm) [mg $(100g)^{-1}$]	12.3	13.5	17.5
Mean plant available magnesium content (0–30 cm) [mg $(100g)^{-1}$]	8.8	13.0	14.3

At a national level, however, southern Germany (and especially the trial site Makofen) tends to be classified as a homogeneous location. In comparison, the arable land in the terminal moraine areas of the Vistula Ice Age in northeastern Germany is particularly heterogeneous, which would influence the results of a method comparison (KOSZINSKI ET AL. 1995; KARPINSKI ET AL. 2015). Therefore, the site in Dürnast was chosen as a heterogeneous and well-studied test site in southern Germany, while at the Makofen site, fields assessed nationally with low yield variability were analyzed to test the accuracy of the methods under these conditions. Future studies should analyze other locations and crops to enable the evaluation and further development of existing technologies independently of the location. However, the fact that the tested methods were able to achieve such good results on a supposedly less-heterogeneous site as in Makofen shows the great potential of the site-specific systems.

5.1.2 Experimental setup

The data generated with different digital methods to record the spatial variability of nitrogen uptake and yield vary in terms of spatial resolution and distribution. Satellite-based data are currently available in a 10 x 10 m grid, while sensor-based data only measure parts of the field, with the distance between two steering lines having a decisive influence on the proportion of the measured field area to the total field area (MUÑOZ-HUERTA ET AL. 2013; WECKESSER ET AL. 2021). In the case of combine harvester data, on the other hand, the working width is decisive for the spatial resolution and distribution of the data. Furthermore, in field experiments to record yields, each area can only be harvested once, so when obtaining ground truth data using a plot harvester, this and the combine harvester with a

yield sensor must drive directly next to each other. However, as the distance between two measurement points decreases, the variance in the difference decreases. This is the basis for geostatistical methods (kriging interpolation), which are used in many studies on yield variability (SONG ET AL. 2009; GAVIOLI ET AL. 2016; VALLENTIN ET AL. 2020; MITTERMAYER ET AL. 2021). Therefore, this procedure provides ground truth data with a very high measurement accuracy.

However, these circumstances make it difficult to compare these methods, since the data are in different spatial resolutions and distributions. For this reason, plot experiments were set up in these investigations, which were appropriately adapted to the spatial resolution of the data. The plot trials for yield recording were arranged according to the spatial resolution of the satellite data and the working width of the combine harvester, while the plot trials for the nitrogen uptake were directly adapted to the grid of the satellite data. With the additional use of a handheld multispectral sensor, the sensor measurements could also be carried out independently of steering lines in all plots. In this way, data per plot could be generated with all methods, which enables good evaluation of the method comparison. This approach has also proven itself in other studies. For example, WANG ET AL. (2019), HAUSER ET AL. (2021), and MITTERMAYER ET AL. (2021) used a similar principle to examine yield data with combine harvesters, sensors, and biomass samples. CAO ET AL. (2015, 2018), PREY AND SCHMIDHALTER (2019), and WESTERMEIER AND MAIDL (2019) calculated the correlations between the nitrogen uptake and different vegetation indices based on sensor data and biomass samples using a similar experimental setup.

5.2 Discussion of results

5.2.1 Yield data

Overall, the field experiments showed a clear variation in the winter wheat yield of 5–11 t ha^{-1}, which can be classified as normal for the region examined. For example, HÜLSBERGEN ET AL. (2020) and MITTERMAYER ET AL. (2021) also analyzed the yield variation in winter wheat in southern Germany and obtained very similar results (5–10 t ha^{-1}). Further investigations showed yield variations of 4–7 t ha^{-1} in eastern Germany (HAUSER ET AL. 2021), 2–5 t ha^{-1} in southern Italy (DIACONO ET AL. 2012), and 0.5–5 t ha^{-1} in the Wheatbelt of Western Australia (ROBERTSON ET AL. 2008). Thus, the study region can be classified as a high-yield location for winter wheat on a global level. Table 9 shows in

detail the wheat yields of the individual test fields determined using different digital methods.

Table 9: Wheat yields determined in this study based on different digital methods

Method	Year	Field	Unit	Minimum yield	Maximum yield	Average yield
Plot harvester	2018	D2	t ha^{-1}	6.1	10.9	8.1
Sensor data	2018	D2	t ha^{-1}	6.1	10.4	8.1
Satellite data	2018	D2	t ha^{-1}	3.1	5.6	4.2
Combine harvester	2018	D2	t ha^{-1}	6.1	10.9	8.8
Plot harvester	2020	Kapellenacker	t ha^{-1}	8.4	10.1	9.3
Sensor data	2020	Kapellenacker	t ha^{-1}	6.8	10.4	9.4
Satellite data	2020	Kapellenacker	t ha^{-1}	8.3	10.1	9.3
Combine harvester	2020	Kapellenacker	t ha^{-1}	8.4	10.2	9.8
Plot harvester	2021	Loher Weg links	t ha^{-1}	4.5	7.5	5.9
Sensor data	2021	Loher Weg links	t ha^{-1}	4.4	7.2	5.9
Satellite data	2021	Loher Weg links	t ha^{-1}	7.2	9.6	8.5
Combine harvester	2021	Loher Weg links	t ha^{-1}	3.7	7.8	5.7

The results show that basically all three tested methods are able to record the absolute yield of winter wheat. In 2020, there were only minor deviations (<5%), and in 2018 and 2021, the deviations in the combine harvester with yield mapping and the sensor data were also small. The high deviations in the absolute yield of the satellite data occurred due to underestimation (−48%) on field D2 and overestimation (+44%) on the field Loher Weg links. This is very problematic since the absolute height is very important for yield maps, which are used as a basis for site-specific nitrogen fertilization (HÜLSBERGEN ET AL. 2020; HAUSER ET AL. 2021; MITTERMAYER ET AL. 2021). These clear deviations would lead to over- or under-fertilization and counteract the goal of lower N balances. In the case of relative zone maps, which are used as a basis for soil sampling, for example, this would be less of a problem, but this is an exclusion criterion for fertilization (MAIDL 2011; MUÑOZ-HUERTA ET AL. 2013; WECKESSER ET AL. 2021). The reason for these significant deviations could be the occurrence of weather extremes during the growing season (e.g., persistent dry periods, excessive precipitation, etc.). The year 2018 was characterized by heat and droughts, while 2021 was moderately cool and rained above average. The plant growth model PROMET models the absolute level of wheat yield based on satellite data and other input data

(agricultural management, crop specifications, dynamic environmental driver variables, and static environmental parameters) (HANK ET AL. 2015). In this context, the model may react too strongly to weather data, which would explain the underestimation due to the drought in crop year 2018 and the overestimation based on the heavy rainfall in crop year 2021. Similar results were also obtained by HANK ET AL. (2015) in their investigations, which also found a tendency to overestimate yields in extreme weather conditions. Further investigations are therefore urgently needed at this point to assess this assumption more precisely. The relative yield distribution, on the other hand, can be mapped moderately with the satellite data over all three test years, as the examination of the correlative relationships with the ground truth data shows ($R^2 = 0.53$–0.68) (Table 10).

Table 10: Yield data calculated by digital technologies in relation to the ground truth data

R^2	Year	Sensor	Satellite	Combine
Plot harvester (linear)	2018	0.74	0.68	0.69
Plot harvester (polynomial)	2018	0.75	0.68	0.69
Plot harvester (linear)	2020	0.69	0.51	0.25
Plot harvester (polynomial)	2020	0.71	0.53	0.30
Plot harvester (linear)	2021	0.67	0.54	0.72
Plot harvester (polynomial)	2021	0.71	0.56	0.72

HANK ET AL. (2015), who compared PROMET yield data with combine harvester data and found a good correlation ($R^2 = 0.82$), came to the same conclusion. Other studies that analyzed satellite data with yield data from biomass samples and combine harvester data also found moderate-to-good correlations ($R^2 = 0.54$–0.76) (TOSCANO ET AL. 2019; ZHAO ET AL. 2020). These results and the development of agriculturally used satellites regarding an increasing overflight frequency with a higher spatial resolution (3 x 3 m) make satellite data an interesting tool for agricultural practices in the future (WEIS 2019; PLANET 2022). The results of the sensor data show consistently strong relationships ($R^2 = 0.71$–0.75) to the ground truth data over all three years and are therefore well suited for the creation of absolute yield potential maps for fertilization. HAUSER ET AL. (2021) and MITTERMAYER ET AL. (2021) also compared yield estimates based on sensor data and the algorithms of MAIDL ET AL. (2019) with ground truth data and came to similar results ($R^2 = 0.63$–0.70). KAIVOSOJA ET AL. (2017) also showed a strong correlation comparing sensor data with combine harvester data ($R^2 = 0.82$). The results of the yield mapping of the combine harvester in the years 2018

and 2021 (R^2 = 0.69–0.72) were at a similarly good level. In 2020, on the other hand, the correlation (R^2 = 0.30) of the combine harvester data to the ground truth data was weak. This significant variation brings uncertainty when using combine harvester data and confirms the susceptibility to deviations that have already been discussed in several studies (ARSLAN AND COLVIN 2002; SIMBAHAN ET AL. 2004; NOACK 2006; BACHMAIER 2007). Above all, sensor errors, operating errors, and errors due to operating conditions and in data processing are mentioned as the main factors for inaccurate data. However, many of these can be avoided through further developments by combine harvester manufacturers and intensive driver training. Only errors due to changing operating conditions such as different material moisture levels, abrupt changes in speed, and grain plants lying on the ground will continue to influence the precision of combine harvester data in the future and must be considered in data processing (STEINMAYR 2002; TOSCANO ET AL. 2019). However, uniformly maturing crop stands and the reduction of plants lying on the ground are strived by the farmer through appropriate crop management anyway, so that these factors should not generally influence the yield maps. If corresponding impairments occur due to adverse harvesting conditions, these maps can still be sorted out through targeted data management, so they are not considered when creating yield potential maps for fertilization. In principle, however, it is possible to use combine harvester yield sensors to record the absolute wheat yield during harvesting, as shown by the results from 2018 and 2021 and by HAUSER ET AL. (2021) (R^2 = 0.70) and MITTERMAYER ET AL. (2021) (R^2 = 0.66). Technological advances such as John Deere's Active Yield also help to improve combine harvester data, as evidenced by the clear difference in the precision of the data between 2020 (R^2 = 0.30) and 2021 (R^2 = 0.72). A John Deere S780 combine harvester was used in both years under identical conditions (driver, calibration, model, working width, etc.) with the only difference being that Active Yield was installed in 2021 as additional equipment (JOHN DEERE 2019; STETTMER ET AL. 2022b). However, to be able to confirm this assumption, further manufacturer-independent investigations with ground truth data on yield sensors in combine harvesters are urgently needed.

5.2.2 Nitrogen uptake data

The absolute nitrogen uptake was investigated in the field trials for four characteristic growth stages that are relevant for nitrogen fertilization. The two early dates BBCH 31 and BBCH 39 are particularly important for promoting the yield, while nitrogen fertilization at the two

later dates BBCH 55 and BBCH 65 primarily influences the level of crude protein content and is therefore decisive for the quality of the wheat (MAIDL ET AL. 1998; MOHAMMED ET AL. 2013; DICK ET AL. 2016). Therefore, the highest precision of the digital measurement methods is required, especially during these growth stages, to avoid environmentally harmful influences on the agroecosystems through nitrogen losses. Table 11 shows the nitrogen uptake determined with different digital methods for the respective growth stages.

Table 11: Nitrogen uptake determined in this study based on different digital methods

Method	Year	BBCH	Unit	Minimum N uptake	Maximum N uptake	Average N uptake
Biomass samples	2020	31	kg N ha^{-1}	33.2	64.1	50.2
Satellite data	2020	31	kg N ha^{-1}	23.3	35.8	30.4
Sensor data	2020	31	kg N ha^{-1}	24.6	66.2	42.7
Biomass samples	2020	39	kg N ha^{-1}	109.2	125.2	118.2
Satellite data	2020	39	kg N ha^{-1}	84.9	141.6	116.9
Sensor data	2020	39	kg N ha^{-1}	68.8	169.1	124.1
Biomass samples	2020	55	kg N ha^{-1}	167.1	199.5	186.8
Satellite data	2020	55	kg N ha^{-1}	121.6	163.0	144.9
Sensor data	2020	55	kg N ha^{-1}	143.5	247.3	203.6
Biomass samples	2020	65	kg N ha^{-1}	211.8	235.2	225.5
Satellite data	2020	65	kg N ha^{-1}	164.1	188.3	178.1
Sensor data	2020	65	kg N ha^{-1}	166.9	320.2	248.5
Biomass samples	2021	31	kg N ha^{-1}	29.4	63.0	45.2
Satellite data	2021	31	kg N ha^{-1}	33.8	47.6	40.8
Sensor data	2021	31	kg N ha^{-1}	23.5	62.1	43.9
Biomass samples	2021	39	kg N ha^{-1}	124.1	195.8	144.3
Satellite data	2021	39	kg N ha^{-1}	100.8	161.0	123.4
Sensor data	2021	39	kg N ha^{-1}	103.8	217.5	143.0
Biomass samples	2021	55	kg N ha^{-1}	142.6	225.9	192.3
Satellite data	2021	55	kg N ha^{-1}	146.4	202.8	170.0
Sensor data	2021	55	kg N ha^{-1}	118.3	275.7	199.9
Biomass samples	2021	65	kg N ha^{-1}	182.4	260.8	218.3
Satellite data	2021	65	kg N ha^{-1}	140.8	225.5	183.4
Sensor data	2021	65	kg N ha^{-1}	147.2	308.5	232.1

The results show that both the satellite-based and sensor-based approaches are able to map the absolute nitrogen uptake of winter wheat at characteristically important growth stages. Only in 2020 did both methods in BBCH 31 show clearer deviations, which can be explained by a pronounced early summer drought. In 2020, at the time of the measurements in BBCH 31, it was far too dry, so the wheat plants suffered from drought stress. Drought stress, plant diseases, soil compaction, and deficiencies in other nutrients influence the reflection signature in sensor- or satellite-based reflection measurements, so incorrectly interpreted measured values can occur as a result (FRANKE AND MENZ 2007; WANG ET AL. 2011). The spatial distribution of the nitrogen uptake was moderately-to-well mapped with both methods over both test years, as the examination of the correlative relationships to the ground truth data shows (R^2 = 0.57–0.83) (Table 12).

Table 12: Nitrogen uptake calculated by digital technologies in relation to the ground truth data

R^2 (linear)	Year	BBCH	Sensor	Satellite
Biomass samples	2020	31	0.74	0.60
Biomass samples	2020	39	0.83	0.80
Biomass samples	2020	55	0.77	0.74
Biomass samples	2020	65	0.67	0.67
Biomass samples	2021	31	0.66	0.48
Biomass samples	2021	39	0.76	0.57
Biomass samples	2021	55	0.72	0.63
Biomass samples	2021	65	0.65	0.59

In BBCH 31, a weak correlation (R^2 = 0.48) with the satellite data was obtained only in 2021, which can also be explained by external influences. At the time of the measurements in BBCH 31, cloudy and rainy weather was predominant over a longer period. As a result, this weak correlation highlights the impact of one of the main disadvantages of satellite data, namely its dependence on cloud-free satellite images. In the absence of current satellite images, the nitrogen uptake is estimated based on older images, which can lead to discrepancies. Due to the ever-shorter intervals until the satellites fly over again with the simultaneous higher spatial resolution (3 x 3 m) of new agricultural satellite systems, the impact of this disadvantage is becoming less and less (WEIS 2019; PLANET 2022). Overall, both the sensor- and satellite-data-based approaches are well suited to recording the absolute nitrogen uptake and deriving the nitrogen fertilization using algorithms. This conclusion was

also reached in other studies that determined the correlative relationships between the nitrogen uptake and various vegetation indices based on sensor data and achieved precise results with the REIP ($R^2 = 0.59$–0.90), which is also used in the algorithms of MAIDL (2011) (PREY AND SCHMIDHALTER 2019; WESTERMEIER AND MAIDL 2019; MITTERMAYER ET AL. 2021). Other studies also obtained good results with reflection-optical sensor measurements ($R^2 = 0.57$–0.89) (CAO ET AL. 2015; PAVULURI ET AL. 2015; CAO ET AL. 2018). CHEN (2015) calculated correlations between remote sensing data and the nitrogen uptake of winter wheat at different growth stages and found a strong correlation ($R^2 = 0.86$). JIA ET AL. (2011) and MAGNEY ET AL. (2017) were also able to generate precise results with satellite data ($R^2 = 0.74$–0.81).

Ultimately, both measurement methods have their advantages and disadvantages, which MUÑOZ-HUERTA ET AL. (2013) and WECKESSER ET AL. (2021) also compared; both approaches showed potential in this study. Especially against the backdrop of the already mentioned developments regarding agricultural satellite data, it can be said that satellite data will greatly enrich practical agriculture in the future.

5.3 Conclusions and outlook

The correct delineation of yield zones and the exact recording of the nitrogen uptake are the two basic requirements for site-specific nitrogen fertilization in winter wheat cultivation. The results of these investigations show that site-specific agricultural technology can provide very precise data and reveal great potential for practice. Absolute yield potential maps can be generated well with sensor and combine harvester data, but the combine harvester data are prone to uncertainty. Therefore, in the future, the various yield recording systems in combine harvesters should be examined across manufacturers at several locations and in different crops to reduce the level of uncertainty in combine harvester data in the future. This would be very important in practice since modern combine harvesters are usually equipped with yield sensors and the corresponding technology, so yield maps could be generated very easily during harvesting. Furthermore, the results show that good relative zone maps can be generated with satellite data, but the plant growth model PROMET reveals problems in modeling the absolute yield height when weather extremes occur. At this point, further investigations should be carried out urgently to concretely provide an answer to this assumption. This would be a significant development as satellite data, available free of charge, are used more and more on farms; therefore, the validation of such applications is of

great importance. Furthermore, the tested digital methods for yield recording can not only function as a database for site-specific nitrogen fertilization but are also very interesting for other areas of application. For example, for the installation of tree strips, flower strips, or agroforestry systems, long-term low-yield areas can be identified, or soil investigations can be planned afterwards. This area of application is very interesting for both conventional and organic farms. The recording of the current nitrogen uptake is easily possible based on both sensor and satellite data, as the results of these investigations show. Both approaches have advantages and disadvantages, which must be weighted differently depending on the size and type of the farm. Future investigations should deal with a higher spatial resolution of satellite data (e.g., 3 x 3 m) and other wavelengths in optical reflection measurements to improve and further develop vegetation indices. In addition to winter wheat, evaluations should also take place in other important arable crops. Another future research field should be the application of remote sensing data to reduce the use of pesticides.

In summary, based on the results of this work, it can be said that the methods examined could open up numerous scientific and practical applications that would help to better harmonize successful arable farming with environmental protection. The foreseeable improvement in the performance of digital technologies and the availability of digital data justify further scientific investigations in this research field.

6 References

Argento, F., Anken, T., Abt, F., Vogelsanger, E., Walter, A., Liebisch, F. (2021): Site-specific nitrogen management in winter wheat supported by low-altitude remote sensing and soil data. *Precision Agriculture* 22(2), 364–386.

Arslan, S., Inanc, F., Gray, J. N., Colvin, T. S. (2000): Grain flow measurements with X-ray techniques. *Computers and electronics in agriculture* 26(1), 65–80.

Arslan, S., Colvin, T. S. (2002): Grain yield mapping: Yield sensing, yield reconstruction, and errors. *Precision Agriculture* 3(2), 135–154.

Auernhammer, H. (2001): Precision farming—the environmental challenge. *Computers and electronics in agriculture* 30(1–3), 31–43.

Bachmaier, M. (2007): Using a robust variogram to find an adequate butterfly neighborhood size for one-step yield mapping using robust fitting paraboloid cones. *Precision Agriculture* 8(1), 75–93.

Berg, J. (2020): Detektion der Biomassebildung und der Stickstoffaufnahme von Mais mittels Reflexionsmessungen als Voraussetzung für eine teilflächenspezifische Stickstoffdüngung. Master-Thesis. Technische Universität München, Weihenstephan. Organic Agriculture and Agronomy.

Blackmore, S., Godwin, R. J., Fountas, S. (2003): The analysis of spatial and temporal trends in yield map data over six years. *Biosystems engineering* 84(4), 455–466.

Blasch, G., Li, Z., Taylor, J. A. (2020): Multi-temporal yield pattern analysis method for deriving yield zones in crop production systems. *Precision Agriculture* 21(6), 1263–1290.

Boogaard, H., Wolf, J., Supit, I., Niemeyer, S., van Ittersum, M. (2013): A regional implementation of WOFOST for calculating yield gaps of autumn-sown wheat across the European Union. *Field Crops Research* 143, 130–142.

Bundesministerium für Ernährung und Landwirtschaft (2021): Erntebericht 2021. Available online: https://www.bmel.de/SharedDocs/Downloads/DE/_Landwirtschaft/Pflanzenbau/Ernte-Bericht/ernte-2021.pdf?__blob=publicationFile&v=2 (accessed on 19 October 2022).

Bundessortenamt (2022): Beschreibende Sortenliste – Getreide, Mais, Öl- und Faserpflanzen, Leguminosen, Rüben, Zwischenfrüchte – 2022. Available online: https://www.bundessortenamt.de/bsa/media/Files/BSL/bsl_getreide_2022.pdf (accessed on 25 October 2022).

Cammarano, D., Fitzgerald, G. J., Casa, R., Basso, B. (2014): Assessing the robustness of vegetation indices to estimate wheat N in Mediterranean environments. *Remote Sensing* 6(4), 2827–2844.

Cao, Q., Cui, Z., Chen, X., Khosla, R., Dao, T. H., Miao, Y. (2012): Quantifying spatial variability of indigenous nitrogen supply for precision nitrogen management in small scale farming. *Precision Agriculture* 13(1), 45–61.

Cao, Q., Miao, Y., Feng, G., Gao, X., Li, F., Liu, B., Yue, S., Cheng, S., Ustin, S. L., Khosla, R. (2015): Active canopy sensing of winter wheat nitrogen status: An evaluation of two sensor systems. *Computers and Electronics in Agriculture* 112, 54–67.

Cao, Q., Miao, Y., Shen, J., Yuan, F., Cheng, S., Cui, Z. (2018): Evaluating two crop circle active canopy sensors for in-season diagnosis of winter wheat nitrogen status. *Agronomy* 8(10), 201.

6 References

Chen, P. (2015): A comparison of two approaches for estimating the wheat nitrogen nutrition index using remote sensing. *Remote Sensing* 7(4), 4527–4548.

Chung, S. O., Choi, M. C., Lee, K. H., Kim, Y. J., Hong, S. J., Li, M. (2016): Sensing technologies for grain crop yield monitoring systems: A review. *Journal of Biosystems Engineering* 41(4), 408–417.

Claas (2020): N-Spezial – Düngung auf den Punkt. Available online: https://www.claas.de/blueprint/servlet/resource/blob/2590046/bbda7d292e7a8b5810b7ef40 113378e2/trends-02-2020-pionier-data.pdf (accessed on 14 November 2022).

Cui, Z., Zhang, F., Chen, X., Dou, Z., Li, J. (2010): In-season nitrogen management strategy for winter wheat: Maximizing yields, minimizing environmental impact in an over-fertilization context. *Field crops research* 116(1–2), 140–146.

Dalgaard, T., Bienkowski, J. F., Bleeker, A., Dragosits, U., Drouet, J. L., Durand, P., Cellier, P. (2012): Farm nitrogen balances in six European landscapes as an indicator for nitrogen losses and basis for improved management. *Biogeosciences* 9(12), 5303–5321.

Dataväxt (2022): CropSat. Available online: https://cropsat.com/ (accessed on 14 November 2022).

Demmel, M. (2001): Ertragsermittlung im Mähdrescher – Ertragsmessgeräte für die lokale Ertragsermittlung. Available online: https://www.dlg.org/fileadmin/downloads/landwirtschaft/themen/publikationen/merkblaett er/dlg-merkblatt_303.pdf (accessed on 16 November 2022).

Demmel, M. (2013): Site-specific recording of yields. In *Precision in Crop Farming* (pp. 313–329). Springer, Dordrecht, Netherlands.

Diacono, M., Castrignanò, A., Troccoli, A., De Benedetto, D., Basso, B., Rubino, P. (2012): Spatial and temporal variability of wheat grain yield and quality in a Mediterranean environment: A multivariate geostatistical approach. *Field Crops Research* 131, 49–62.

Diacono, M., Rubino, P., Montemurro, F. (2013): Precision nitrogen management of wheat. A review. *Agronomy for Sustainable Development* 33(1), 219–241.

Dick, C. D., Thompson, N. M., Epplin, F. M., & Arnall, D. B. (2016): Managing late-season foliar nitrogen fertilization to increase grain protein for winter wheat. *Agronomy Journal* 108(6), 2329–2338.

Döös, B. R. (2002): Population growth and loss of arable land. *Global Environmental Change* 12(4), 303–311.

Dowell, F. E., Maghirang, E. B., Xie, F. E. N. G., Lookhart, G. L., Pierce, R. O., Seabourn, B. W., Bean, S. R., Wilson, J. D., Chung, O. K. (2006): Predicting wheat quality characteristics and functionality using near-infrared spectroscopy. *Cereal chemistry* 83(5), 529–536.

Ebertseder, T., Gutser, R., Hege, U., Brandhuber, R., Schmidhalter, U. (2003): Strategies for site-specific nitrogen fertilization with respect to long-term environmental demands. In *Proc. Fourth European Conf. on Precision Agriculture, Berlin* (pp. 193–198).

Ehlert, D., Hammen, V., Adamek, R. (2003): On-line sensor pendulum-meter for determination of plant mass. *Precision agriculture* 4(2), 139–148.

Erdle, K., Mistele, B., Schmidhalter, U. (2011): Comparison of active and passive spectral sensors in discriminating biomass parameters and nitrogen status in wheat cultivars. *Field Crops Research* 124(1), 74–84.

Erekul, O., Ellmer, F., Köhn, W., Öncan, F. (2005): Einfluss differenzierter Stickstoffdüngung auf Kornertrag und Backqualität von Winterweizen:(Effect of different nitrogen fertilization on

yield and bread-making quality of winter wheat). *Archives of Agronomy and Soil Science* 51(5), 523–540.

Farid, H. U., Bakhsh, A., Ahmad, N., Ahmad, A., Mahmood-Khan, Z. (2016): Delineating site-specific management zones for precision agriculture. *The Journal of Agricultural Science* 154(2), 273–286.

FarmFacts (2022a): Site-specific fertilization. Available online: https://www.nextfarming.com/farmer/field/site-specific-fertilisation (accessed on 14 November 2022).

FarmFacts (2022b): NEXT GreenSeeker - Stickstoff-Sensor für die Landwirtschaft. Available online: https://www.nextfarming.de/hardware/stickstoff-sensor/next-greenseeker/ (accessed on 14 November 2022).

Franke, J., Menz, G. (2007): Multi-temporal wheat disease detection by multi-spectral remote sensing. *Precision Agriculture* 8(3), 161–172.

Fritzmeier (2021): ISARIA. Available online: https://isaria-digitalfarming.com/wp-content/uploads/2021/07/DV_Isaria_ISARIA-PRO-Active-Spray_Broschuere_2021.pdf (accessed on 14 November 2022).

Frogbrook, Z. L., Oliver, M. A. (2007): Identifying management zones in agricultural fields using spatially constrained classification of soil and ancillary data. *Soil Use and Management* 23(1), 40–51.

Fulton, J., Hawkins, E., Taylor, R., Franzen, A. (2018): Yield monitoring and mapping. *Precision agriculture basics* 63–77.

Gabriel, D., Pfitzner, C., Haase, N. U., Hüsken, A., Prüfer, H., Greef, J. M., Rühl, G. (2017): New strategies for a reliable assessment of baking quality of wheat–Rethinking the current indicator protein content. *Journal of cereal science* 77, 126–134.

Gaj, R., Górski, D., Przybyl, J. (2013): Effect of differentiated phosphorus and potassium fertilization on winter wheat yield and quality. *Journal of Elementology* 18(1).

Gandorfer, M. (2006): Bewertung von Precision Farming dargestellt am Beispiel der teilflächenspezifischen Stickstoffdüngung (Evaluation of Precision Farming illustrated using Site-Specific Nitrogen Fertilization as an Example). Doctoral dissertation. Technische Universität München, Weihenstephan. Chair of Agricultural Economics.

Gavioli, A., de Souza, E. G., Bazzi, C. L., Guedes, L. P. C., Schenatto, K. (2016): Optimization of management zone delineation by using spatial principal components. *Computers and Electronics in Agriculture* 127, 302–310.

Gu, B., Ge, Y., Chang, S. X., Luo, W., Chang, J. (2013): Nitrate in groundwater of China: Sources and driving forces. *Global Environmental Change* 23(5), 1112–1121.

Guastaferro, F., Castrignanò, A., De Benedetto, D., Sollitto, D., Troccoli, A., Cafarelli, B. (2010): A comparison of different algorithms for the delineation of management zones. *Precision agriculture* 11(6), 600–620.

Hadjimitsis, D. G., Papadavid, G., Agapiou, A., Themistocleous, K., Hadjimitsis, M. G., Retalis, A., Michaelides, S., Chrysoulakis, N., Toulios, L., Clayton, C. R. I. (2010): Atmospheric correction for satellite remotely sensed data intended for agricultural applications: impact on vegetation indices. *Natural Hazards and Earth System Sciences* 10(1), 89–95.

Hank, T. B., Bach, H., Mauser, W. (2015): Using a remote sensing-supported hydro-agroecological model for field-scale simulation of heterogeneous crop growth and yield: Application for wheat in central Europe. *Remote Sensing* 7(4), 3934–3965.

Hauser, J., Maidl, F. X., Wagner, P. (2021): Untersuchung der teilflächenspezifischen Ertragserfassung von Großmähdreschern in Winterweizen (Investigation of site-specific yield mapping of combine harvesters in winter wheat). In *Proceedings of the 41st GIL-Jahrestagung*, *Potsdam, Germany* (pp. 133–138).

Hawkesford, M. J. (2014): Reducing the reliance on nitrogen fertilizer for wheat production. *Journal of cereal science* 59(3), 276–283.

Heijting, S., De Bruin, S., Bregt, A. K. (2011): The arable farmer as the assessor of within-field soil variation. *Precision Agriculture* 12(4), 488–507.

Heil, K., Schmidhalter, U. (2017): Improved evaluation of field experiments by accounting for inherent soil variability. *European Journal of Agronomy* 89, 1–15.

Hoffland, E., Dicke, M., Van Tintelen, W., Dijkman, H., Van Beusichem, M. L. (2000): Nitrogen availability and defense of tomato against two-spotted spider mite. *Journal of Chemical Ecology* 26(12), 2697–2711.

Huang, T., Ju, X., Yang, H. (2017): Nitrate leaching in a winter wheat-summer maize rotation on a calcareous soil as affected by nitrogen and straw management. *Scientific Reports* 7(1), 1–11.

Hülsbergen, K. J., Maidl, F. X., Forster, F., Prücklmaier, J. (2017): Minderung von Nitrataustägen in Trinkwassereinzugsgebieten durch optimiertes Stickstoffmanagement am Beispiel der Gemeinde Hohenthann (Niederbayern) mit intensiver landwirtschaftlicher Flächennutzung (Reduction of nitrate emissions in drinking water catchment areas through optimized nitrogen management). Forschungsbericht an das Bayerische Staatsministerium für Ernährung, Landwirtschaft und Forsten, Technische Universität München. Available online: https://www.lfu.bayern.de/wasser/gw_gefaehrdung_schutz/gwschutz_landwirtschaft/projekte_hohenthann/doc/tum_bericht_hohenthann.pdf (accessed on 27 October 2022).

Hülsbergen, K. J., Maidl, F. X., Mittermayer, M., Weng, J., Kern, A., Leßke, F., Gilg, A. (2020): Digital Basiertes Stickstoffmanagement in Landwirtschaftlichen Betrieben–Emissionsminderung durch Optimierte Stickstoffkreisläufe und Sensorgestützte Teilflächenspezifische Düngung (Digitally Based Nitrogen Management in Agricultural Farms–Emission Reduction through Optimized Nitrogen Cycles and Sensor Based Site-Specific Fertilization). Forschungsbericht an Deutsche Bundesstiftung Umwelt, Technische Universität München. Available online: https://www.dbu.de/projekt_30743/01_db_2848.html (accessed on 25 October 2022).

Hunt, M. L., Blackburn, G. A., Carrasco, L., Redhead, J. W., Rowland, C. S. (2019): High resolution wheat yield mapping using Sentinel-2. *Remote Sensing of Environment* 233, 111410.

Igrejas, G., Branland, G. (2020): The importance of wheat. In *Wheat quality for improving processing and human health* (pp. 1–7). Springer, Cham, Germany.

Jia, L., Yu, Z., Li, F., Gnyp, M., Koppe, W., Bareth, G., Miao, Y., Chen, X., Zhang, F. (2011): Nitrogen status estimation of winter wheat by using an Ikonos satellite image in the north china plain. In *International Conference on Computer and Computing Technologies in Agriculture* (pp. 174–184). Springer, Berlin, Heidelberg, Germany.

Jin, Z., Azzari, G., Lobell, D. B. (2017): Improving the accuracy of satellite-based high-resolution yield estimation: A test of multiple scalable approaches. *Agricultural and forest meteorology* 247, 207–220.

6 References
_____

John Deere (2019): Active Yield – Betrieb und Einstellung. Available online: https://www.deere.de/assets/docs/region-2/parts-and-service/manuals-and-training/combines/s-series/Active-Yield-DE.pdf (accessed on 16 November 2022).

Kaivosoja, J., Näsi, R., Hakala, T., Viljanen, N., Honkavaara, E. (2017): Different remote sensing data in relative biomass determination and in precision fertilization task generation for cereal crops. In *Proceedings of the 8th International Conference on Information and Communication Technologies in Agriculture, Food & Environment, Chania, Greece,* (pp. 164–176).

Karpinski, I., Schuler, J., Müller, K. (2015): A new approach to support site-specific farming and economic decision making for precision agriculture in East Germany: The heterogeneity indicator. *Outlook on AGRICULTURE* 44(4), 283–289.

Kormann, G., Demmel, M., Auernhammer, H. (1998): Testing stand for yield measurement systems in combine harvesters. In *Proceedings of the ASAE Annual International Conference, Coronado Springs Resort, Orlando, FL, USA* (Paper No. 98 31 02).

Koszinski, S., Wendroth, O., Lehfeldt, J. (1995): Field scale heterogeneity of soil structural properties in a moraine landscape of north-eastern Germany. *International agrophysics* 9(3).

Kucke, M., Kleeberg, P. (1997): Nitrogen balance and soil nitrogen dynamics in two areas with different soil, climatic and cropping conditions. *European Journal of Agronomy* 6(1–2), 89–100.

Küstermann, B., Christen, O., Hülsbergen, K. J. (2010): Modelling nitrogen cycles of farming systems as basis of site-and farm-specific nitrogen management. *Agriculture, ecosystems & environment* 135(1–2), 70–80.

Landesamt für Digitalisierung, Breitband und Vermessung (2022): Bodenschätzung – Bewertung der natürlichen Ertragsfähigkeit landwirtschaftlicher Flächen. Available online: https://www.ldbv.bayern.de/produkte/kataster/boden.html#:~{}:text=Unter%20Bodensch%C3%A4tzung%20versteht%20man%20die,in%20Acker%2D%20und%20Gr%C3%BCnland%20unterteilt (accessed on 29 November 2022).

Li, F., Miao, Y., Hennig, S. D., Gnyp, M. L., Chen, X., Jia, L., Bareth, G. (2010): Evaluating hyperspectral vegetation indices for estimating nitrogen concentration of winter wheat at different growth stages. *Precision Agriculture* 11(4), 335–357.

Limbrunner, B., Maidl, F. X. (2006): Ermittlung des optimalen Stickstoff-Versorgungszustands bei Winterweizen (Triticum aestivum) mittels Laser-induzierter Chlorophyll-Fluoreszenz. In *Mitteilungen der Gesellschaft für Pflanzenbauwissenschaften 18* (pp. 294–295).

Liu, G., Zhang, L., Zhang, Q., Musyimi, Z. (2015): The response of grain production to changes in quantity and quality of cropland in Yangtze River Delta, China. *Journal of the Science of Food and Agriculture* 95(3), 480–489.

Liu, H., Whiting, M. L., Ustin, S. L., Zarco-Tejada, P. J., Huffman, T., Zhang, X. (2018): Maximizing the relationship of yield to site-specific management zones with object-oriented segmentation of hyperspectral images. *Precision agriculture* 19(2), 348–364.

Lopez-Lozano, R., Casterad, M. A., Herrero, J. (2010): Site-specific management units in a commercial maize plot delineated using very high resolution remote sensing and soil properties mapping. *Computers and Electronics in Agriculture* 73(2), 219–229.

Macholdt, J., Honermeier, B. (2017): Yield stability in winter wheat production: a survey on German farmers' and advisors' views. *Agronomy* 7(3), 45.

Magney, T. S., Eitel, J. U., Vierling, L. A. (2017): Mapping wheat nitrogen uptake from RapidEye vegetation indices. *Precision Agriculture* 18(4), 429–451.

Maidl, F. X., Sticksel, E., Retzer, F., Fischbeck, G. (1998): Effect of varied N-fertilization on yield formation of winter wheat under particular consideration of mainstems and tillers. *Journal of Agronomy and Crop Science* 180(1), 15–22.

Maidl, F. X., Brunner, R., Sticksel, E., Fischbeck, G. (1999): Ursachen kleinräumiger Ertragsschwankungen im bayerischen Tertiärhügelland und Folgerungen für eine teilschlagbezogene Düngung. *Journal of Plant Nutrition and Soil Science* 162(3), 337–342.

Maidl, F. X., Schächtl, J., Huber, G. (2004): Strategies for site-specific nitrogen fertilization on winter wheat. In *Proceedings of the 7th International Conference on Precision Agriculture and Other Precision Resources Management, Hyatt Regency, Minneapolis, MN, USA* (pp. 1938–1948). Precision Agriculture Center, Minnesota, USA.

Maidl, F. X. (2011): Verfahren zur Bestimmung des Düngebedarfs, Insbesondere des Stickstoff-Düngerbedarfs und Vorrichtung zur Durchführung des Verfahrens. Patentnr. DE 102011050877.

Maidl, F. X. (2016): Minderung von Nitrataust-trägen in Trinkwassereinzugsgebieten durch optimiertes Stickstoffmanagement. Available online: https://www.hef.tum.de/fileadmin/Veranstaltungen/2016/26_Oktober_Wasser/Vortrag_Maidl_26Okt_freigegeben.pdf (accessed on 14 November 2022).

Maidl, F. X., Spicker, A., Weng, J., Hülsbergen, K. J. (2019): Ableitung des teilflächenspezifischen Kornertrags von Getreide aus Reflexionsdaten (Derivation of the site-specific grain yield from reflection data). In *Proceedings of the 39th GIL-Jahrestagung, Wien, Austria* (pp. 131–134).

Mauser, W., Bach, H. (2009): PROMET–Large scale distributed hydrological modelling to study the impact of climate change on the water flows of mountain watersheds. *Journal of Hydrology* 376(3–4), 362–377.

Meyer, D., Kolbe, H. (2021): Improvement of Nitrogen-Fertilizer Recommendation by Consideration of Long-Term Site and Cultivation Effected Mineralization. *Agronomy* 11(12), 2492.

Migdall, S., Bach, H., Bobert, J., Wehrhan, M., Mauser, W. (2009): Inversion of a canopy reflectance model using hyperspectral imagery for monitoring wheat growth and estimating yield. *Precision Agriculture* 10(6), 508–524.

Mittermayer, M., Gilg, A., Maidl, F. X., Nätscher, L., Hülsbergen, K. J. (2021): Site-specific nitrogen balances based on spatially variable soil and plant properties. *Precision Agriculture* 22(5), 1416–1436.

Mittermayer, M., Maidl, F. X., Nätscher, L., Hülsbergen, K. J. (2022): Analysis of site-specific N balances in heterogeneous croplands using digital methods. *European Journal of Agronomy* 133, 126442.

Mittermayer, M. (2022): Analysis of site-specific N balances using digital methods in heterogeneous croplands in southern Germany. Doctoral dissertation. Technische Universität München, Weihenstephan. Organic Agriculture and Agronomy.

Mohammed, Y. A., Kelly, J., Chim, B. K., Rutto, E., Waldschmidt, K., Mullock, J., Torres, G., Desta, K. G., Raun, W. (2013): Nitrogen fertilizer management for improved grain quality and yield in winter wheat in Oklahoma. *Journal of plant nutrition* 36(5), 749–761.

Mulla, D. J. (2013): Twenty five years of remote sensing in precision agriculture: Key advances and remaining knowledge gaps. *Biosystems engineering* 114(4), 358–371.

Muñoz-Huerta, R. F., Guevara-Gonzalez, R. G., Contreras-Medina, L. M., Torres-Pacheco, I., Prado-Olivarez, J., Ocampo-Velazquez, R. V. (2013): A review of methods for sensing the nitrogen status in plants: advantages, disadvantages and recent advances. *Sensors* 13(8), 10823–10843.

Noack, P.O. (2006): Entwicklung fahrspurbasierter Algorithmen zur Korrektur von Ertragsdaten im Precision Farming (Development of Lane-Based Algorithms for the Correction of Yield Data in Precision Farming). Doctoral dissertation. Technische Universität München, Weihenstephan. Agricultural Systems Engineering.

Noack, P. O. (2007): Ertragskartierung im Getreidebau. In: *KTBL-Heft* (70). KTBL, Darmstadt, Germany.

Ostermeier, R., Rogge, H. I., Auernhammer, H. (2007): Multisensor data fusion implementation for a sensor based fertilizer application system. *Agricultural Engineering International: CIGR Journal* 9, 1–13.

Öttl, S., Sixt, T. (2021): Ertragserfassung am Mähdrescher im Vergleich zu sensor- und satellitengestützten Systemen. Wissenschaftliche Arbeit im Rahmen des Masterstudiengangs Agrarsystemwissenschaften, Modul Projekt Agrarsysteme. Technische Universität München, Weihenstephan. Organic Agriculture and Agronomy.

Patzold, S., Mertens, F. M., Bornemann, L., Koleczek, B., Franke, J., Feilhauer, H., Welp, G. (2008): Soil heterogeneity at the field scale: a challenge for precision crop protection. *Precision Agriculture* 9(6), 367–390.

Pavuluri, K., Chim, B. K., Griffey, C. A., Reiter, M. S., Balota, M., Thomason, W. E. (2015): Canopy spectral reflectance can predict grain nitrogen use efficiency in soft red winter wheat. *Precision agriculture* 16(4), 405–424.

Peralta, N. R., Costa, J. L., Balzarini, M., Franco, M. C., Córdoba, M., Bullock, D. (2015): Delineation of management zones to improve nitrogen management of wheat. *Computers and Electronics in Agriculture* 110, 103–113.

Perez-Munoz, F., Colvin, T. S. (1996): Continuous grain yield monitoring. *Transactions of the ASAE* 39(3), 775–783.

Pfeiffer, D. W., Hummel, J. W., Miller, N. R. (1993): Real-time corn yield sensor. In *Summer meeting of the American Society of Agricultural Engineers, Spokane, WA, USA* (Paper No. 93 10 13).

Pfleger, F. (2015): Charakterisierung von Weizensorten hinsichtlich ihrer Eignung in der bäckereitechnischen Anwendung aus der Sicht eines Mühlenunternehmens. Bachelor-Thesis. Hochschule für angewandte Wissenschaften Hamburg. Department of Ecotrophology.

Planet (2022): PlanetScope. Available online: https://docs.sentinel-hub.com/api/latest/data/planet/planet-scope/ (accessed on 20 November 2022).

Prey, L., Schmidhalter, U. (2019): Sensitivity of Vegetation Indices for Estimating Vegetative N Status in Winter Wheat. *Sensors* 19(17), 3712.

Prücklmaier, J. (2020): Feldexperimentelle Analysen zur Ertragsbildung und Stickstoffeffizienz bei organisch-mineralischer Düngung auf heterogenen Standorten und Möglichkeiten zur Effizienzsteigerung durch computer- und sensorgestützte Düngesysteme (Field Experimental Analyses of Yield Effects and Nitrogen Efficiency of Fertilizer Application

Systems). Doctoral dissertation. Technische Universität München, Weihenstephan. Organic Agriculture and Agronomy.

Quemada, M., Baranski, M., Nobel-de Lange, M. N. J., Vallejo, A., Cooper, J. M. (2013): Meta-analysis of strategies to control nitrate leaching in irrigated agricultural systems and their effects on crop yield. *Agriculture, ecosystems & environment* 174, 1–10.

Reckleben, Y. (2014): Sensoren für die Stickstoffdüngung—Erfahrungen in 12 Jahren praktischem Einsatz. *Journal für Kulturpflanzen* 66(2), 42–47.

Reinke, R., Dankowicz, H., Phelan, J., Kang, W. (2011): A dynamic grain flow model for a mass flow yield sensor on a combine. *Precision Agriculture* 12(5), 732–749.

Reyniers, M., Vrindts, E., De Baerdemaeker, J. (2006): Comparison of an aerial-based system and an on the ground continuous measuring device to predict yield of winter wheat. *European Journal of Agronomy* 24(2), 87–94.

Robertson, M. J., Lyle, G., Bowden, J. W. (2008): Within-field variability of wheat yield and economic implications for spatially variable nutrient management. *Field Crops Research* 105(3), 211–220.

Roßkopf, N., Fell, H., Zeitz, J. (2015): Organic soils in Germany, their distribution and carbon stocks. *Catena* 133, 157–170.

Saint-Denis, T., Goupy, J. (2004): Optimization of a nitrogen analyser based on the Dumas method. *Analytica Chimica Acta* 515(1), 191–198.

Saleh, A., Belal, A. (2014): Delineation of site-specific management zones by fuzzy clustering of soil and topographic attributes: A case study of East Nile Delta, Egypt. In *IOP Conference Series: Earth and Environmental Science* (Vol. 18, No. 1, p. 012046). IOP Publishing, Kuching, Malaysia.

Schächtl, J. (2004): Sensorgestützte Bonitur von Aufwuchs und Stickstoffversorgung bei Weizen- und Kartoffelbeständen (Sensor-based determination of biomass growth and nitrogen uptake in wheat and potato stocks). Doctoral dissertation. Technische Universität München, Weihenstephan. Organic Agriculture and Agronomy.

Schächtl, J., Huber, G., Maidl, F. X., Sticksel, E., Schulz, J., Haschberger, P. (2005): Laser-induced chlorophyll fluorescence measurements for detecting the nitrogen status of wheat (Triticum aestivum L.) canopies. *Precision Agriculture* 6(2), 143–156.

Schmidhalter, U., Maidl, F. X., Heuwinkel, H., Demmel, M., Auernhammer, H., Noack, P. O., Rothmund, M. (2008): Precision farming–adaptation of land use management to small scale heterogeneity. In *Perspectives for agroecosystem management* (pp. 121–199). Elsevier, Amsterdam, Netherlands.

Schmidhalter, U. (2014): Sensorgestützte Ermittlung des Nährstoffbedarfs. *VDLUFA-Schriftenreihe* 70, 57–66.

Schröer, D., Buhk, J. H., Latacz-Lohmann, U. (2022): Betriebswirtschaftliche Auswirkungen der Düngeverordnung 2020: Erwerbsverlustkalkulationen und Prüfung auf Existenzgefährdung für fünf bayrische Betriebe. *Berichte über Landwirtschaft-Zeitschrift für Agrarpolitik und Landwirtschaft*. Available online: https://www.buel.bmel.de/index.php/buel/article/view/383/613 (accessed on 26 October 2022).

Schuster, J., Mittermayer, M., Maidl, F. X., Nätscher, L., Hülsbergen, K. J. (2022): Spatial variability of soil properties, nitrogen balance and nitrate leaching using digital methods on heterogeneous arable fields in southern Germany. *Precision Agriculture,* 1–30.

Servadio, P., Bergonzoli, S., Verotti, M. (2017): Delineation of management zones based on soil mechanical-chemical properties to apply variable rates of inputs throughout a field (VRA). *Engineering in agriculture, environment and food* 10(1), 20–30.

Simbahan, G. C., Dobermann, A., Ping, J. L. (2004): Screening yield monitor data improves grain yield maps. *Agronomy Journal* 96(4), 1091–1102.

Sinfield, J. V., Fagerman, D., Colic, O. (2010): Evaluation of sensing technologies for on-the-go detection of macro-nutrients in cultivated soils. *Computers and Electronics in Agriculture* 70(1), 1–18.

Skudra, I., Linina, A. (2011): The influence of meteorological conditions and nitrogen fertilizer on wheat grain yield and quality. In *6th Baltic Conference on Food Science and Technology: Innovations for Food Science and Production, FOODBALT-2011-Conference Proceedings*, 23–26.

Song, X., Wang, J., Huang, W., Liu, L., Yan, G., Pu, R. (2009): The delineation of agricultural management zones with high resolution remotely sensed data. *Precision agriculture* 10(6), 471–487.

Song, Y., Wang, J., Shang, J., Liao, C. (2020): Using UAV-based SOPC derived LAI and SAFY model for biomass and yield estimation of winter wheat. *Remote Sensing* 12(15), 2378.

Spicker, A.B. (2016): Entwicklung von Verfahren der teilflächenspezifischen Stickstoffdüngung zu Wintergerste (Hordeum vulgare L.) und Winterraps (Brassica napus L.) auf Grundlage Reflexionsoptischer Messungen (Development of Sensor-Based Nitrogen Fertilization Systems for Oilseed Rape (Brassica napus L.) and winter barley (Hordeum vulgare L.)). Doctoral dissertation. Technische Universität München, Weihenstephan. Organic Agriculture and Agronomy.

Stamatiadis, S., Schepers, J. S., Evangelou, E., Tsadilas, C., Glampedakis, A., Glampedakis, M., Dercas, N., Spyropoulos, N., Dalezios, N. R., Eskridge, K. (2018): Variable-rate nitrogen fertilization of winter wheat under high spatial resolution. *Precision Agriculture* 19(3), 570–587.

Statistisches Bundesamt (2022): Destatis - Wachstum und Ernte - Feldfrüchte 2021. Available online: https://www.destatis.de/DE/Themen/Branchen-Unternehmen/Landwirtschaft-Forstwirtschaft-Fischerei/Feldfruechte-Gruenland/Publikationen/Downloads-Feldfruechte/feldfruechte-jahr-2030321217164.pdf;jsessionid=782D75005809F0A555867381E127195E.live731?__blob=publicationFile (accessed on 19 October 2022).

Steinmayr, T. (2002): Fehleranalyse und Fehlerkorrektur bei der lokalen Ertragsermittlung im Mähdrescher zur Ableitung eines Standardisierten Algorithmus für die Ertragskartierung (Error Analysis and Correction of Yield Recording in Combine Harvesters to Derive a Standardized Algorithm for Yield Mapping). Doctoral dissertation. Technische Universität München, Weihenstephan. Agricultural Systems Engineering.

Stettmer, M., Maidl, F. X., Schwarzensteiner, J., Hülsbergen, K. J., Bernhardt, H. (2022a): Analysis of Nitrogen Uptake in Winter Wheat Using Sensor and Satellite Data for Site-Specific Fertilization. *Agronomy* 12(6), 1455.

Stettmer, M., Mittermayer, M., Maidl, F. X., Schwarzensteiner, J., Hülsbergen, K. J., Bernhardt, H. (2022b): Three Methods of Site-Specific Yield Mapping as a Data Source for the Delineation of Management Zones in Winter Wheat. *Agriculture* 12(8), 1128.

Strebel, O., Duynisveld, W. H. M., Böttcher, J. (1989): Nitrate pollution of groundwater in western Europe. *Agriculture, ecosystems & environment* 26(3–4), 189–214.

Strubbe, G., Missotten, B., De Baerdemaeker, J. (1996): Performance evaluation of a three-dimensional optical volume flow meter. *Applied Engineering in Agriculture* 12(4), 403–409.

Svoboda, N., Strer, M., Hufnagel, J. (2015): Rainfed winter wheat cultivation in the North German Plain will be water limited under climate change until 2070. *Environmental Sciences Europe* 27(1), 1–7.

Tarkalson, D. D., Payero, J. O., Ensley, S. M., Shapiro, C. A. (2006): Nitrate accumulation and movement under deficit irrigation in soil receiving cattle manure and commercial fertilizer. *Agricultural water management* 85(1–2), 201–210.

Tec5 (2022): Spektrometer Systeme, Version 2.13. Available online: https://tec5.com/de/ (accessed on 08 December 2022).

Thorburn, P. J., Biggs, J. S., Weier, K. L., Keating, B. A. (2003): Nitrate in groundwaters of intensive agricultural areas in coastal Northeastern Australia. *Agriculture, ecosystems & environment* 94(1), 49–58.

Thoren, D., Schmidhalter, U. (2009): Nitrogen status and biomass determination of oilseed rape by laser-induced chlorophyll fluorescence. *European Journal of Agronomy* 30(3), 238–242.

Toscano, P., Castrignanò, A., Di Gennaro, S. F., Vonella, A. V., Ventrella, D., Matese, A. (2019): A precision agriculture approach for durum wheat yield assessment using remote sensing data and yield mapping. *Agronomy* 9(8), 437.

Tremblay, N., Fallon, E., Ziadi, N. (2011): Sensing of crop nitrogen status: Opportunities, tools, limitations, and supporting information requirements. *HortTechnology* 21(3), 274–281.

USDA Foreign Agricultural Service (2022a): Grain: World Markets and Trade. Available online: https://apps.fas.usda.gov/psdonline/circulars/grain.pdf (accessed on 19 October 2022).

USDA Foreign Agricultural Service (2022b): World Agricultural Production. Available online: https://apps.fas.usda.gov/psdonline/circulars/production.pdf (accessed on 19 October 2022).

Vallentin, C., Dobers, E. S., Itzerott, S., Kleinschmit, B., Spengler, D. (2020): Delineation of management zones with spatial data fusion and belief theory. *Precision Agriculture* 21(4), 802–830.

Verhoef, W., Bach, H. (2003): Simulation of hyperspectral and directional radiance images using coupled biophysical and atmospheric radiative transfer models. *Remote sensing of environment* 87(1), 23–41.

Verhoef, W., Bach, H. (2007): Coupled soil–leaf-canopy and atmosphere radiative transfer modeling to simulate hyperspectral multi-angular surface reflectance and TOA radiance data. *Remote Sensing of Environment* 109(2), 166–182.

Vinzent, B., Fuß, R., Maidl, F. X., Hülsbergen, K. J. (2017): Efficacy of agronomic strategies for mitigation of after-harvest N2O emissions of winter oilseed rape. *European Journal of Agronomy* 89, 88–96.

Wang, H., Ju, X., Wei, Y., Li, B., Zhao, L., Hu, K. (2010): Simulation of bromide and nitrate leaching under heavy rainfall and high-intensity irrigation rates in North China Plain. *Agricultural water management* 97(10), 1646–1654.

Wang, T. C., Ma, B. L., Xiong, Y. C., Saleem, M. F., Li, F. M. (2011): Optical sensing estimation of leaf nitrogen concentration in maize across a range of water-stress levels. *Crop and Pasture Science* 62(6), 474–480.

6 References

Wang, K., Huggins, D. R., Tao, H. (2019): Rapid mapping of winter wheat yield, protein, and nitrogen uptake using remote and proximal sensing. *International Journal of Applied Earth Observation and Geoinformation* 82, 101921.

Weckesser, F., Leßke, F., Luthardt, M., Hülsbergen, K. J. (2021): Conceptual Design of a Comprehensive Farm Nitrogen Management System. *Agronomy* 11(12), 2501.

Weis, M. (2019): Satellitendaten für die Landwirtschaft – Digitalisierung als Trend. Available online: https://lel.landwirtschaft-bw.de/pb/site/pbs-bw-mlr/get/documents_E1002901778/MLR.LEL/PB5Documents/lel/Abteilung_1/Landinfo/Landinfo_extern/2019/05_2019/pdf_einzeln/Weiss.pdf?attachment=true (accessed on 20 November 2022).

Welsh, J. P., Wood, G. A., Godwin, R. J., Taylor, J. C., Earl, R., Blackmore, S., Knight, S. M. (2003): Developing strategies for spatially variable nitrogen application in cereals, part II: wheat. *Biosystems Engineering* 84(4), 495–511.

Wendland, F., Bergmann, S., Eisele, M., Gömann, H., Herrmann, F., Kreins, P., Kunkel, R. (2020): Model-based analysis of nitrate concentration in the leachate—The North Rhine-Westfalia case study, Germany. *Water* 12(2), 550.

Westermeier, M., Maidl, F. X. (2019): Comparison of spectral indices to detect nitrogen uptake in winter wheat. *Journal für Kulturpflanzen* 71(8/9), 238–248.

Whelan, B. (2018): Site-specific crop management. In *Pedometrics* (pp. 597–622). Springer, Cham, Germany.

Wintersteiger (2022): Plot combine. Available online: https://www.wintersteiger.com/us/Plant-Breeding-and-Research/Products/Product-range/Plot-combine (accessed on 07 December 2022).

Wu, J., Wang, D., Bauer, M. E. (2005): Image-based atmospheric correction of QuickBird imagery of Minnesota cropland. *Remote Sensing of Environment* 99(3), 315–325.

Yara (2022): Atfarm. Available online: https://www.at.farm/de/ (accessed on 14 November 2022).

Zecevic, V., Knezevic, D., Boskovic, J., Micanovic, D., Dozet, G. (2010): Effect of nitrogen fertilization on winter wheat quality. *Cereal Research Communications* 38(2), 243–249.

Zhang, X., Davidson, E. A., Mauzerall, D. L., Searchinger, T. D., Dumas, P., Shen, Y. (2015): Managing nitrogen for sustainable development. *Nature* 528(7580), 51–59.

Zhang, X. (2017): A plan for efficient use of nitrogen fertilizers. *Nature* 543(7645), 322–323.

Zhao, Y., Potgieter, A. B., Zhang, M., Wu, B., Hammer, G. L. (2020): Predicting wheat yield at the field scale by combining high-resolution Sentinel-2 satellite imagery and crop modelling. *Remote Sensing* 12(6), 1024.

Zimmer, Y. (2016): Ranking: Spitzenweizenerträge der EU-Bauern. Available online: https://www.agrarheute.com/pflanze/getreide/ranking-spitzenweizenertraege-eu-bauern-519343 (accessed on 21 October 2022).

7 Eidesstattliche Erklärung

Hiermit erkläre ich an Eides statt, dass ich die vorliegende wissenschaftliche Arbeit selbstständig verfasst und keine anderen als die angegebenen Quellen und Hilfsmittel benutzt habe.

Mit dieser Arbeit wurden noch keine vergeblichen Promotionsversuche unternommen.

Des Weiteren erkenne ich, dass keine Strafverfahren gegen mich anhängig sind.

Waidholz, 23.03.2023

Matthias Johannes Stettmer

Appendix A – Curriculum vitae

Personal Details

Name   Matthias Johannes Stettmer
Date of Birth   July 04, 1994
Place of Birth   Bogen

Profession

Since 03/2020	**Research assistant,** OG Düngeoptimierung Niederbayern, Irlbach (Germany); Institute of Agricultural Systems Engineering, Technische Universität München, Freising (Germany)
03/2019 - 10/2019	**Farm Manager,** Landwirtschaftlicher Betrieb Christian Pentzlin, Weitendorf (Germany)
08/2018 - 10/2018	**Internship,** Wecker Farms Ltd., Sedley SK (Canada)
11/2017 - 07/2018	**Internship,** Farmtastic Consulting GmbH, Irlbach (Germany)
08/2017 - 10/2017	**Internship,** Agrar e.G. Hagemann, Groß Salitz (Germany)
03/2017 - 06/2017	**Internship,** AGCO GmbH, Marktoberdorf (Germany)
07/2016 - 09/2016	**Internship,** Agrar e.G. Hagemann, Groß Salitz (Germany)
08/2015 - 09/2015	**Internship,** ROPA Fahrzeug- und Maschinenbau GmbH, Herrngiersdorf (Germany)
08/2014 - 09/2014	**Internship,** Gut Derenburg, Derenburg (Germany)

University

03/2020 - 03/2023	**Ph.D.,** Institute of Agricultural Systems Engineering, Technische Universität München, Freising (Germany)
04/2017 - 02/2020	**M.Sc. in Agricultural Management,** Technische Universität München, Freising (Germany); Specialization: Arable Farming
10/2013 - 03/2017	**B.Sc. in Agricultural Sciences,** Technische Universität München, Freising (Germany)

School

09/2005 - 06/2013	**Abitur,** Veit-Höser-Gymnasium, Bogen (Germany)
09/2001 - 07/2005	**Elementary School,** Degernbach (Germany)

Appendix B – Publication reprints

The next pages show two reprints of the publications used in this thesis.

The publication "Analysis of nitrogen uptake in winter wheat using sensor and satellite data for site-specific fertilization" is open access (MDPI). No restrictions to reprint apply.

The publication "Three methods of site-specific yield mapping as a data source for the delineation of management zones in winter wheat" is open access (MDPI). No restrictions to reprint apply.

Article

Analysis of Nitrogen Uptake in Winter Wheat Using Sensor and Satellite Data for Site-Specific Fertilization

Matthias Stettmer [1,*] **, Franz-Xaver Maidl** [2] **, Jürgen Schwarzensteiner** [3] **, Kurt-Jürgen Hülsbergen** [2] **and Heinz Bernhardt** [1]

1 Agricultural Systems Engineering, TUM School of Life Sciences, Technical University of Munich, Dürnast 10, 85354 Freising, Germany; heinz.bernhardt@tum.de
2 Organic Agriculture and Agronomy, TUM School of Life Sciences, Technical University of Munich, Liesel-Beckmann-Straße 2, 85354 Freising, Germany; maidl@tum.de (F.-X.M.); kurt.juergen.huelsbergen@tum.de (K.-J.H.)
3 Farmtastic Consulting GmbH, Graf-von-Bray-Straße 14, 94342 Irlbach, Germany; js@farmtastic.consulting
* Correspondence: matthias.stettmer@tum.de

Abstract: Sensor- and satellite-based determination of nitrogen uptake provides critical data in site-specific fertilization algorithms. Therefore, two basic noncontact measurement methods (sensor and satellite) were investigated in winter wheat, and their precision was evaluated in this study. Nitrogen uptake at four characteristic growth stages (BBCH 31, BBCH 39, BBCH 55, and BBCH 65) was determined using algorithms based on sensor and satellite data. As a reference, nitrogen uptake was determined using biomass samples in the laboratory (ground truth data). The precision of the tested methods was evaluated using statistical indicators (mean, median, minimum, maximum, and standard deviation) and correlation analyses between the nitrogen uptake of the ground truth data and that of the respective method. The results showed moderate to strong correlations with the nitrogen uptake of the ground truth data for both methods ($R^2 = 0.57$–0.83). Both sensor and satellite data best represented nitrogen uptake in BBCH 39 and 55 ($R^2 = 0.63$–0.83). In sum, there were only slight deviations in the absolute amount of nitrogen uptake ($\leq \pm 15\%$). Clear deviations can be explained by external influences during measurement. Overall, the investigations showed that the nitrogen uptake could be appropriately determined as a data basis for site-specific fertilization systems using sensor and satellite data.

Keywords: nitrogen uptake; sensor data; satellite data; site-specific fertilization; winter wheat

1. Introduction

Harmonizing successful crop production with environmental protection is a key requirement of modern fertilization systems. A particular focus is placed on nitrogen (N) fertilization. Nitrogen uptake by wheat in the field can vary noticeably. Spatial variability of nitrogen uptake depends on numerous overlapping influencing factors and their interactions (edaphic factors, climatic factors, and agricultural management practices) [1–6]. Particularly, soil properties, such as soil texture, available water capacity, humus content, nutrient content, and pH, vary on a very small scale, resulting in varying nitrogen uptakes [7–10]. This effect can be further intensified by prevalent uniform fertilization due to different nutrient removals in the high- and low-yield zones of a field [11–14]. This results in small-scale fluctuating nitrogen balances and stocks in soil, causing high nitrate leaching in low-yield zones with overfertilization [5,15]. Therefore, systems adapted to small-scale crop variations for fertilization will be required, which will consider the heterogeneity of fields and their different yield potentials to minimize nitrate losses.

Site-specific nitrogen fertilization is a promising approach to minimizing nitrate leaching [16–20]. The literature shows that this method can balance the nitrogen surplus and improve nitrogen efficiency [21–24]. In this context, various methods for site-specific nitrogen fertilization have been developed and tested. These approaches can be divided into

three categories: "mapping", "online", and "mapping + online" [16,25,26]. Site conditions (e.g., soil texture or yield potential) are used with the mapping approach, whereas crop biomass and/or nitrogen uptake are determined by field measurements (sensor/satellite) and algorithms in the online approach. The mapping + online approach is a combination of both. Fertilizer systems based on the mapping + online approach, which uses sensor or satellite data, have been established [16,22,23,27]. These systems use different methods to determine the nitrogen uptake of the crops in the field on a small scale. Based on the determined nitrogen uptake, these fertilizer systems calculate the amount of nitrogen fertilizer to be applied using algorithms and other data, such as the yield potential, quality target, or weather data [28,29]. Studies on this show that the accuracy of determining nitrogen uptake can vary significantly depending on the method [30,31]. For example, the use of different vegetation indices in reflection–optical measurements results in clear differences in nitrogen uptake [32–35]. The literature shows that some vegetation indices are more or less suitable for determining biomass growth and nitrogen uptake, whereas the suitability of other vegetation indices varies based on the crop's growth stage [36–38]. Studies on this show that the vegetation index red edge inflection point (REIP) can provide robust and accurate data on nitrogen uptake, particularly for winter wheat [4,39–41]. The precision of the determination is crucial since current nitrogen uptake is a significant parameter in fertilization algorithms. Deviations in the determination of nitrogen uptake lead to incorrect calculations, resulting in yield losses and environmental pollution [42,43]. Therefore, a precise evaluation of the most recent site-specific fertilization methods, particularly the determination of nitrogen uptake, with ground truth data is crucial for harmonizing successful crop production with environmental protection.

This study examines the accuracy of recording nitrogen uptake with two basic non-contact measurement methods of site-specific nitrogen fertilization in winter wheat. The aim was to evaluate their precision and suitability as important data for site-specific fertilization algorithms. Thus, plot trials were conducted in 2020 and 2021 at two different locations in southern Germany. The trials analyzed the accuracy of the individual methods in mapping the nitrogen uptake of winter wheat at different growth stages (BBCH 31, BBCH 39, BBCH 55, and BBCH 65) in a sub-area, as this is decisive for the precision of the fertilizer applications generated with fertilizer algorithms. Therefore, the following were investigated: (a) how accurately the relative differences in the field were identified by the methods and (b) how accurately the methods estimated absolute nitrogen uptake. In the trial plots, nitrogen uptake was determined using biomass samples (ground truth data) and digital, georeferenced methods (sensor and satellite). Correlation analyses evaluated the relationships among the nitrogen uptake data determined using different methods. Based on the results, the accuracy, precision, and suitability of the tested methods for recording the spatial variability of nitrogen uptake in winter wheat at different growth stages were evaluated.

2. Materials and Methods

2.1. Site and Weather Conditions

Two heterogeneous fields in which the experiments were conducted in 2020 and 2021 were selected. Both fields belong to the Makofen Research Farm (48°81′55″ N 12°74′31″ E), which is 15 km southeast of Straubing (320 m a.s.l.). The trial fields of the Makofen Research Farm are flat and characterized by extremely fertile loess soil. Table 1 shows the most important soil parameters in the trial fields.

Table 2 provides an overview of temperature and precipitation at Makofen Research Farm. The 20-year mean annual precipitation at the trial sites is 781 mm, and the mean annual temperature is 9.5 °C.

Table 1. Soil data—Makofen Research Farm.

Property	Unit	Field A	Field B
Soil classification		Cambisol	Cambisol
Soil type		Silty loam	Silty loam
Soil fertility index *		75–85	70–80
Sand (0–30 cm)	%	6.0	6.9
Silt (0–30 cm)	%	70.1	69.4
Clay (0–30 cm)	%	23.9	23.7
Available water capacity (in 10 cm)	Vol.%	24.0	23.2
Soil organic carbon content (0–30 cm)	% DM	1.2	1.4
Soil total nitrogen content (0–30 cm)	% DM	0.14	0.12
Plant available phosphorus content (0–30 cm)	mg $(100 \text{ g})^{-1}$	14.8	17.9
Plant available potassium content (0–30 cm)	mg $(100 \text{ g})^{-1}$	17.7	18.4
pH (0–30 cm)		6.5	6.9

* The soil fertility index is a quantitative assessment of soil fertility given in integers in a range of 0–100, with 100 representing the most fertile soil in Germany.

Table 2. Mean temperature and precipitation—Makofen Research Farm.

	Unit	January to March	April to June	July to September	October to December	Year
2000–2020 Makofen						
Temperature $\bar{x}$	°C	1.4	14.4	17.3	4.7	9.5
Precipitation $\sum$	mm	170	209	230	172	781
2020 Makofen						
Temperature $\bar{x}$	°C	3.7	13.9	18.3	5.1	10.3
Precipitation $\sum$	mm	149	189	176	141	655
2021 Makofen						
Temperature $\bar{x}$	°C	1.8	13.1	17.3	4.4	9.2
Precipitation $\sum$	mm	129	268	250	165	812

2.2. Crop Management

In 2020 and 2021, the RGT Meister winter wheat variety was grown on the trial fields. The previous crop grown in the fields was sugar beets. Sowing, plant protection, and fertilization were conducted uniformly on the trial fields. Fertilization was conducted according to the Fertilizer Ordinance based on the Nmin content at the beginning of the spring growing season (2020: 66 kg N ha^{-1}; 2021: 62 kg N ha^{-1}). Plant protection was conducted according to the infestation situation. Table 3 shows an overview of crop management.

2.3. Experimental Design

The experimental setup was precisely adapted to the 10 m × 10 m grid of the satellite data. Both the plot size (10 m × 10 m) and the trial alignment in the field were based on the satellite data grid. This is critical for the high accuracy of the satellite data [5,44]. New plots were available for each growth stage, since the cutting of the biomass samples in the individual plots would influence the reflection measurements with the sensor and satellite at the subsequent growth stage. The experimental setup was the same in both experimental years, and only the number of plots differed (2020: *n* = 30; 2021: *n* = 45). Figure 1 shows the experimental setup in 2020.
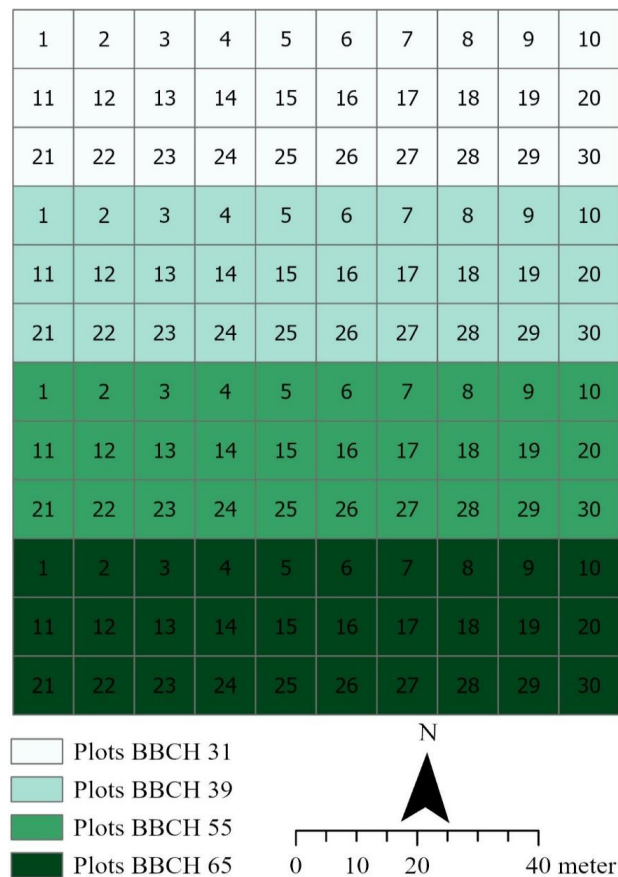
2.4. Methods of Determining Nitrogen Uptake

Nitrogen uptake per plot was determined using the following methods:

- Biomass samples (ground truth data) [45,46];
- An algorithm based on reflection measurements using a multispectral sensor [28,47];
- Radiative transfer model (soil–leaf–canopy) based on satellite data [29,48].

Table 3. Crop management of the trial fields.

| Field	Treatment	Unit	Amount	Product	Date
A	Sowing	kg/ha^{-1}	156	Meister	27 October 2019
A	First N fertilization	kg/ha^{-1}	60	ASN	28 March 2020
A	Second N fertilization	kg/ha^{-1}	80	CAN	30 April 2020
A	Third N fertilization	kg/ha^{-1}	40	CAN	20 May 2020
A	N fertilization, total	kg/ha^{-1}	180		
A	Plant protection	kg/ha^{-1}	0.05/0.07	Biathlon, Concert	7 April 2020
A	Plant protection	L/ha^{-1}	0.5	CCC 720	7 April 2020
A	Plant protection	L/ha^{-1}	1.25/0.075	Capalo/Karate	16 May 2020
A	Plant protection	L/ha^{-1}	2.0	Osiris	13 June 2020
B	Sowing	kg/ha^{-1}	205	Meister	10 November 2020
B	First N fertilization	kg/ha^{-1}	78	ASN	4 March 2021
B	Second N fertilization	kg/ha^{-1}	54	CAN	8 May 2021
B	Third N fertilization	kg/ha^{-1}	40	CAN	4 June 2021
B	N fertilization, total	kg/ha^{-1}	172		
B	Plant protection	kg/ha^{-1}	0.13	Broadway	22 April 2021
B	Plant protection	L/ha^{-1}	0.25/0.5	Pixxaro/CCC 720	22 April 2021
B	Plant protection	L/ha^{-1}	1.0/0.3	Revystar/Flexity	20 May 2021
B	Plant protection	L/ha^{-1}	1.0/0.075	Ascra Xpro/Karate	11 June 2021

Figure 1. Experimental setup (Field A, 2020).

Nitrogen uptake was determined using the respective methods in the growth stages, BBCH 31, BBCH 39, BBCH 55, and BBCH 65. Thus, an area of 2.5 m^2 of plants was manually cut off in each plot for the ground truth data. These samples were weighed, chopped, and dried at 105 °C. This resulted in the above-ground biomass yield. The Dumas method was used to analyze the nitrogen content of the samples, and the nitrogen uptake of the plot

was determined [45,46]. The reflection measurements with the multispectral sensor were conducted in the respective growth stages in the individual plots. The REIP 700 vegetation index was calculated based on these measurements, and the algorithms used to estimate the nitrogen uptake were based on this index considering further data, such as yield potential and variety properties [28]. Depending on the availability, the radiative transfer model used up-to-date satellite data to estimate nitrogen uptake. Based on the satellite data, the radiative transfer model calculated the nitrogen uptake at the respective growth stages considering additional data, such as observational parameters, soil reflectance information, leaf optical properties, and canopy properties [29,48].

2.5. Data Processing

Considering the corresponding methodology, nitrogen uptake was determined using different methods. Point data were generated using digital contactless measuring systems. Next, these point data were visualized using geoinformation system software, ArcGIS [49], and assigned to the digitized plots via their coordinates. Data points on or outside the plot edges were removed. The recorded data points varied in spatial resolution and distribution based on the method. Figure 2 shows the detailed structure and data distribution of a plot. Subsequently, the mean was calculated using all available data points per plot and method. Thus, the nitrogen uptake per plot in kg N ha^{-1} was determined for each method.
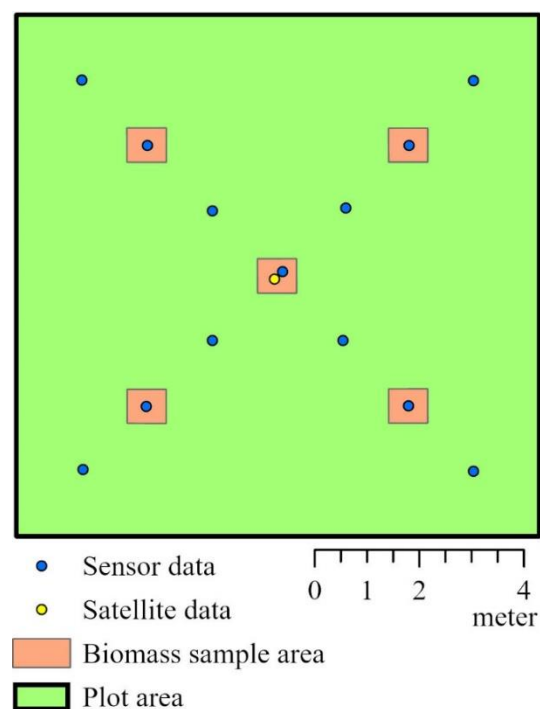
Figure 2. Structure and data distribution in the plot.

2.6. Descriptive Statistics

The mean, median, minimum, maximum, and standard deviation were calculated for each method using R.

2.7. Correlation Analysis

Correlation analyses based on the nitrogen uptake per plot in kg N ha^{-1} determined the relationships between the data of the tested digital methods and the ground truth data. The coefficients of determination (R^2) were classified as very strong ($R^2 > 0.9$), strong ($0.9 > R^2 > 0.7$), moderate ($0.7 > R^2 > 0.5$), weak ($0.5 > R^2 > 0.3$), or very weak ($R^2 < 0.3$).

3. Results

3.1. Spatial Variation in Nitrogen Uptake in 2020 (Field A)

Different methods for the site-specific determination of nitrogen uptake at characteristic growth stages produced different results in the nitrogen distribution pattern, nitrogen variation, and mean nitrogen uptake in Field A (Figure 3, Table 4). The nitrogen uptake of the biomass samples (ground truth data) in BBCH 31 varied between 33.2 and 64.1 kg N ha^{-1}. The nitrogen uptake estimated by the radiative transfer model based on satellite data in BBCH 31 (23.3–35.8 kg N ha^{-1}) was also characterized by variability; however, the variation was not as great as in those obtained with the other methods, and a significantly lower nitrogen level was noticeable. The nitrogen uptake estimated using algorithms based on sensor data in BBCH 31 (24.6–66.2 kg N ha^{-1}) was more similar to the measured values of the ground truth data. All the methods in BBCH 39 showed almost the same mean nitrogen uptake and a similar nitrogen distribution, but the variation was higher for both satellite and sensor data (Figure 3).
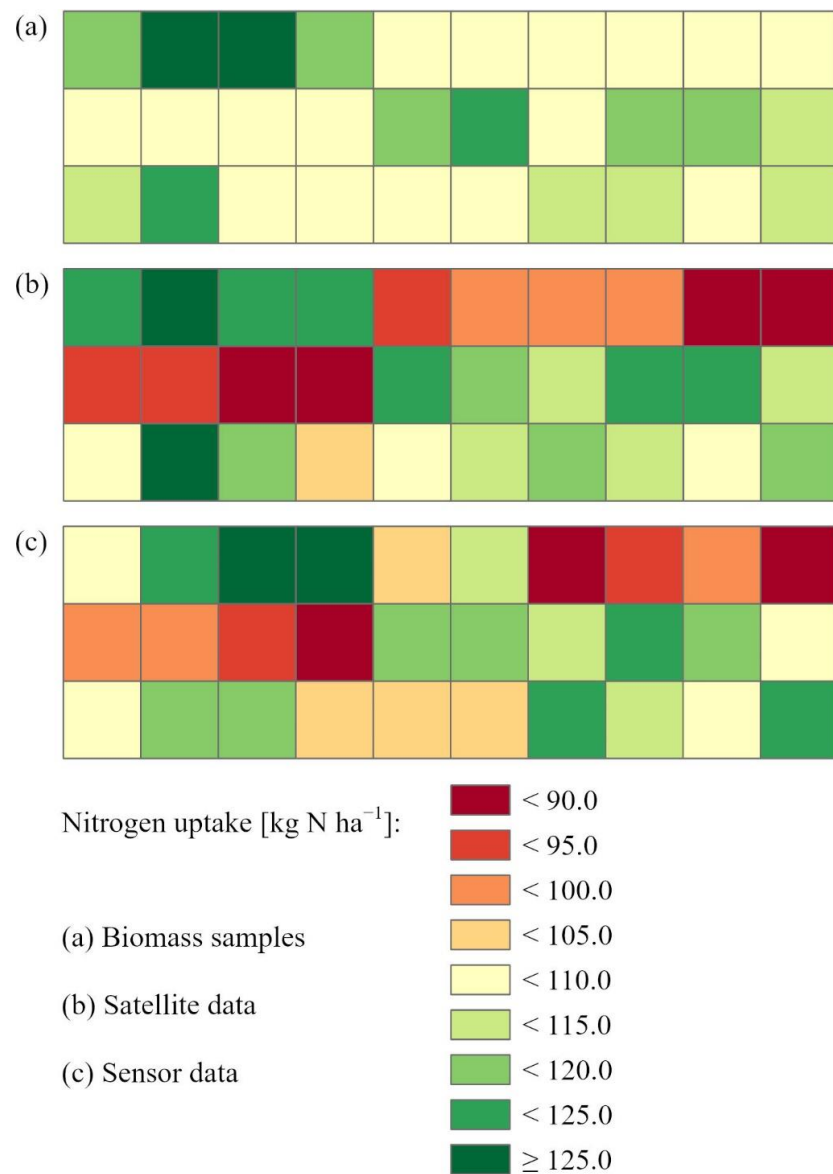
Figure 3. Nitrogen uptake 2020, BBCH 39. Nitrogen uptake was determined from the biomass samples, sensor data, and satellite data.

Table 4. Descriptive statistics of the nitrogen uptake data in kg N ha^{-1} analyzed in this study.

| Variable	*n*	Year	BBCH	Unit	Mean	Median	Minimum	Maximum	Standard Deviation	Skewness
Biomass samples	30	2020	31	kg N ha^{-1}	50.2	50.9	33.2	64.1	7.9	−0.41
Satellite data	30	2020	31	kg N ha^{-1}	30.4	30.7	23.3	35.8	3.4	−0.36
Sensor data	30	2020	31	kg N ha^{-1}	42.7	43.7	24.6	66.2	9.8	0.28
Biomass samples	30	2020	39	kg N ha^{-1}	118.2	118.4	109.2	125.2	3.7	−0.34
Satellite data	30	2020	39	kg N ha^{-1}	116.9	122.7	84.9	141.6	17.2	−0.51
Sensor data	30	2020	39	kg N ha^{-1}	124.1	127.1	68.8	169.1	27.2	−0.37
Biomass samples	30	2020	55	kg N ha^{-1}	186.8	187.9	167.1	199.5	9.6	−0.45
Satellite data	30	2020	55	kg N ha^{-1}	144.9	145.4	121.6	163.0	11.9	−0.34
Sensor data	30	2020	55	kg N ha^{-1}	203.6	216.1	143.5	247.3	32.2	−0.52
Biomass samples	30	2020	65	kg N ha^{-1}	225.5	225.9	211.8	235.2	6.1	−0.37
Satellite data	30	2020	65	kg N ha^{-1}	178.1	181.2	164.1	188.3	7.9	−0.57
Sensor data	30	2020	65	kg N ha^{-1}	248.5	255.3	166.9	320.2	37.9	−0.30
Biomass samples	45	2021	31	kg N ha^{-1}	45.2	44.9	29.4	63.0	7.5	0.12
Satellite data	45	2021	31	kg N ha^{-1}	40.8	40.5	33.8	47.6	1.9	−0.11
Sensor data	45	2021	31	kg N ha^{-1}	43.9	44.9	23.5	62.1	9.7	−0.34
Biomass samples	45	2021	39	kg N ha^{-1}	144.3	142.2	124.1	195.8	13.9	1.17
Satellite data	45	2021	39	kg N ha^{-1}	123.4	120.4	100.8	161.0	16.0	0.9
Sensor data	45	2021	39	kg N ha^{-1}	143.0	133.7	103.8	217.5	31.2	0.51
Biomass samples	45	2021	55	kg N ha^{-1}	192.3	192.1	142.6	225.9	16.1	−0.74
Satellite data	45	2021	55	kg N ha^{-1}	170.0	169.2	146.4	202.8	12.5	0.47
Sensor data	45	2021	55	kg N ha^{-1}	199.9	191.6	118.3	275.7	44.1	0.24
Biomass samples	45	2021	65	kg N ha^{-1}	218.3	217.5	182.4	260.8	17.5	0.52
Satellite data	45	2021	65	kg N ha^{-1}	183.4	182.6	140.8	225.5	21.4	0.19
Sensor data	45	2021	65	kg N ha^{-1}	232.1	239.3	147.2	308.5	46.9	0.11

Both the satellite and sensor data in BBCH 55 and 65 showed similar nitrogen distributions, which was consistent with the ground truth data. However, the absolute level of nitrogen uptake was noticeably lower with the satellite data than with the ground truth data, whereas it was higher with the sensor data. A deviation of −20% in the mean nitrogen uptake with the satellite data and +10% with the sensor data was observed in BBCH 55 and 65.

3.2. Spatial Variation in Nitrogen Uptake in 2021 (Field B)

The nitrogen uptake data determined using different digital measuring systems and methods for the examined growth stages in Field B produced results similar to those in Field A (Figure 4, Table 4). Thus, the nitrogen uptake of the ground truth data in BBCH 31 (29.4–63.0 kg N ha^{-1}) varied in a similar range as in 2020. The estimate of nitrogen uptake by the radiative transfer model based on satellite data in BBCH 31 (33.8–47.6 kg N ha^{-1}) was also characterized by variability, but the variation was again lower and at a lower nitrogen level, whereas the estimate from the sensor data (23.5–62.1 kg N ha^{-1}) was similar to the measured values of the ground truth data (Figure 4). All methods in BBCH 39 showed a similar nitrogen distribution; however, the variation was slightly lower with the satellite data and was slightly higher with the sensor data. The satellite and sensor data in BBCH 55 and 65 showed similar nitrogen distribution patterns, which were consistent with the ground truth data. However, it was also noticed that the absolute level of nitrogen uptake was lower with the satellite data than with the ground truth data, whereas it was slightly higher with the sensor data. In BBCH 55 and 65, there were slight deviations from the mean nitrogen uptake of −14% with the satellite data and +5% with the sensor data.

3.3. Correlation between Variables

Table 5 shows the coefficients of determination (R^2) of the linear relationships of the nitrogen uptake data determined using various digital methods.
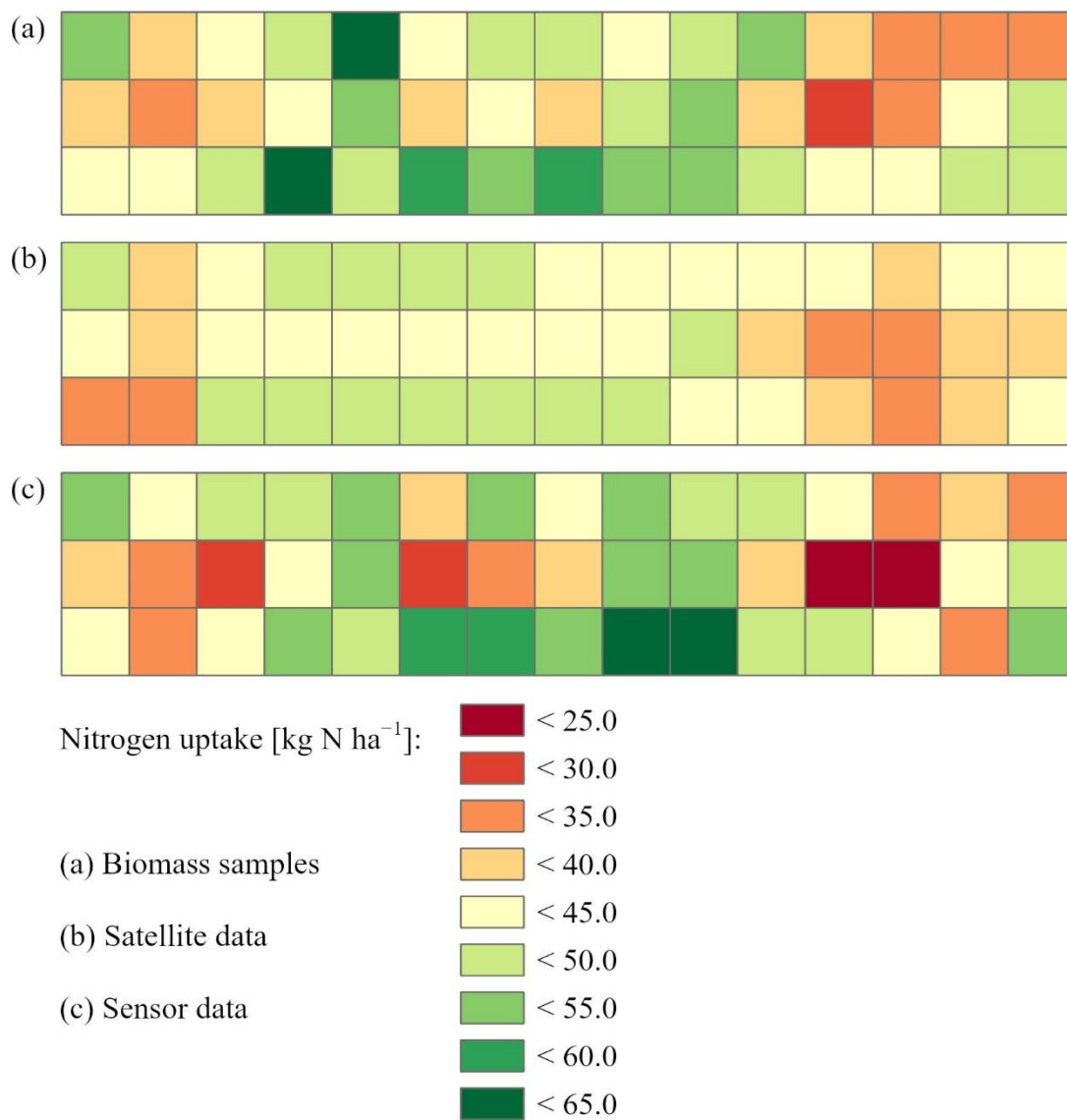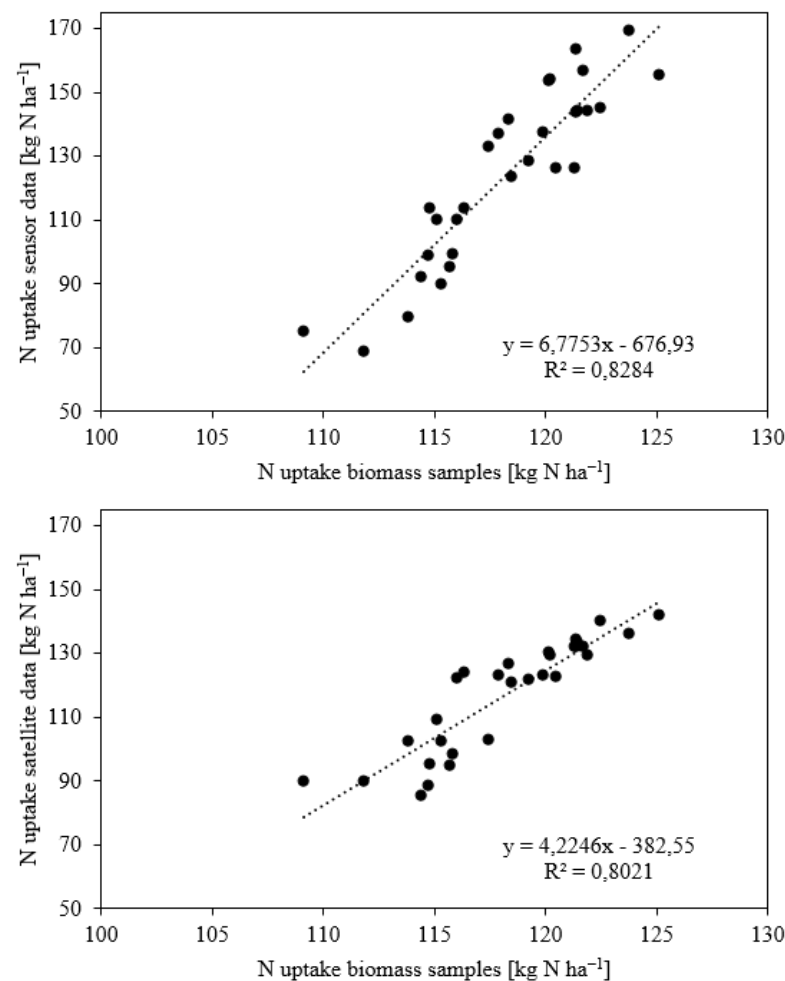
Figure 4. Nitrogen uptake 2021, BBCH 31. Nitrogen uptake was determined from the biomass samples, sensor data, and satellite data.

Table 5. Coefficients of determination (R^2): nitrogen uptake data for 2020 ($n = 30$) and 2021 ($n = 45$).

R^2	BBCH	Sensor 2020	Satellite 2020	Sensor 2021	Satellite 2021
Biomass samples 2020	31	0.74	0.60		
Biomass samples 2020	39	0.83	0.80		
Biomass samples 2020	55	0.77	0.74		
Biomass samples 2020	65	0.67	0.67		
Biomass samples 2021	31			0.66	0.48
Biomass samples 2021	39			0.76	0.57
Biomass samples 2021	55			0.72	0.63
Biomass samples 2021	65			0.65	0.59

3.3.1. Field A (2020)

Overall, all tested methods achieved similar correlations and could at least moderately map the nitrogen uptake for all growth stages examined. In BBCH 31, the correlation analysis showed a strong relationship between the ground truth data and the estimate from the sensor data (R^2 = 0.74). The nitrogen uptake in BBCH 31 determined by the radiative transfer model based on satellite data (R^2 = 0.60) was moderately correlated with the ground truth data. In BBCH 39 and 55, both the estimates from the sensor data (R^2 = 0.77–0.83) and those from the satellite data (R^2 = 0.74–0.80) were strongly correlated with the ground truth data (Figure 5). The results from the sensor and satellite data in BBCH 65 were identical and showed a moderate correlation with the ground truth data (R^2 = 0.67).

Figure 5. The linear relationships between nitrogen uptake of ground truth data and sensor data (**above**) and satellite data (**below**) in BBCH 39 in Field A in 2020.

3.3.2. Field B (2021)

In 2021, the correlations were considerably similar to those of the previous year. All methods except the satellite data in BBCH 31 mapped nitrogen uptake at least moderately. There was a moderate correlation between the ground truth data and the sensor data (R^2 = 0.66) in BBCH 31, but only a weak correlation with the satellite data (R^2 = 0.48). In BBCH 39 and 55, the estimates from the sensor data (R^2 = 0.72–0.76) were strongly correlated with the ground truth data, and with those from the satellite data (R^2 = 0.57–0.63) moderately. The results of the sensor (R^2 = 0.65) and satellite data (R^2 = 0.59) in BBCH 65 were repeatedly similar and showed a moderate correlation with the ground truth data.

4. Discussion

4.1. Discussion of the Methods

4.1.1. Site Selection

This study investigated the recording of nitrogen uptake using two basic noncontact measurement methods of site-specific nitrogen fertilization in winter wheat at characteristic growth stages in heterogeneous fields at two locations in southern Germany. The precision of the methods was tested by comparing the statistical indicators (mean, median, minimum, maximum, and standard deviation) and examining correlative relationships. The aim of this was to identify the variability in nitrogen uptake and analyze its absolute amount.

4.1.1. Site Selection

The expression of the spatial variability of nitrogen uptake has a significant impact on the results of this method's comparison [50,51]. Therefore, heterogeneous fields were selected for this study. The heterogeneity of the trial sites was assessed based on the soil parameters, biomass maps, and a farm manager's expertise. Heijting et al. [52] showed that a farm manager's expertise is a suitable basis for evaluating the heterogeneity of a field. Furthermore, other studies revealed that small-scale variations in the soil properties and crop stands are characteristic of the study region [5,53].

4.1.2. Ground Truth Data

The nitrogen uptake data were determined using two digital methods. Suitable ground truth data (biomass samples) are crucial in evaluating the different estimation methods for comparing the modeled data with the measured data [5]. Therefore, in this study, biomass samples were cut in all plots for each examined growth stage (BBCH 31, BBCH 39, BBCH 55, and BBCH 65), and the nitrogen uptake was determined in the laboratory [45,46]. The biomass samples enabled accurate determination of the nitrogen uptake per plot and the evaluation of the estimates obtained using digital methods. However, the measuring effort for biomass samples is extremely high and a limiting factor for large areas. For example, Mittermayer et al. [5] investigated the variability of nitrogen uptake in an area of 13.1 ha and used 50 biomass samples; the data analysis was conducted using geostatistical methods. Other studies analyzed even larger fields of more than 1000 ha and only compared the sensor and satellite data. Mezera et al. [51] and Gozdowski et al. [54] achieved similar results with both measurement methods and found moderate to strong correlations ($R^2 = 0.51$–0.79). The results of this study confirmed this. For example, both methods correlated strongly ($R^2 = 0.76$) in BBCH 39 in 2020; however, there was a higher variation in absolute nitrogen uptake with both digital methods than with the ground truth data. Because the absolute height of nitrogen uptake is also crucial for site-specific fertilization, the ground truth data of the biomass samples were of immense importance for the precise evaluation of the two digital methods in this study.

4.2. Discussion of the Results

4.2.1. Sensor Data

The nitrogen uptake estimate based on multispectral sensor data, the REIP vegetation index, and a crop-specific algorithm [28] provided reliable results in both test years. The method recognized the spatial nitrogen distribution in all tested growth stages as moderate to strong ($R^2 = 0.65$–0.83). Apart from BBCH 31 in 2020 (-15%), there were only small deviations ($\leq \pm 10\%$) in the nitrogen uptake's mean absolute level. This deviation may have been due to drought stress. There was a pronounced early summer drought at the time of the measurements in BBCH 31. Drought stress, plant diseases, soil compaction, and lack of other nutrients can influence the reflection signature in reflection–optical measurements, resulting in incorrectly interpreted measured values [55–57]. Further, the correlation quality of the sensor data typically improved with the increasing growth stage toward a peak in BBCH 39 and then slightly decreased again. Nevertheless, no clear saturation occurred, as, for example, with systems based on simple vegetation indices, such as NDVI or SAVI, and good precision was shown even with high nitrogen uptake [36,38,58]. Similar results

were also obtained by Prey and Schmidhalter [38,58], who investigated the sensitivity of different vegetation indices for estimating nitrogen uptake in winter wheat and consistently achieved moderate results with the REIP (R^2 = 0.59). Westermeier and Maidl [36] made the same conclusions in their study and even found correlations of up to R^2 = 0.9 for the REIP 700 index. Further investigations with reflection–optical sensor measurements presented moderate to very strong correlations with nitrogen uptake in winter wheat at the relevant growth stages (R^2 = 0.57–0.89) [4,5,59,60]. Consequently, the sensor data are suitable for both early and late site-specific fertilization measures. In addition, the sensor measurements from BBCH 65 can be used to calculate yield estimates and yield potential maps [61,62]. These results confirm the significant potential of modern sensor technology for recording nitrogen uptake as a basis for site-specific fertilization. The prerequisites for the successful implementation of this method are multispectral sensors with high measurement accuracy, suitable vegetation indices, and science-based algorithms [5,36,38,58,60].

4.2.2. Satellite Data

The nitrogen uptake estimate with the radiative transfer model based on satellite data also achieved good results in both test years. The method identified the spatial nitrogen distribution in all tested growth stages, except in BBCH 31 in 2021 (R^2 = 0.48), moderately to strongly (R^2 = 0.57–0.80). This deviation can be explained by the dependence of this method on clear, cloud-free satellite images [63–65]. In BBCH 31, it was frequently cloudy in 2021, and the availability of cloud-free satellite images was extremely limited. Consequently, older satellite images had to be used to estimate nitrogen uptake, which can result in deviations. The mean absolute level of nitrogen uptake of the satellite data in the years 2020 ($\leq -20\%$) and 2021 ($\leq -15\%$) showed slightly larger deviations compared to those with the sensor data. An exception to this was BBCH 31 in 2020 (-40%), since there was a significant deviation, which can be explained by drought stress. Drought stress, plant diseases, soil compaction, and a lack of other nutrients can affect the reflection signature of multispectral satellite images in the same way as with the sensor data, resulting in incorrectly interpreted measured values [55,56]. Other literature also presented good results using satellite data. Chen [66] conducted correlation analyses between remote sensing data and the nitrogen concentration in winter wheat at different growth stages and achieved strong correlations (R^2 = 0.86). Magney et al. [67] compared satellite data with biomass samples and successfully mapped the nitrogen uptake with high precision (R^2 = 0.81). Further investigations into mapping the nitrogen uptake of winter wheat using satellite data also showed good results (R^2 = 0.74) [68]. Consequently, with current data availability, satellite data are also suitable as a basis for early and late site-specific fertilization measures. Further, yield estimates and yield potential maps can also be generated using satellite images [29,69]. These results confirm that remote sensing methods can be used to record parameters such as nitrogen uptake with good precision and use them for site-specific fertilization measures.

5. Conclusions

Current nitrogen uptake is a crucial parameter in site-specific fertilization algorithms. The more precisely the nitrogen uptake is determined by noncontact measuring methods, the more precise the result of the site-specific fertilization. The results of these investigations show the suitability of both measurement methods. Nitrogen uptake can be determined appropriately using the tested methods for both BBCH 31 and 39, which are crucial growth stages for yield fertilization, and BBCH 55 and 65, which are relevant for quality fertilization or for deriving yield estimates. Significant deviations, such as those in BBCH 31 in 2020, can be explained by external influences. Further, data generated by sensor measurements close to plants are somewhat more precise, particularly when determining the absolute level of nitrogen uptake. In addition, the sensor technology is unaffected by cloud cover and is particularly superior at times when there are no cloud-free satellite images. On the other hand, the sensor technology is extremely expensive and requires a high level of

user qualification. However, with the satellite data, the finished application map is sent to the machine and is, therefore, very easy to use. Furthermore, the satellite data depict the entire field and do not only measure partial areas. In summary, both measurement methods have advantages and disadvantages. However, both methods prove their potential and are suitable for determining the nitrogen uptake for site-specific fertilization systems in winter wheat. Referring to the great relevance of the topic and the environmental effects of inappropriate fertilization, noncontact measuring methods for determining plant parameters such as nitrogen uptake require urgent further investigation to improve the precision, particularly with the absolute level of nitrogen uptake. The focus should be on the higher spatial resolution of satellite data (e.g., 5 m $\times$ 5 m) and other wavelengths in reflection–optical measurements to improve and develop vegetation indices.

References

1. Kucke, M.; Kleeberg, P. Nitrogen balance and soil nitrogen dynamics in two areas with different soil, climatic and cropping conditions. *Eur. J. Agron.* **1997**, *6*, 89–100. [CrossRef]
2. Wang, H.; Ju, X.; Wei, Y.; Li, B.; Zhao, L.; Hu, K. Simulation of bromide and nitrate leaching under heavy rainfall and high-intensity irrigation rates in North China plain. *Agric. Water Manag.* **2010**, *97*, 1646–1654. [CrossRef]
3. Tarkalson, D.D.; Payero, J.O.; Ensley, S.M.; Shapiro, C.A. Nitrate accumulation and movement under deficit irrigation in soil receiving cattle manure and commercial fertilizer. *Agric. Water Manag.* **2006**, *85*, 201–210. [CrossRef]
4. Cao, Q.; Miao, Y.; Shen, J.; Yuan, F.; Cheng, S.; Cui, Z. Evaluating two crop circle active canopy sensors for in-season diagnosis of winter wheat nitrogen status. *Agronomy* **2018**, *8*, 201. [CrossRef]
5. Mittermayer, M.; Gilg, A.; Maidl, F.-X.; Nätscher, L.; Hülsbergen, K.-J. Site-specific nitrogen balances based on spatially variable soil and plant properties. *Precis. Agric.* **2021**, *22*, 1416–1436. [CrossRef]
6. Strebel, O.; Duynisveld, W.H.M.; Böttcher, J. Nitrate pollution of groundwater in western Europe. *Agric. Ecosyst. Environ.* **1989**, *26*, 189–214. [CrossRef]
7. Maidl, F.X.; Brunner, R.; Sticksel, E.; Fischbeck, G. Ursachen kleinräumiger Ertragsschwankungen im bayerischen Tertiärhügelland und Folgerungen für eine teilschlagbezogene Düngung [Reasons of small-scale yield variations in the Bavarian tertiary hill country and conclusions for site-specific fertilization]. *J. Plant Nutr. Soil Sci.* **1999**, *162*, 337–342. [CrossRef]
8. Lopez-Lozano, R.; Casterad, M.A.; Herrero, J. Site-specific management units in a commercial maize plot delineated using very high-resolution remote sensing and soil properties mapping. *Comput. Electron. Agric.* **2010**, *73*, 219–229. [CrossRef]
9. Farid, H.U.; Bakhsh, A.; Ahmad, N.; Ahmad, A.; Mahmood-Khan, Z. Delineating site-specific management zones for precision agriculture. *J. Agric. Sci.* **2016**, *154*, 273–286. [CrossRef]
10. Servadio, P.; Bergonzoli, S.; Verotti, M. Delineation of management zones based on soil mechanical-chemical properties to apply variable rates of inputs throughout a field (VRA). *Eng. Agric. Environ. Food* **2017**, *10*, 20–30. [CrossRef]
11. Frogbrook, Z.L.; Oliver, M.A. Identifying management zones in agricultural fields using spatially constrained classification of soil and ancillary data. *Soil Use Manag.* **2007**, *23*, 40–51. [CrossRef]
12. Hülsbergen, K.J.; Maidl, F.X.; Forster, F.; Prücklmaier, J. *Minderung von Nitrataustägen in Trinkwassereinzugsgebieten durch Optimiertes Stickstoffmanagement am Beispiel der Gemeinde Hohenthann (Niederbayern) mit Intensiver Landwirtschaftlicher Flächennutzung [Reduction of Nitrate Emissions in Drinking Water Catchment Areas through Optimized Nitrogen Management]*; Forschungsbericht an das Bayerische Staatsministerium für Ernährung, Landwirtschaft und Forsten, Technische Universität München: Freising, Germany, 2017. Available online: https://www.lfu.bayern.de/wasser/gw_gefaehrdung_schutz/gwschutz_landwirtschaft/projekte_hohenthann/doc/tum_bericht_hohenthann.pdf (accessed on 8 March 2022).

13. Stamatiadis, S.; Schepers, J.S.; Evangelou, E.; Tsadilas, C.; Glampedakis, A.; Glampedakis, M.; Dercas, N.; Spyropoulos, N.; Dalezios, N.R.; Eskridge, K. Variable-rate nitrogen fertilization of winter wheat under high spatial resolution. *Precis. Agric.* **2018**, *19*, 570–587. [CrossRef]

14. Wang, K.; Huggins, D.R.; Tao, H. Rapid mapping of winter wheat yield, protein, and nitrogen uptake using remote and proximal sensing. *Int. J. Appl. Earth Obs. Geoinf.* **2019**, *82*, 101921. [CrossRef]

15. Dalgaard, T.; Bienkowski, J.F.; Bleeker, A.; Dragosits, U.; Drouet, J.L.; Durand, P.; Frumau, A.; Hutchings, N.J.; Kedziora, A.; Magliulo, V.; et al. Farm nitrogen balances in six European landscapes as an indicator for nitrogen losses and basis for improved management. *Biogeosciences* **2012**, *9*, 5303–5321. [CrossRef]

16. Maidl, F.X.; Schächtl, J.; Huber, G. Strategies for site-specific nitrogen fertilization on winter wheat. In Proceedings of the 7th International Conference on Precision Agriculture and Other Precision Resources Management, Minneapolis, MN, USA, 25–28 July 2004; pp. 1938–1948.

17. Diacono, M.; Rubino, P.; Montemurro, F. Precision nitrogen management of wheat. A review. *Agron. Sustain. Dev.* **2013**, *33*, 219–241. [CrossRef]

18. Mulla, D.J. Twenty-five years of remote sensing in precision agriculture: Key advances and remaining knowledge gaps. *Biosyst. Eng.* **2013**, *114*, 358–371. [CrossRef]

19. Liu, H.; Whiting, M.L.; Ustin, S.L.; Zarco-Tejada, P.J.; Huffman, T.; Zhang, X. Maximizing the relationship of yield to site-specific management zones with object-oriented segmentation of hyperspectral images. *Precis. Agric.* **2018**, *19*, 348–364. [CrossRef]

20. Prücklmaier, J. Feldexperimentelle Analysen zur Ertragsbildung und Stickstoffeffizienz bei Organisch-Mineralischer Düngung auf Heterogenen Standorten und Möglichkeiten zur Effizienzsteigerung Durch Computer- und Sensorgestützte Düngesysteme [Field Experimental Analyses of Yield Effects and Nitrogen Efficiency of Fertilizer Application Systems]. Ph.D. Thesis, Technische Universität München, Munich, Germany, 2020.

21. Peralta, N.R.; Costa, J.L.; Balzarini, M.; Franco, M.C.; Córdoba, M.; Bullock, D. Delineation of management zones to improve nitrogen management of wheat. *Comput. Electron. Agric.* **2015**, *110*, 103–113. [CrossRef]

22. Spicker, A.B. Entwicklung von Verfahren der teilflächenspezifischen Stickstoffdüngung zu Wintergerste (*Hordeum vulgare* L.) und Winterraps (*Brassica napus* L.) auf Grundlage Reflexionsoptischer Messungen [Development of Sensor-Based Nitrogen Fertilization Systems for Oilseed Rape (*Brassica napus* L.) and winter barley (*Hordeum vulgare* L.)]. Ph.D. Thesis, Technische Universität München, Munich, Germany, 2016.

23. Vinzent, B.; Fuß, R.; Maidl, F.X.; Hülsbergen, K.J. Efficacy of agronomic strategies for mitigation of after-harvest N_2O emissions of winter oilseed rape. *Eur. J. Agron.* **2017**, *89*, 88–96. [CrossRef]

24. Argento, F.; Anken, T.; Abt, F.; Vogelsanger, E.; Walter, A.; Liebisch, F. Site-specific nitrogen management in winter wheat supported by low-altitude remote sensing and soil data. *Precis. Agric.* **2021**, *22*, 364–386. [CrossRef]

25. Gandorfer, M. Bewertung von Precision Farming Dargestellt am Beispiel der Teilflächenspezifischen Stickstoffdüngung [Evaluation of Precision Farming Illustrated Using Site-Specific Nitrogen Fertilization as an Example]. Ph.D. Thesis, Technische Universität München, Munich, Germany, 2006.

26. Weckesser, F.; Leßke, F.; Luthardt, M.; Hülsbergen, K.-J. Conceptual design of a comprehensive farm nitrogen management system. *Agronomy* **2021**, *11*, 2501. [CrossRef]

27. Schmidhalter, U. Sensorgestützte Ermittlung des Nährstoffbedarfs. *VDLUFA-Schriftenreihe* **2014**, *70*, 57–66.

28. Maidl, F.X. *Verfahren zur Bestimmung des Düngebedarfs, Insbesondere des Stickstoff-Düngerbedarfs und Vorrichtung zur Durchführung des Verfahrens*; Patentnr. DE 102011050877; Technische Universität München: Munich, Germany, 2011.

29. Hank, T.B.; Bach, H.; Mauser, W. Using a remote sensing-supported hydro-agroecological model for field-scale simulation of heterogeneous crop growth and yield: Application for wheat in central Europe. *Remote Sens.* **2015**, *7*, 3934–3965. [CrossRef]

30. Auernhammer, H. Precision farming—The environmental challenge. *Comput. Electron. Agric.* **2001**, *30*, 31–43. [CrossRef]

31. Ebertseder, T.; Gutser, R.; Hege, U.; Brandhuber, R.; Schmidhalter, U. Strategies for site-specific nitrogen fertilization with respect to long-term environmental demands. In Proceedings of the Fourth European Conference on Precision Agriculture, Berlin, Germany, 15–19 June 2003; pp. 193–198.

32. Perry, E.M.; Davenport, J.R. Spectral and spatial differences in response of vegetation indices to nitrogen treatments on apple. *Comput. Electron. Agric.* **2007**, *59*, 56–65. [CrossRef]

33. Maresma, Á.; Ariza, M.; Martínez, E.; Lloveras, J.; Martínez-Casasnovas, J.A. Analysis of vegetation indices to determine nitrogen application and yield prediction in maize (*Zea mays* L.) from a standard UAV service. *Remote Sens.* **2016**, *8*, 973. [CrossRef]

34. Herrera, J.M.; Rubio, G.; Häner, L.L.; Delgado, J.A.; Lucho-Constantino, C.A.; Islas-Valdez, S.; Pellet, D. Emerging and established technologies to increase nitrogen use efficiency of cereals. *Agronomy* **2016**, *6*, 25. [CrossRef]

35. Feng, W.; Zhang, H.Y.; Zhang, Y.S.; Qi, S.L.; Heng, Y.R.; Guo, B.B.; Ma, D.Y.; Guo, T.C. Remote detection of canopy leaf nitrogen concentration in winter wheat by using water resistance vegetation indices from in-situ hyperspectral data. *Field Crops Res.* **2016**, *198*, 238–246. [CrossRef]

36. Westermeier, M.; Maidl, F.X. Vergleich von Spektralindizes zur Erfassung der Stickstoffaufnahme bei Winterweizen (*Triticum aestivum* L.). *J. Kulturpfl.* **2019**, *71*, 238–248.

37. Li, F.; Miao, Y.; Hennig, S.D.; Gnyp, M.L.; Chen, X.; Jia, L.; Bareth, G. Evaluating hyperspectral vegetation indices for estimating nitrogen concentration of winter wheat at different growth stages. *Precis. Agric.* **2010**, *11*, 335–357. [CrossRef]

38. Prey, L.; Schmidhalter, U. Sensitivity of vegetation indices for estimating vegetative n status in winter wheat. *Sensors* **2019**, *19*, 3712. [CrossRef] [PubMed]

39. Erdle, K.; Mistele, B.; Schmidhalter, U. Comparison of active and passive spectral sensors in discriminating biomass parameters and nitrogen status in wheat cultivars. *Field Crops Res.* **2011**, *124*, 74–84. [CrossRef]

40. Cammarano, D.; Fitzgerald, G.J.; Casa, R.; Basso, B. Assessing the robustness of vegetation indices to estimate wheat N in mediterranean environments. *Remote Sens.* **2014**, *6*, 2827–2844. [CrossRef]

41. Li, F.; Miao, Y.; Feng, G.; Yuan, F.; Yue, S.; Gao, X.; Liu, Y.; Liu, B.; Ustin, S.L.; Chen, X. Improving estimation of summer maize nitrogen status with red edge-based spectral vegetation indices. *Field Crops Res.* **2014**, *157*, 111–123. [CrossRef]

42. Cui, Z.; Zhang, F.; Chen, X.; Miao, Y.; Li, J.; Shi, L.; Xu, J.; Ye, Y.; Liu, C.; Yang, Z.; et al. On-farm evaluation of an in-season nitrogen management strategy based on soil Nmin test. *Field Crops Res.* **2008**, *105*, 48–55. [CrossRef]

43. Li, X.; Hu, C.; Delgado, J.A.; Zhang, Y.; Ouyang, Z. Increased nitrogen use efficiencies as a key mitigation alternative to reduce nitrate leaching in north china plain. *Agric. Water Manag.* **2007**, *89*, 137–147. [CrossRef]

44. Devaux, N.; Crestey, T.; Leroux, C.; Tisseyre, B. Potential of sentinel-2 satellite images to monitor vine fields grown at a territorial scale. *OENO One* **2019**, *53*, 52–59. [CrossRef]

45. Ebeling, M.E. The dumas method for nitrogen in feeds. *J. Assoc. Off. Anal. Chem.* **1968**, *51*, 766–770. [CrossRef]

46. Saint-Denis, T.; Goupy, J. Optimization of a nitrogen analyser based on the Dumas method. *Anal. Chim. Acta* **2004**, *515*, 191–198. [CrossRef]

47. TEC5, Spektrometer Systeme, Version 2.13. Available online: https://tec5.com/de/ (accessed on 14 March 2022).

48. Verhoef, W.; Bach, H. Coupled soil–leaf-canopy and atmosphere radiative transfer modeling to simulate hyperspectral multi-angular surface reflectance and TOA radiance data. *Remote Sens. Environ.* **2007**, *109*, 166–182. [CrossRef]

49. ArcGIS. Map Creation and Analysis: Location Intelligence for Everyone. Available online: https://www.esri.com/de-de/arcgis/products/arcgis-online/overview (accessed on 15 March 2022).

50. Patzold, S.; Mertens, F.M.; Bornemann, L.; Koleczek, B.; Franke, J.; Feilhauer, H.; Welp, G. Soil heterogeneity at the field scale: A challenge for precision crop protection. *Precis. Agric.* **2008**, *9*, 367–390. [CrossRef]

51. Mezera, J.; Lukas, V.; Horniaček, I.; Smutný, V.; Elbl, J. Comparison of proximal and remote sensing for the diagnosis of crop status in site-specific crop management. *Sensors* **2022**, *22*, 19. [CrossRef]

52. Heijting, S.; De Bruin, S.; Bregt, A.K. The arable farmer as the assessor of within-field soil variation. *Precis. Agric.* **2011**, *12*, 488–507. [CrossRef]

53. Heil, K.; Schmidhalter, U. Improved evaluation of field experiments by accounting for inherent soil variability. *Eur. J. Agron.* **2017**, *89*, 1–15. [CrossRef]

54. Gozdowski, D.; Stępień, M.; Panek, E.; Varghese, J.; Bodecka, E.; Rozbicki, J.; Samborski, S. Comparison of winter wheat NDVI data derived from landsat 8 and active optical sensor at field scale. *Remote Sens. Appl. Soc. Environ.* **2020**, *20*, 100409. [CrossRef]

55. Wang, T.C.; Ma, B.L.; Xiong, Y.C.; Saleem, M.F.; Li, F.M. Optical sensing estimation of leaf nitrogen concentration in maize across a range of water-stress levels. *Crop Pasture Sci.* **2011**, *62*, 474–480. [CrossRef]

56. Franke, J.; Menz, G. Multi-temporal wheat disease detection by multi-spectral remote sensing. *Precis. Agric.* **2007**, *8*, 161–172. [CrossRef]

57. Sensoren für die Variable Stickstoffdüngung–Funktionsprinzipien und Marktübersicht. Available online: https://www.lwk-niedersachsen.de/lwk/news/33577_Sensoren_f%C3%BCr_die_variable_Stickstoffd%C3%BCngung_-_Funktionsprinzipien_und_Markt%C3%BCbersicht (accessed on 22 March 2022).

58. Prey, L.; Schmidhalter, U. Simulation of satellite reflectance data using high-frequency ground based hyperspectral canopy measurements for in-season estimation of grain yield and grain nitrogen status in winter wheat. *ISPRS J. Photogramm. Remote Sens.* **2019**, *149*, 176–187. [CrossRef]

59. Pavuluri, K.; Chim, B.K.; Griffey, C.A.; Reiter, M.S.; Balota, M.; Thomason, W.E. Canopy spectral reflectance can predict grain nitrogen use efficiency in soft red winter wheat. *Precis. Agric.* **2015**, *16*, 405–424. [CrossRef]

60. Cao, Q.; Miao, Y.; Feng, G.; Gao, X.; Li, F.; Liu, B.; Yue, S.; Cheng, S.; Ustin, S.L.; Khosla, R. Active canopy sensing of winter wheat nitrogen status: An evaluation of two sensor systems. *Comput. Electron. Agric.* **2015**, *112*, 54–67. [CrossRef]

61. Maidl, F.X.; Spicker, A.; Weng, J.; Hülsbergen, K.J. Ableitung des teilflächenspezifischen Kornertrags von Getreide aus Reflexionsdaten (Derivation of the site-specific grain yield from reflection data). In Proceedings of the 39th GIL-Jahrestagung, Wien, Austria, 18–19 February 2019; pp. 131–134.

62. Hauser, J.; Maidl, F.X.; Wagner, P. Untersuchung der teilflächenspezifischen Ertragserfassung von Großmähdreschern in Winterweizen (Investigation of site-specific yield mapping of combine harvesters in winter wheat). In Proceedings of the 41st GIL-Jahrestagung, Potsdam, Germany, 8–9 March 2021; pp. 133–138.

63. Georgi, C.; Spengler, D.; Itzerott, S.; Kleinschmit, B. Automatic delineation algorithm for site-specific management zones based on satellite remote sensing data. *Precis. Agric.* **2018**, *19*, 684–707. [CrossRef]

64. Kumhalova, J.; Matějková, Š. Yield variability prediction by remote sensing sensors with different spatial resolution. *Int. Agrophys.* **2017**, *31*, 195–202. [CrossRef]

65. Domínguez, J.A.; Kumhálová, J.; Novák, P. Winter oilseed rape and winter wheat growth prediction using remote sensing methods. *Plant Soil Environ.* **2015**, *61*, 410–416.

66. Chen, P. A comparison of two approaches for estimating the wheat nitrogen nutrition index using remote sensing. *Remote Sens.* **2015**, *7*, 4527–4548. [CrossRef]
67. Magney, T.S.; Eitel, J.U.H.; Vierling, L.A. Mapping wheat nitrogen uptake from RapidEye vegetation indices. *Precis. Agric.* **2017**, *18*, 429–451. [CrossRef]
68. Jia, L.; Yu, Z.; Li, F.; Gnyp, M.; Koppe, W.; Bareth, G.; Miao, Y.; Chen, X.; Zhang, F. Nitrogen status estimation of winter wheat by using an Ikonos satellite image in the north china plain. In Proceedings of the International Conference on Computer and Computing Technologies in Agriculture, Beijing, China, 29–31 October 2011; pp. 174–184.
69. Mauser, W.; Bach, H. PROMET–Large scale distributed hydrological modelling to study the impact of climate change on the water flows of mountain watersheds. *J. Hydrol.* **2009**, *376*, 362–377. [CrossRef]

Three Methods of Site-Specific Yield Mapping as a Data Source for the Delineation of Management Zones in Winter Wheat

Matthias Stettmer [1,*], Martin Mittermayer [2], Franz-Xaver Maidl [2], Jürgen Schwarzensteiner [3], Kurt-Jürgen Hülsbergen [2] and Heinz Bernhardt [1]

1. Agricultural Systems Engineering, TUM School of Life Sciences, Technical University of Munich, 85354 Freising, Germany; heinz.bernhardt@tum.de
2. Organic Agriculture and Agronomy, TUM School of Life Sciences, Technical University of Munich, 85354 Freising, Germany; martin.mittermayer@tum.de (M.M.); maidl@tum.de (F.-X.M.); kurt.juergen.huelsbergen@tum.de (K.-J.H.)
3. Farmtastic Consulting GmbH, 94342 Irlbach, Germany; js@farmtastic.consulting
* Correspondence: matthias.stettmer@tum.de

Abstract: In this study, three digital, site-specific, yield-mapping methods for winter wheat were examined, and their precision was evaluated. The crop yields of heterogeneous fields at three locations were determined on a site-specific basis using a yield-recording system composed of a combine harvester and algorithms based on reflection measurements made via satellites, as well as a tractor-mounted sensor. As a reference, the yield was determined with a plot harvester (ground truth data). The precision of the three methods was evaluated via statistical indicators (mean, median, minimum, maximum, and standard deviation) and correlation analyses between the yield of the ground truth data and the respective method. The results show a yield variation of 4.5–10.9 t ha^{-1} in the trial fields. The yield of the plot harvester was strongly correlated with the yield estimate from the sensor data (R^2 = 0.71–0.75), it was moderately correlated with the yield estimate from the satellite data (R^2 = 0.53–0.68), and it ranged from strongly to weakly correlated with the yield map of the combine harvester (R^2 = 0.30–0.72). The absolute yield can be estimated using sensor data. Slight deviations (<10%) in the absolute yield are observed with the combine harvester, and there are clear deviations ($\pm$48%) when using the satellite data. The study shows differences in the precision and accuracy of the investigated methods. Further research and optimization are urgently needed to determine the exactness of the individual methods.

Keywords: management zones; yield variability; site-specific farming; winter wheat; sensor data; remote sensing

1. Introduction

Yield is the most important target criterion in crop production [1]. The crop yield determines the resource efficiency (nitrogen efficiency and energy efficiency) [2,3], environmental impact [4,5], and profitability of crop production [6,7]. The literature shows enormous differences in yields among fields in different soil and/or climatic areas around the world [8,9]. Various studies on the yield of winter wheat show a variation of 6.3 to 12.9 t ha^{-1} in southern Germany [5], 3.8 to 6.9 t ha^{-1} in eastern Germany [10], and 0.6 to 4.9 t ha^{-1} in the wheatbelt of Western Australia [11]. The crop yield depends on numerous overlapping influencing factors (genetic potential of the variety, fertilization, crop protection, and yield potentials of the soil and climate) [12–14]. The major reasons for these strong yield fluctuations are the differences in the yield potential of the soil, the topography, and the complex interactions with the climate and weather [15–17]. Soil properties such as soil texture, available water capacity, humus content, nutrient content, and pH vary at very small scales, leading to yield variations [5,18,19]. This results in small-scale fluctuating nutrient balances and nutrient stocks in soil, resulting in high emissions and nitrate losses

in areas with low yield potential and overfertilization [5,20]. Nitrate loss into groundwater is a major problem [21]. Therefore, systems that are adapted to small-scale yield variations in crop management and fertilization will be required in the future. Site-specific land management, especially site-specific nitrogen fertilization, is promising [22–25]. This method can reduce the N surplus while increasing the N efficiency [4,5,26,27]. A prerequisite for the successful use of these digital methods is the delineation of management zones. Various parameters, such as yield maps (combine harvester data and hand sampling), biomass maps (satellite data), and soil parameters (available nitrogen, soil organic carbon, pH, available potassium, and bulk density), can be used to define the management zones of a field [28,29]. These parameters can be determined using different modern technologies such as multi- or hyperspectral measurements by sensors, drones or satellites, and georeferenced soil sampling.

Yield maps are one of the most important data sources for the delineation of management zones for site-specific fertilization; they can be supplemented with current crop measurements (e.g., nitrogen uptake with sensors or satellites) [1,30–32]. Recording the relative yield variability and absolute yield is important for precise site-specific fertilization [33]. A prerequisite for the development and use of yield maps is the availability of georeferenced yield data, which can be determined using various digital technologies [30,34,35]. Yield maps that are modeled based on these technologies may tend to over- or underestimate yield [36]. Additionally, there are various methods of filtering yield data based on the presence of outliers. Filter functions based on yield limits, moisture limits, travel distance, and yield surges are often used for this [37].

In this study, three different site-specific yield-mapping methods (sensor, satellite, and combine harvester) for winter wheat were investigated to evaluate their precision and suitability as a data basis for the delineation of yield and management zones for site-specific land management. For this purpose, plot trials were conducted in 2018, 2020, and 2021 at three different locations in southern Germany. The trials analyzed the precision of individual methods when mapping the harvested yield in the partial area, which is important to ensure the accuracy of the yield maps generated by these methods. The following aspects were investigated: (a) how accurately can the relative yield variation in the field be identified by the methods, and (b) how accurately can the methods estimate the absolute yield. In the trial plots, the yield was determined using a plot combine harvester (ground truth data) and digital georeferenced methods (sensor, satellite, and combine harvester). Correlation analyses that were determined using different methods evaluated the relationships among. Based on the results, the tested methods' accuracy, precision, and suitability as the data basis for the delineation of management zones are evaluated.

2. Materials and Methods

2.1. Site and Weather Conditions

Three fields were selected for the study: in 2018, a field at the Dürnast Research Station (48°40′66″ N 11°69′49″ E), 3 km west of Freising (485 m a. s. l.), was selected, and in 2020 and 2021, experiments were conducted in two fields of the Makofen Research Farm (48°81′55″ N 12°74′31″ E), 15 km southeast of Straubing (320 m a. s. l.) (Figure 1). The trial field in Dürnast consists of medium-quality soil with hilly relief. The trial fields in Makofen are flat and characterized by very fertile loess soil. This classification is based on the soil fertility index [38]. Table 1 shows the most important soil parameters of the trial fields.

An overview of temperature and precipitation at the trial sites is provided in Table 2. The 20-year mean annual precipitation is 789 mm, and the mean annual temperature is 8.7 °C at the Dürnast Research Station (Table 2). At the Makofen Research Farm, the 20-year mean annual precipitation is 781 mm, and the mean annual temperature is 9.5 °C (Table 2).
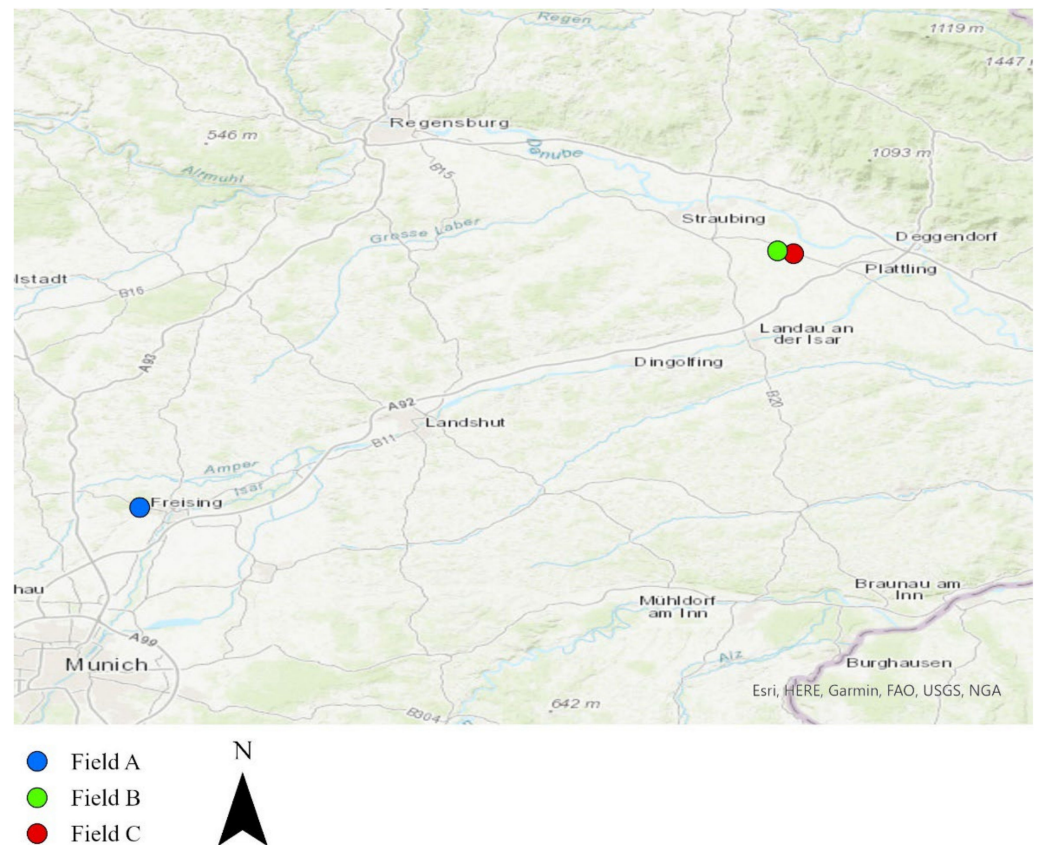
Field A
Field B
Field C

N

Figure 1. Trial sites.

Table 1. Soil data—Dürnast Research Station and Makofen.

Property	Unit	Field A	Field B	Field C
Soil classification		Cambisol	Cambisol	Cambisol
Soil type		Silty loam	Silty loam	Silty loam
Soil fertility index *		55–60	75–85	70–80
Sand (0–30 cm)	%	40.5	6.0	6.9
Silt (0–30 cm)	%	39.5	70.1	69.4
Clay (0–30 cm)	%	20.0	23.9	23.7
Available water capacity (in 10 cm)	Vol.%	17.0	24.0	23.2
Soil organic carbon content (0–30 cm)	% DM	1.4	1.2	1.4
Soil total nitrogen content (0–30 cm)	% DM	0.13	0.14	0.12
Plant available phosphorus content (0–30 cm)	mg $(100 \text{ g})^{-1}$	13.7	14.8	17.9
Plant available potassium content (0–30 cm)	mg $(100 \text{ g})^{-1}$	15.2	17.7	18.4
pH (0–30 cm)		6.2	6.5	6.9

* The soil fertility index is a quantitative assessment of soil fertility given in integers in a range of 0–100, with 100 representing the most fertile soil in Germany [38].

2.2. Crop Management

In 2018, the Reform winter wheat variety was grown on the trial field after grain corn. In 2020 and 2021, the Meister variety was grown on trial fields after sugar beet. In all trial years, the seedbed preparation was performed with plow and rotary harrow. Sowing, plant protection, and fertilization were uniformly conducted on the trial fields. Fertilization was conducted according to the fertilizer ordinance. Plant protection was conducted according to the infestation situation. Table 3 shows the crop management.

Table 2. Mean temperature and precipitation—Dürnast Research Station and Makofen.

	Unit	January to March	April to June	July to September	October to December	Year
2000–2020 Dürnast						
Temperature x̄	°C	1.1	13.2	16.8	3.8	8.7
Precipitation ∑	mm	151	257	236	145	789
2018 Dürnast						
Temperature x̄	°C	1.3	15.7	18.0	5.7	10.2
Precipitation∑	mm	143	218	209	158	728
2000–2020 Makofen						
Temperature x̄	°C	1.4	14.4	17.3	4.7	9.5
Precipitation ∑	mm	170	209	230	172	781
2020 Makofen						
Temperature x̄	°C	3.7	13.9	18.3	5.1	10.3
Precipitation ∑	mm	149	189	176	141	655
2021 Makofen						
Temperature x̄	°C	1.8	13.1	17.3	4.4	9.2
Precipitation ∑	mm	129	268	250	165	812

Table 3. Crop management of the trial fields.

Field	Treatment	Unit	Amount	Product	Date
A	Sowing	kg/ha^{-1}	158	Reform	26 October 2017
A	First N fertilization	kg/ha^{-1}	58	Inno Fert Star	4 April 2018
A	Second N fertilization	kg/ha^{-1}	59	CAN	8 May 2018
A	Third N fertilization	kg/ha^{-1}	50	CAN	29 May 2018
A	N fertilization, total	kg/ha^{-1}	167		
A	Plant protection	L/ha^{-1}	0.8	CCC 720	14 April 2018
A	Plant protection	kg/ha^{-1}	0.22	Broadway	14 April 2018
A	Plant protection	L/ha^{-1}	2.0/0.075	Adexar/Karate	26 May 2018
B	Sowing	kg/ha^{-1}	156	Meister	27 October 2019
B	First N fertilization	kg/ha^{-1}	60	ASN	28 March 2020
B	Second N fertilization	kg/ha^{-1}	80	CAN	30 April 2020
B	Third N fertilization	kg/ha^{-1}	40	CAN	20 May 2020
B	N fertilization, total	kg/ha^{-1}	180		
B	Plant protection	kg/ha^{-1}	0.05/0.07	Biathlon, Concert	7 April 2020
B	Plant protection	L/ha^{-1}	0.5	CCC 720	7 April 2020
B	Plant protection	L/ha^{-1}	1.25/0.075	Capalo/Karate	16 May 2020
B	Plant protection	L/ha^{-1}	2.0	Osiris	13 June 2020
C	Sowing	kg/ha^{-1}	205	Meister	10 November 2020
C	First N fertilization	kg/ha^{-1}	78	ASN	4 March 2021
C	Second N fertilization	kg/ha^{-1}	54	CAN	8 May 2021
C	Third N fertilization	kg/ha^{-1}	40	CAN	4 June 2021
C	N fertilization, total	kg/ha^{-1}	172		
C	Plant protection	kg/ha^{-1}	0.13	Broadway	22 April 2021
C	Plant protection	L/ha^{-1}	0.25/0.5	Pixxaro/CCC 720	22 April 2021
C	Plant protection	L/ha^{-1}	1.0/0.3	Revystar/Flexity	20 May 2021
C	Plant protection	L/ha^{-1}	1.0/0.075	Ascra Xpro/Karate	11 June 2021

2.3. Experimental Design

The trial fields were divided into a grid of 15 m × 30 m plots. The outer 25 m of the trial fields were not included in the data analysis to avoid evaluating data from areas that did not belong to the field. This is important for methods based on satellite data in a 10 × 10 m grid to exclude measurement errors along the field edges [39]. The experimental

setup was the same for all three experimental years, and only the number of plots differed (2018: *n* = 93; 2020: *n* = 106; 2021: *n* = 150) due to the different field sizes over the years. Figure 2 shows the experimental setup in 2020.
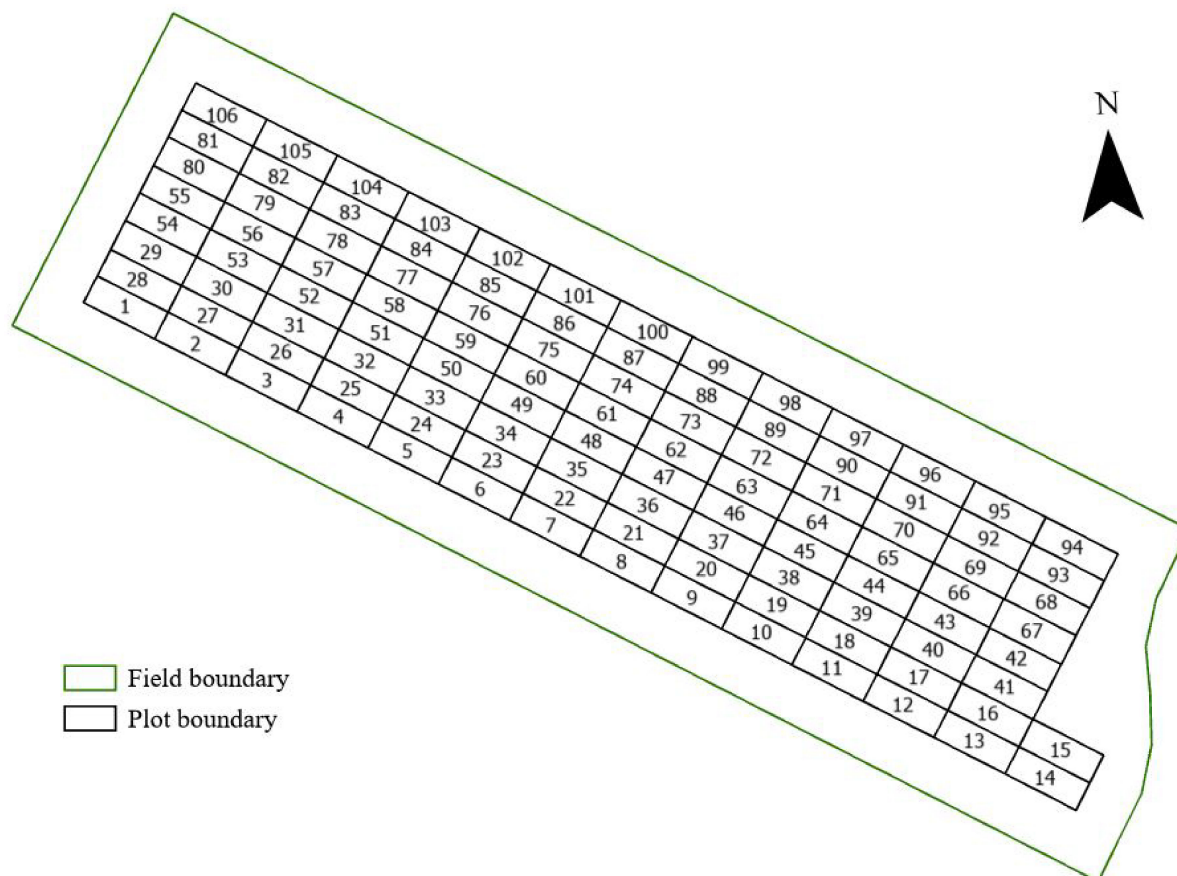
Figure 2. Experimental setup (Field B, 2020).

2.4. Methods of Determining Yield

The wheat yield per plot was determined using the following methods:

- Plot harvester (ground truth data) [40];
- Combine harvester with yield mapping (mass flow sensor) [34];
- Process of Radiation, Mass, and Energy Transfer (PROMET) plant growth model based on satellite data (Sentinel-2) [41];
- Algorithm based on reflection measurements using a tractor-mounted multispectral sensor [42,43].

The winter wheat yield was determined with the plot harvester and the combine harvester with yield mapping (mass flow sensor) in the trial years on harvest dates of 27 July 2018, 30 July 2020, and 10 August 2021. A New Holland CX 8050 was used in 2018, and a John Deere S780 was used in 2020 and 2021 to map yields with a combine harvester. The PROMET estimate data were made available by the developer Vista GmbH. Depending on the availability, the PROMET plant growth model used satellite data shortly before the harvest date to estimate the yield [36]. Based on satellite data, the PROMET plant growth model calculated the yield considering further data [36]. The PROMET model requires four groups of model inputs that affect the spatial simulation of crop yield:

- Agricultural management (sowing date, fertilization events, harvest date);
- Crop specifications (variety, photoperiod sensitivity, assimilation rate);
- Dynamic environmental driver variables (temperature, precipitation, radiation, wind);
- Static environmental parameters (location, terrain, and soil properties) [36].

The reflection measurement for the algorithm by Maidl et al. [42] was conducted in the BBCH 65 growth stage. Based on this measurement, the REIP 700 vegetation index was calculated, and the algorithms used to estimate the yield were based on this index [42].

2.5. Data Processing

Considering the corresponding methodology, different digital methods were used to determine the yield for the entire field. Yield maps were generated based on point data. Next, these point data were visualized using geoinformation system software, ArcGIS [44], and assigned to the digitized plots via their coordinates. Data points on or outside the plot edges were eliminated. Depending on the method, the recorded yield data varied in terms of the spatial resolution and distribution in the plots. The plot combine harvester and combine harvester were driven immediately next to each other throughout the plot. Figure 3 shows the structure and data distribution of a plot in detail. The mean was calculated using all available yield values per plot. Thus, the yield per plot in t ha^{-1} was determined for each method for further analysis.
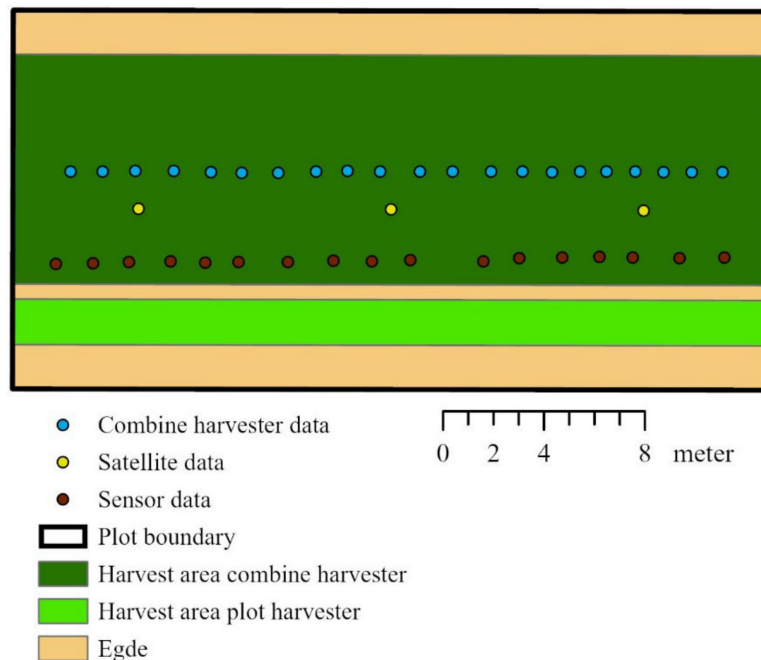
Figure 3. Structure and data distribution in the plot.

2.6. Descriptive Statistics

The mean, median, minimum, maximum, and standard deviation were calculated for each method using R.

2.7. Correlation Analysis

Correlation analyses based on the yield per plot in t ha^{-1} determined the relationships between the yield values of the tested digital methods and the ground truth data. The coefficients of determination (R^2) were classified as very strong ($R^2 > 0.9$), strong ($0.9 > R^2 > 0.7$), moderate ($0.7 > R^2 > 0.5$), weak ($0.5 > R^2 > 0.3$), or very weak ($R^2 < 0.3$) [45].

3. Results

3.1. Spatial Variation in the Wheat Yield in 2018 (Field A)

Different site-specific yield mapping methods in 2018 led to different results for the yield distribution pattern, yield variation, and mean wheat yield in Field A (Figure 4, Table 4). The wheat yield, as determined by the plot harvester, varied between 6.1 and 10.9 t ha^{-1}. The wheat yield measured by the mass flow sensor of the combine harvester

(6.1–10.9 t ha^{-1}) and the yield estimation made using algorithms based on sensor data (6.1–10.4 t ha^{-1}) also varied, quite similarly to the ground truth data. The yield estimate made by the PROMET plant growth model based on satellite data (3.1–5.6 t ha^{-1}) was also characterized by variability, but the yield variation of this method was not as great as those with the other methods, and a significantly lower yield level was noticeable (Figure 4). The mean wheat yield in field A, determined with the plot harvester, was 8.1 t ha^{-1}, exactly corresponding to the sensor data yield; furthermore, when determined by the mass flow sensor of the combine harvester it was higher at 8.8 t ha^{-1} and when based on the satellite data it was lower at 4.2 t ha^{-1}. This resulted in a deviation of +9% in the mean wheat yield of the combine harvester (mass flow sensor) and −48% when based on the satellite data compared to the ground truth data.
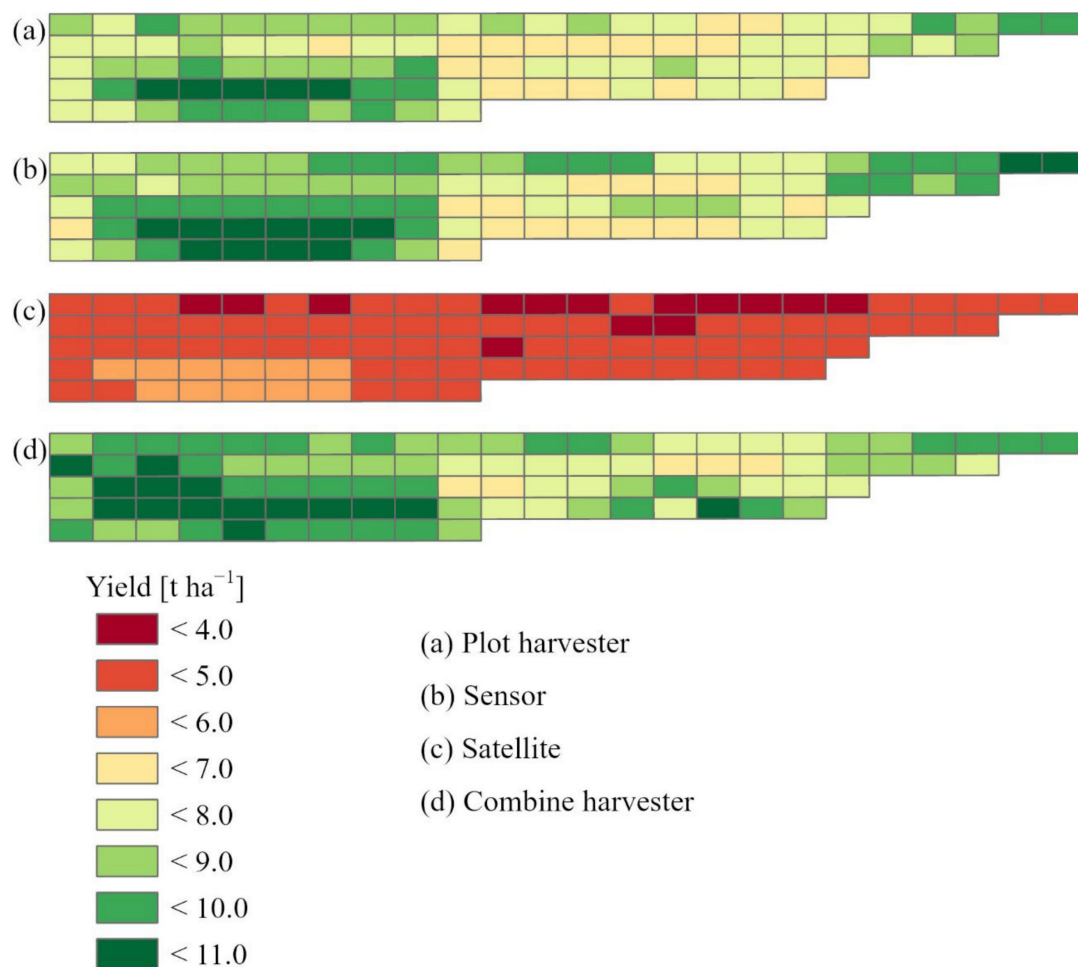
Figure 4. Yield maps 2018, Field A. Yield determined from the plot harvester, sensor data, satellite data, and combine harvester.
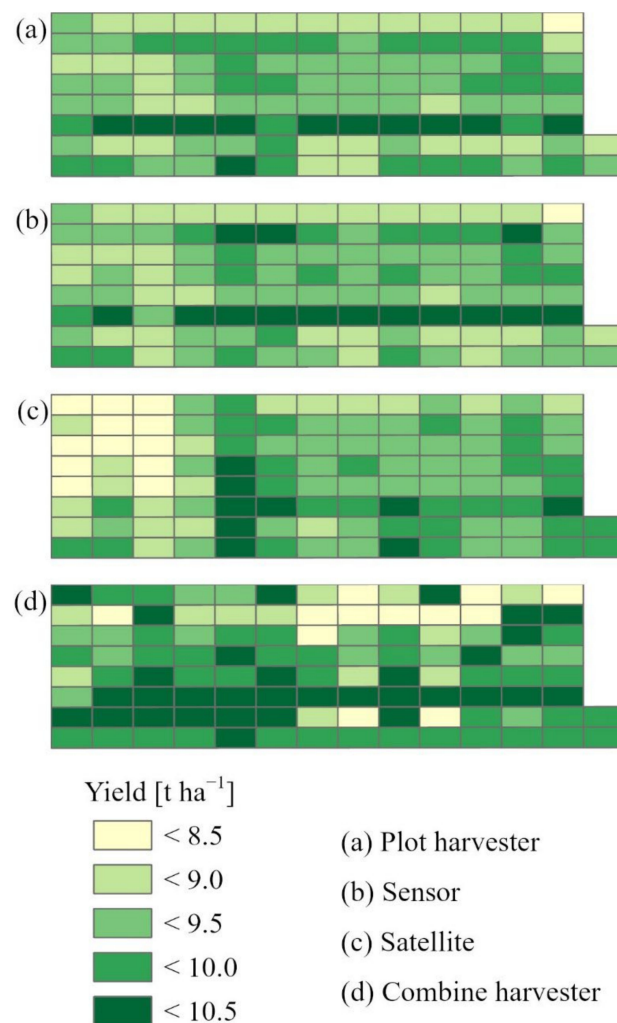
3.2. Spatial Variation in the Wheat Yield in 2020 (Field B)

The yields in 2020, determined using different digital methods, led to similar overall results. In contrast to 2018, the yield variability was significantly lower in 2020 (Figure 5, Table 4). The yield variation based on satellite data (8.3–10.1 t ha^{-1}) and determined by the mass flow sensor of the combine harvester (8.4–10.2 t ha^{-1}) corresponded to the ground truth data (8.4–10.1 t ha^{-1}). The yield estimate based on the sensor data showed a slightly higher yield variability (6.8–10.4 t ha^{-1}). However, the yield distribution pattern matched the ground truth data well (Figure 5). The mean wheat yield of the ground truth data for field B was 9.3 t ha^{-1} and corresponded with the yields based on the sensor and satellite

data, while that determined by the mass flow sensor of the combine harvester (9.8 t ha^{-1}) was slightly higher. Overall, the deviations in the mean wheat yields were small (<5%).

**Table 4.** Descriptive statistics of the yield data in t ha^{-1} analyzed in this study.

Variable	n	Year	Field	Unit	Mean	Median	Minimum	Maximum	Standard Deviation	Skewness
Plot harvester	93	2018	A	t ha^{-1}	8.1	8.0	6.1	10.9	1.1	0.42
Sensor data	93	2018	A	t ha^{-1}	8.1	8.1	6.1	10.4	1.0	0.18
Satellite data	93	2018	A	t ha^{-1}	4.2	4.3	3.1	5.6	0.7	0.08
Combine harvester	93	2018	A	t ha^{-1}	8.8	8.9	6.1	10.9	1.1	−0.11
Plot harvester	106	2020	B	t ha^{-1}	9.3	9.3	8.4	10.1	0.2	0.2
Sensor data	106	2020	B	t ha^{-1}	9.4	9.3	6.8	10.4	0.9	−0.4
Satellite data	106	2020	B	t ha^{-1}	9.3	9.3	8.3	10.1	0.3	−0.74
Combine harvester	106	2020	B	t ha^{-1}	9.8	9.8	8.4	10.2	0.2	−2.7
Plot harvester	150	2021	C	t ha^{-1}	5.9	5.9	4.5	7.5	0.5	0.35
Sensor data	150	2021	C	t ha^{-1}	5.9	6.0	4.4	7.2	0.5	−0.61
Satellite data	150	2021	C	t ha^{-1}	8.5	8.6	7.2	9.6	0.5	−0.34
Combine harvester	150	2021	C	t ha^{-1}	5.7	5.7	3.7	7.8	0.7	0.13

Yield [t ha^{-1}]
< 8.5
< 9.0
< 9.5
< 10.0
< 10.5

(a) Plot harvester
(b) Sensor
(c) Satellite
(d) Combine harvester

Figure 5. Yield maps 2020, Field B. Yield determined from the plot harvester, sensor data, satellite data, and combine harvester.

3.3. Spatial Variation in the Wheat Yield in 2021 (Field C)

In 2021, there were differences in the results of various digital methods (Figure 6, Table 4). As in 2018, the yields determined using satellite data with the PROMET model clearly differed from the results of the other yield-mapping systems. However, the yields based on the satellite data were much higher in 2021 and much lower than the results of the other measurement systems in 2018 (Figures 4 and 6). The yields of the combine harvester (3.7–7.8 t ha^{-1}) and the sensor data (4.4–7.2 t ha^{-1}) were very similar to the ground truth data (4.5–7.5 t ha^{-1}) in terms of yield variation and distribution pattern. The yield estimate based on the satellite data (7.2–9.6 t ha^{-1}) showed less yield variation at a significantly higher yield level (Figure 6), resulting in a deviation of +44% in the mean wheat yield of the satellite data (8.5 t ha^{-1}) compared to the ground truth data (5.9 t ha^{-1}) in field C. The mean wheat yields of the combine harvester and sensor data corresponded to the ground truth data.
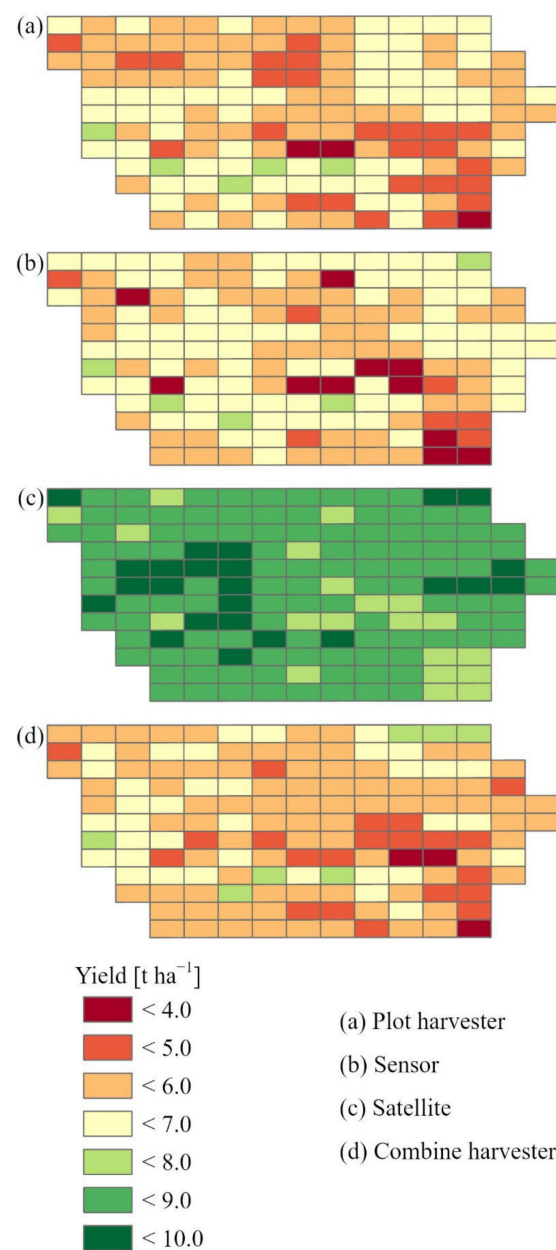
Figure 6. Yield maps 2021, Field C. Yield determined from the plot harvester, sensor data, satellite data, and combine harvester.

3.4. Correlation between Variables

Table 5 shows the coefficients of determination (R^2) of the linear and polynomial relationships (second degree) of the wheat yields, determined using various digital methods.

Table 5. Coefficients of determination (R^2): yield data for 2018 ($n = 93$), 2020 ($n = 106$), and 2021 ($n = 150$).

| R^2	Sensor 2018	Satellite 2018	Combine 2018	Sensor 2020	Satellite 2020	Combine 2020	Sensor 2021	Satellite 2021	Combine 2021
Plot harvester (linear) 2018	0.74	0.68	0.69						
Plot harvester (polynomial) 2018	0.75	0.68	0.69						
Plot harvester (linear) 2020				0.69	0.51	0.25			
Plot harvester (polynomial) 2020				0.71	0.53	0.30			
Plot harvester (linear) 2021							0.67	0.54	0.72
Plot harvester (polynomial) 2021							0.71	0.56	0.72

3.4.1. Field A (2018)

In 2018, the correlation analysis showed a strong relationship between the ground truth data and the yield estimate from the sensor data ($R^2 = 0.75$). The yield estimate from the satellite data ($R^2 = 0.68$) and the yield map from the combine harvester ($R^2 = 0.69$) were moderately correlated with the ground truth data.

3.4.2. Field B (2020)

In 2020, the correlations between the yield data of the tested methods were very different. As in the previous year, there was a strong relationship between the ground truth data and the yield estimate based on sensor data ($R^2 = 0.71$). The yield estimates from the satellite data and ground truth data showed a moderate correlation ($R^2 = 0.53$), while that from the combine harvester only weakly correlated with the ground truth data ($R^2 = 0.30$) (Table 5).

3.4.3. Field C (2021)

In 2021, all the methods resulted in moderate or strong relationships. Strong correlations were determined between the ground truth data and the yield data from the combine harvester ($R^2 = 0.72$) as well as the sensor data ($R^2 = 0.71$). The correlation between the ground truth data and the estimate from the satellite data ($R^2 = 0.56$) was moderate (Figure 7 and Table 5).
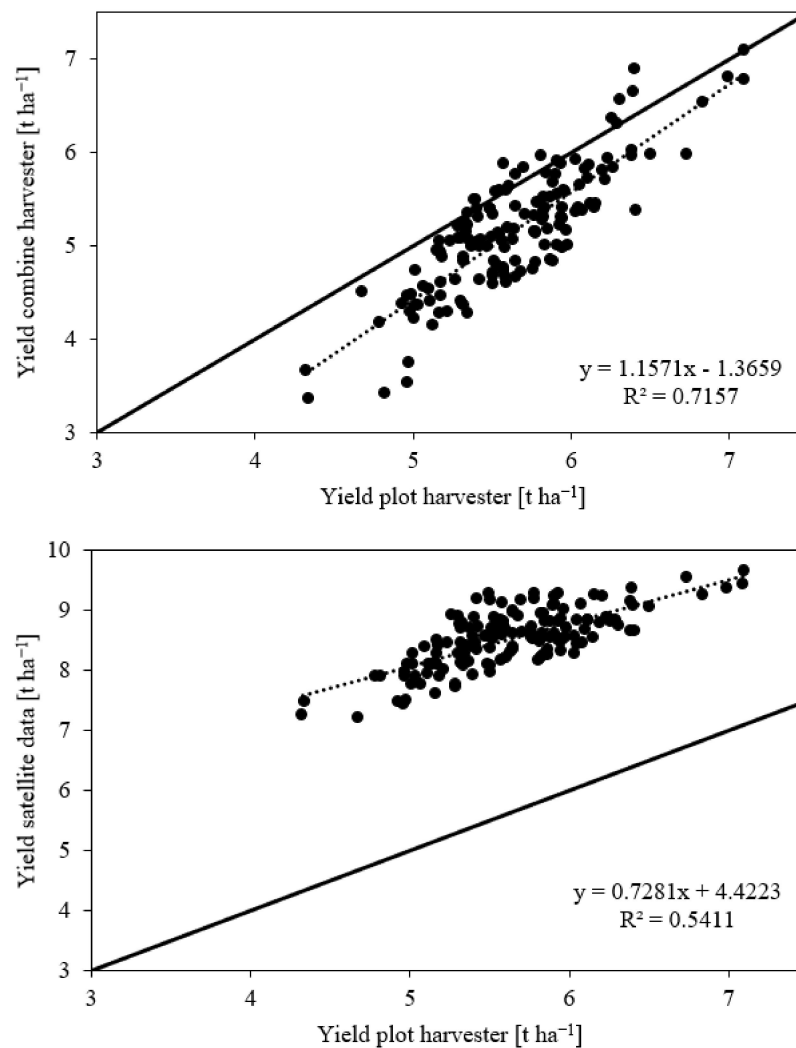
Figure 7. The linear relationships between the yields of ground truth data (plot harvester) and combine harvester (**above**) as well as satellite data (**below**) in field C in 2021.

4. Discussion

4.1. Discussion of the Methods

In this study, three different site-specific yield-mapping methods for winter wheat were tested on heterogeneous fields at three locations in southern Germany. The precision of the methods was tested by comparing the statistical indicators (mean, median, minimum, maximum, and standard deviation), mapping the yield distribution patterns and investigating the correlative relationships. The aim was to identify the yield distribution patterns and analyze the absolute wheat yields.

4.1.1. Site Selection

The yield variability results were particularly influenced by the heterogeneity of the trial fields [46,47]. In homogeneous fields, a lower yield variation was expected; therefore, these fields were not suitable for a comparison of the methods [5,48]. As a result, heterogeneous fields were selected for this investigation. The heterogeneity was assessed based on soil properties, biomass maps, and the expertise of the farm managers. The expertise of the farm managers was a suitable basis for assessing the heterogeneity of a field [49]. Furthermore, the literature shows that small-scale variations in the soil parameters and yield are characteristic of the study region [50].

4.1.2. Ground Truth Data

The yield data were determined using various digital methods. Suitable ground truth data (yield measurements) were crucial in evaluating the various digital yield-mapping methods so that the modeled data could be compared with the measured data [5]. Therefore, in this study, all plots were harvested by a plot harvester with a weighing system [40]. The plot harvester facilitated the determination of the correct wheat yield per plot and the evaluation of the yield maps determined using digital methods. The plot harvester and combine harvester could not harvest the same area, resulting in minor deviations in their measured values. They drove next to each other through the plots. However, the variance in the difference decreases with the distance between two measurement points, which is the basis for the geostatistical methods (kriging interpolation) used in many studies on yield variability [5,51–53]. Therefore, this approach provided ground truth data with very high measurement accuracy.

Since the use of a plot harvester is labor-intensive and can hardly be implemented for large fields, similar studies compared the modeled yield data with the yield map data from a combine harvester [1,32,54]. However, this requires high precision when mapping yields with a combine harvester. Investigations showed considerable uncertainties in mapping yields using a combine harvester due to various error sources. Sensor errors, operating errors, errors due to operating conditions, and data processing were the most common causes of uncertainty [34,55,56]. In particular, constantly changing operating conditions during harvest, different measurement systems, and principles for combine harvesters from different manufacturers and, sometimes, missing or inaccurate calibration led to uncertainties in the combine harvester data [57–59]. Despite further development of the yield-mapping systems in combine harvesters, the fluctuation in the correlations between the ground truth data and the combine harvester data from R^2 = 0.30 to 0.72 showed clear differences in the precision of the combine harvester data in this study. In a study by Hülsbergen et al. [60], the combine harvester data from individual fields were strongly correlated with ground truth data (plot harvester and biomass samples), while this correlation was weak in other fields. Therefore, the ground truth data from the plot harvester were of immense importance to the evaluation of various methods in this study. Alternatively, georeferenced biomass samples can also provide ground truth data. However, the measurement effort is a limiting factor. Mittermayer et al. [5] collected 50 biomass samples in a 13.1 ha area in his investigations, determined the yield with a laboratory thresher, and conducted data analysis using geostatistical methods.

4.2. Discussion of the Results

The yield variation in the three trial years (2018: 6.1 to 10.9 t ha^{-1}, 2020: 8.4 to 10.1 t ha^{-1}, and 2021: 4.5 to 7.5 t ha^{-1}) was clear. By analyzing several fields and research years, the optimal conditions to evaluate the precision of various digital yield-mapping methods were given. Several scientific studies addressed the mapping of the yield variability of winter wheat, but most of these studies only used one method [10,23,32,36,52]. Only a few studies compared ground truth data with data from different digital systems.

4.2.1. Sensor Data

The yield estimate based on multispectral sensor data, the REIP vegetation index, and a crop-specific yield algorithm [42] provided high-precision yield maps in all three years (2018: R^2 = 0.75, 2020: R^2 = 0.71, and 2021: R^2 = 0.71). In addition, this method showed only minor deviations in the yield variation and the mean wheat yield of max. ±1%. Hauser et al. [10] also compared plot harvester data with sensor data and achieved similar results (R^2 = 0.70). Kaivosoja et al. [54] compared sensor data with combine harvester data and found a strong correlation (R^2 = 0.82). These results confirm the potential of continuously generating very precise yield data from sensor data. The prerequisites for obtaining high yield-mapping accuracy using this method are multispectral sensors

with high measurement accuracy, suitable vegetation indices, and scientific-based yield algorithms [42,61,62].

4.2.2. Combine Harvester

The yield data of the combine harvester (mass flow sensor) provided yield maps of at least moderate or good quality in 2018 and 2021 (2018: R^2 = 0.69 and 2021: R^2 = 0.72). In 2020, however, the combine harvester data were only weakly correlated with the ground truth data (R^2 = 0.30). A maximum deviation in the yield variation and the mean wheat yield of ±9% showed that the bad correlation in 2020 was mainly due to an incorrect mapping of the yield distribution pattern. A New Holland combine harvester was used in 2018, while a John Deere combine harvester was used in 2020 and 2021. All three combine harvesters determined the yield using a mass flow sensor. However, the John Deere combine was equipped with "active yield" in 2021, which means that the mass flow sensor in the grain elevator was continuously calibrated using load cells installed in the grain tank [63]. This possibly led to a considerable improvement in the precision of the combine harvester data between 2020 and 2021, as all other conditions (driver, calibration, model, working width, etc.) were identical for both years. These results confirmed the conclusions of previous studies of the uncertainties in combine harvester data [34,55–57]. The central causes of uncertainties, such as calibration and automatic cutting width detection, can be improved through further developments by the manufacturer. Operating errors can be avoided through intensive driver training. Varying environmental influences and operating conditions, such as different material moisture levels, soiling of the sensors by crop residues, abrupt changes in speed, or grain plants lying on the ground will limit the accuracy of combine harvester data in the future [58,59]. However, the strong correlations in some cases show the combine harvesters' potential for mapping yields and their spatial variability.

4.2.3. Satellite Data

The yield maps of the PROMET plant growth model, based on satellite data, depict the yield distribution pattern moderately in all three years (2018: R^2 = 0.68, 2020: R^2 = 0.53, and 2021 R^2 = 0.56). The method achieved a maximum deviation of ±48% in the yield variation and the mean wheat yield. Since the relative yield distribution pattern was identified at least moderately in all three trial years, these significant deviations resulted from underestimating (2018) and overestimating (2021) the absolute yield. In both years, weather extremes were observed. In 2018, the weather was hotter and drier than average; in 2021, the weather was colder and wetter than average. In addition to satellite data, the PROMET plant growth model requires various groups of model inputs that affect the spatial simulation of plant development, such as agricultural management (sowing date, fertilization events, harvest date, etc.), crop specifications (variety, photoperiod sensitivity, assimilation rate, etc.), dynamic environmental driver variables (temperature, precipitation, radiation, wind, etc.), and static environmental parameters (location, terrain, and soil properties) [36]. The model may react too strongly to weather data, which means that the model can no longer model reliable absolute yield data in years with extreme meteorological conditions. In this context, Hank et al. [36] also found tendencies to overestimate yields in extreme weather conditions. However, further studies are necessary to assess this assumption and the precision of satellite data-based methods in more detail [5,24,64]. Hank et al. [36] also compared the modeled yield data of the PROMET plant growth model with combine harvester data, finding a strong correlation (R^2 = 0.82). Toscano et al. [59] correlated Sentinel 2 and Landsat 8 satellite data with yield data from hand samples and combine harvesters and found correlations varying from moderate to strong (R^2 = 0.54–0.74). Zhao et al. [32] also compared Sentinel 2 satellite data with combine harvester data and found a stronger correlation (R^2 = 0.76). These results confirm the potential to derive yield zones with satellite data. However, the absolute yield can deviate for data modeled with PROMET based on satellite data, leading to crop management problems. For example, in the case of yield maps for fertilization, the absolute yield is important; otherwise, the crop would

be fertilized incorrectly. Therefore, further investigations are urgently needed to reduce deviations, such as those conducted in 2018 and 2021.

5. Conclusions

Yield maps are one of the most important sources of data for the delineation of management zones for site-specific land management. Therefore, precise yield maps are required to derive high-quality management zones. The results of this study show that the yield maps from the sensor data are best suited to delineate management zones. The yield maps of the combine harvester in 2018 and 2021 are also quite suitable, unlike those from 2020. This can lead to faulty management zones. Incorrect management zones result in inefficient crop management, thus causing environmental pollution. Therefore, further investigations are needed to optimize and develop yield-mapping systems for combine harvesters. The aim should be to generate yield maps with consistent quality, using modern combine harvesters to collect high-quality data easily and inexpensively during harvest. The results of the satellite data depict the relative yield distribution patterns as being moderate over all trial years and are, therefore, suitable for the creation of relative biomass maps. However, due to the deviations in the absolute yields, these results are only suitable for yield potential maps to a limited extent, and further research is required to improve the results. Overall, each method shows enormous potential to generate yield maps. Nevertheless, there are individual problems that urgently need further investigation to improve the precision of all methods.

Author Contributions: Conceptualization, M.S. and F.-X.M.; methodology, M.S. and F.-X.M.; investigation, M.S. and M.M.; data curation, M.S. and M.M.; writing—original draft preparation, M.S.; writing—review and editing, M.M., F.-X.M., K.-J.H. and H.B.; project administration, J.S.; funding acquisition, J.S. All authors have read and agreed to the published version of the manuscript.

Institutional Review Board Statement: Not applicable.

Informed Consent Statement: Not applicable.

Data Availability Statement: The data presented in this study are available from the corresponding author upon reasonable request.

Conflicts of Interest: The authors declare no conflict of interest.

References

1. Hunt, M.L.; Blackburn, G.A.; Carrasco, L.; Redhead, J.W.; Rowland, C.S. High resolution wheat yield mapping using Sentinel-2. *Remote Sens. Environ.* **2019**, *233*, 111410. [CrossRef]
2. Barraclough, P.B.; Howarth, J.R.; Jones, J.; Lopez-Bellido, R.; Parmar, S.; Shepherd, C.E.; Hawkesford, M.J. Nitrogen efficiency of wheat: Genotypic and environmental variation and prospects for improvement. *Eur. J. Agron.* **2010**, *33*, 1–11. [CrossRef]
3. Duan, J.; Shao, Y.; He, L.; Li, X.; Hou, G.; Li, S.; Feng, W.; Zhu, Y.; Wang, Y.; Xie, Y. Optimizing nitrogen management to achieve high yield, high nitrogen efficiency and low nitrogen emission in winter wheat. *Sci. Total Environ.* **2019**, *697*, 134088. [CrossRef]
4. Cui, Z.; Zhang, F.; Chen, X.; Dou, Z.; Li, J. In-season nitrogen management strategy for winter wheat: Maximizing yields, minimizing environmental impact in an over-fertilization context. *Field Crops Res.* **2010**, *116*, 140–146. [CrossRef]
5. Mittermayer, M.; Gilg, A.; Maidl, F.X.; Nätscher, L.; Hülsbergen, K.J. Site-specific nitrogen balances based on spatially variable soil and plant properties. *Precis. Agric.* **2021**, *22*, 1416–1436. [CrossRef]
6. Fan, R.; Zhang, X.; Liang, A.; Shi, X.; Chen, X.; Bao, K.; Yang, X.; Jia, S. Tillage and rotation effects on crop yield and profitability on a Black soil in northeast China. *Can. J. Soil Sci.* **2012**, *92*, 463–470. [CrossRef]
7. Klima, K.; Kliszcz, A.; Puła, J.; Lepiarczyk, A. Yield and profitability of crop production in mountain less favoured areas. *Agronomy* **2020**, *10*, 700. [CrossRef]
8. Hakojärvi, M.; Hautala, M.; Ristolainen, A.; Alakukku, L. Yield variation of spring cereals in relation to selected soil physical properties on three clay soil fields. *Eur. J. Agron.* **2013**, *49*, 1–11. [CrossRef]

9. Zebarth, B.J.; Fillmore, S.; Watts, S.; Barrett, R.; Comeau, L.P. Soil factors related to within-field yield variation in commercial potato fields in Prince Edward Island Canada. *Am. J. Potato Res.* **2021**, *98*, 139–148. [CrossRef]

10. Hauser, J.; Maidl, F.X.; Wagner, P. Untersuchung der teilflächenspezifischen Ertragserfassung von Großmähdreschern in Winterweizen (Investigation of site-specific yield mapping of combine harvesters in winter wheat). In Proceedings of the 41st GIL-Jahrestagung, Potsdam, Germany, 8–9 March 2021; pp. 133–138.

11. Robertson, M.J.; Lyle, G.; Bowden, J.W. Within-field variability of wheat yield and economic implications for spatially variable nutrient management. *Field Crops Res.* **2008**, *105*, 211–220. [CrossRef]

12. Bertic, B.; Loncaric, Z.; Vukadinovic, V.; Vukobratovic, Z.; Vukadinovic, V. Winter wheat yield responses to mineral fertilization. *Cereal Res. Commun.* **2007**, *35*, 245–248. [CrossRef]

13. Cabas, J.; Weersink, A.; Olale, E. Crop yield response to economic, site and climatic variables. *Clim. Chang.* **2009**, *101*, 599–616. [CrossRef]

14. Fasoula, V.A.; Fasoula, D.A. Principles underlying genetic improvement for high and stable crop yield potential. *Field Crops Res.* **2002**, *75*, 191–209. [CrossRef]

15. Buttafuoco, G.; Castrignanò, A.; Colecchia, A.S.; Ricca, N. Delineation of management zones using soil properties and a multivariate geostatistical approach. *Ital. J. Agron.* **2010**, *5*, 323–332. [CrossRef]

16. Farid, H.U.; Bakhsh, A.; Ahmad, N.; Ahmad, A.; Mahmood-Khan, Z. Delineating site-specific management zones for precision agriculture. *J. Agric. Sci.* **2016**, *154*, 273–286. [CrossRef]

17. Moral, F.J.; Terrón, J.M.; Rebollo, F.J. Site-specific management zones based on the Rasch model and geostatistical techniques. *Comput. Electron. Agric.* **2011**, *75*, 223–230. [CrossRef]

18. López-Lozano, R.; Casterad, M.A.; Herrero, J. Site-specific management units in a commercial maize plot delineated using very high resolution remote sensing and soil properties mapping. *Comput. Electron. Agric.* **2010**, *73*, 219–229. [CrossRef]

19. Servadio, P.; Bergonzoli, S.; Verotti, M. Delineation of management zones based on soil mechanical-chemical properties to apply variable rates of inputs throughout a field (VRA). *Eng. Agric. Environ.* **2017**, *10*, 20–30. [CrossRef]

20. Dalgaard, T.; Bienkowski, J.F.; Bleeker, A.; Dragosits, U.; Drouet, J.L.; Durand, P.; Frumau, A.; Hutchings, N.J.; Kedziora, A.; Magliulo, V.; et al. Farm nitrogen balances in six European landscapes as an indicator for nitrogen losses and basis for improved management. *Biogeosciences* **2012**, *9*, 5303–5321. [CrossRef]

21. Strebel, O.; Duynisveld, W.H.M.; Böttcher, J. Nitrate pollution of groundwater in western Europe. *Agric. Ecosyst. Environ.* **1989**, *26*, 189–214. [CrossRef]

22. Diacono, M.; Rubino, P.; Montemurro, F. Precision nitrogen management of wheat. A review. *Agron. Sustain. Dev.* **2013**, *33*, 219–241. [CrossRef]

23. Liu, H.; Whiting, M.L.; Ustin, S.L.; Zarco-Tejada, P.J.; Huffman, T.; Zhang, X. Maximizing the relationship of yield to site-specific management zones with object-oriented segmentation of hyperspectral images. *Precis. Agric.* **2018**, *19*, 348–364. [CrossRef]

24. Mulla, D.J. Twenty five years of remote sensing in precision agriculture: Key advances and remaining knowledge gaps. *Biosyst. Eng.* **2013**, *114*, 358–371. [CrossRef]

25. Prücklmaier, J. Feldexperimentelle Analysen zur Ertragsbildung und Stickstoffeffizienz bei Organisch-Mineralischer Düngung auf Heterogenen Standorten und Möglichkeiten zur Effizienzsteigerung durch Computer- und Sensorgestützte Düngesysteme (Field Experimental Analyses of Yield Effects and Nitrogen Efficiency of Fertilizer Application Systems). Ph.D. Thesis, Technische Universität München, Munich, Germany, 2020.

26. Argento, F.; Anken, T.; Abt, F.; Vogelsanger, E.; Walter, A.; Liebisch, F. Site-specific nitrogen management in winter wheat supported by low-altitude remote sensing and soil data. *Precis. Agric.* **2020**, *22*, 364–386. [CrossRef]

27. Vinzent, B.; Fuß, R.; Maidl, F.X.; Hülsbergen, K.J. Efficacy of agronomic strategies for mitigation of after-harvest N_2O emissions of winter oilseed rape. *Eur. J. Agron.* **2017**, *89*, 88–96. [CrossRef]

28. Brock, A.; Brouder, S.M.; Blumhoff, G.; Hofmann, B.S. Defining yield-based management zones for corn-soybean rotations. *Agron. J.* **2005**, *97*, 1115–1128. [CrossRef]

29. Yao, R.J.; Yang, J.S.; Zhang, T.J.; Gao, P.; Wang, X.P.; Hong, L.Z.; Wang, M.W. Determination of site-specific management zones using soil physico-chemical properties and crop yields in coastal reclaimed farmland. *Geoderma* **2014**, *232*, 381–393. [CrossRef]

30. Blasch, G.; Li, Z.; Taylor, J.A. Multi-temporal yield pattern analysis method for deriving yield zones in crop production systems. *Precis. Agric.* **2020**, *21*, 1263–1290. [CrossRef]

31. Jin, Z.; Azzari, G.; Lobell, D.B. Improving the accuracy of satellite-based high-resolution yield estimation: A test of multiple scalable approaches. *Agric. For. Meteorol.* **2017**, *247*, 207–220. [CrossRef]

32. Zhao, Y.; Potgieter, A.B.; Zhang, M.; Wu, B.; Hammer, G.L. Predicting wheat yield at the field scale by combining high-resolution Sentinel-2 satellite imagery and crop modelling. *Remote Sens.* **2020**, *12*, 1024. [CrossRef]

33. Maidl, F.X.; Schächtl, J.; Huber, G. Strategies for site-specific nitrogen fertilization on winter wheat. In Proceedings of the 7th International Conference on Precision Agriculture and other Precision Resources Management, Minneapolis, MN, USA, 25–28 July 2004; pp. 1938–1948.

34. Arslan, S.; Colvin, T.S. Grain yield mapping: Yield sensing, yield reconstruction, and errors. *Precis. Agric.* **2002**, *3*, 135–154. [CrossRef]

35. Birrell, S.J.; Sudduth, K.A.; Borgelt, S.C. Comparison of sensors and techniques for crop yield mapping. *Comput. Electron. Agric.* **1996**, *14*, 215–233. [CrossRef]

36. Hank, T.; Bach, H.; Mauser, W. Using a remote sensing-supported hydro-agroecological model for field-scale simulation of heterogeneous crop growth and yield: Application for wheat in central Europe. *Remote Sens.* **2015**, *7*, 3934–3965. [CrossRef]
37. Beck, A.D.; Searcy, S.W.; Roades, J.P. Yield data filtering techniques for improved map accuracy. *Appl. Eng. Agric.* **2001**, *17*, 423.
38. Bodenschätzung—Bewertung der Natürlichen Ertragsfähigkeit Landwirtschaftlicher Flächen. Available online: https://www.ldbv.bayern.de/produkte/kataster/boden.html#:~{}:text=Unter%20Bodensch%C3%A4tzung%20versteht%20man%20die,in%20Acker%2D%20und%20Gr%C3%BCnland%20unterteilt (accessed on 27 July 2022).
39. Devaux, N.; Crestey, T.; Leroux, C.; Tisseyre, B. Potential of Sentinel-2 satellite images to monitor vine fields grown at a territorial scale. *OENO One* **2019**, *53*, 52–59. [CrossRef]
40. Wintersteiger, Plot Combine. Available online: https://www.wintersteiger.com/us/Plant-Breeding-and-Research/Products/Product-range/Plot-combine (accessed on 30 June 2022).
41. Mauser, W.; Bach, H. PROMET—Large scale distributed hydrological modelling to study the impact of climate change on the water flows of mountain watersheds. *J. Hydrol.* **2009**, *376*, 362–377. [CrossRef]
42. Maidl, F.X.; Spicker, A.; Weng, J.; Hülsbergen, K.J. Ableitung des teilflächenspezifischen Kornertrags von Getreide aus Reflexionsdaten (Derivation of the site-specific grain yield from reflection data). In Proceedings of the 39th GIL-Jahrestagung, Wien, Austria, 18–19 February 2019; pp. 131–134.
43. TEC5, Spektrometer Systeme, Version 2.13. Available online: https://tec5.com/de/ (accessed on 30 June 2022).
44. ArcGIS. Map Creation and Analysis: Location Intelligence for Everyone. Available online: https://www.esri.com/de-de/arcgis/products/arcgis-online/overview (accessed on 30 June 2022).
45. Stettmer, M.; Maidl, F.X.; Schwarzensteiner, J.; Hülsbergen, K.J.; Bernhardt, H. Analysis of Nitrogen Uptake in Winter Wheat Using Sensor and Satellite Data for Site-Specific Fertilization. *Agronomy* **2022**, *12*, 1455. [CrossRef]
46. Jiang, P.; Thelen, K.D. Effect of soil and topographic properties on crop yield in a North-Central corn–soybean cropping system. *Agron. J.* **2004**, *96*, 252–258. [CrossRef]
47. Patzold, S.; Mertens, F.M.; Bornemann, L.; Koleczek, B.; Franke, J.; Feilhauer, H.; Welp, G. Soil heterogeneity at the field scale: A challenge for precision crop protection. *Precis. Agric.* **2008**, *9*, 367–390. [CrossRef]
48. Roßkopf, N.; Fell, H.; Zeitz, J. Organic soils in Germany, their distribution and carbon stocks. *Catena* **2015**, *133*, 157–170. [CrossRef]
49. Heijting, S.; de Bruin, S.; Bregt, A.K. The arable farmer as the assessor of within-field soil variation. *Precis. Agric.* **2011**, *12*, 488–507. [CrossRef]
50. Heil, K.; Schmidhalter, U. Improved evaluation of field experiments by accounting for inherent soil variability. *Eur. J. Agron.* **2017**, *89*, 1–15. [CrossRef]
51. Gavioli, A.; de Souza, E.G.; Bazzi, C.L.; Guedes, L.P.C.; Schenatto, K. Optimization of management zone delineation by using spatial principal components. *Comput. Electron. Agric.* **2016**, *127*, 302–310. [CrossRef]
52. Song, X.; Wang, J.; Huang, W.; Liu, L.; Yan, G.; Pu, R. The delineation of agricultural management zones with high resolution remotely sensed data. *Precis. Agric.* **2009**, *10*, 471–487. [CrossRef]
53. Vallentin, C.; Dobers, E.S.; Itzerott, S.; Kleinschmit, B.; Spengler, D. Delineation of management zones with spatial data fusion and belief theory. *Precis. Agric.* **2020**, *21*, 802–830. [CrossRef]
54. Kaivosoja, J.; Näsi, R.; Hakala, T.; Viljanen, N.; Honkavaara, E. Different remote sensing data in relative biomass determination and in precision fertilization task generation for cereal crops. In Proceedings of the 8th International Conference on Information and Communication Technologies in Agriculture, Food & Environment, Chania, Greece, 21–24 September 2017; pp. 164–176.
55. Bachmaier, M. Using a robust variogram to find an adequate butterfly neighborhood size for one-step yield mapping using robust fitting paraboloid cones. *Precis. Agric.* **2007**, *8*, 75–93. [CrossRef]
56. Simbahan, G.C.; Dobermann, A.; Ping, J.L. Screening yield monitor data improves grain yield maps. *Agron. J.* **2004**, *96*, 1091–1102. [CrossRef]
57. Noack, P.O. Entwicklung fahrspurbasierter Algorithmen zur Korrektur von Ertragsdaten im Precision Farming (Development of Lane-Based Algorithms for the Correction of Yield Data in Precision Farming). Ph.D. Thesis, Technische Universität München, Munich, Germany, 2006.
58. Steinmayr, T. Fehleranalyse und Fehlerkorrektur bei der lokalen Ertragsermittlung im Mähdrescher zur Ableitung Eines Standardisierten Algorithmus für die Ertragskartierung (Error Analysis and Correction of Yield Recording in Combine Harvesters to Derive a Standardized Algorithm for Yield Mapping). Ph.D. Thesis, Technische Universität München, Munich, Germany, 2002.
59. Toscano, P.; Castrignanò, A.; Di Gennaro, S.F.; Vonella, A.V.; Ventrella, D.; Matese, A. A Precision agriculture approach for durum wheat yield assessment using remote sensing data and yield mapping. *Agronomy* **2019**, *9*, 437. [CrossRef]
60. Hülsbergen, K.J.; Maidl, F.X.; Mittermayer, M.; Weng, J.; Kern, A.; Leßke, F.; Gilg, A. *Digital Basiertes Stickstoffmanagement in Landwirtschaftlichen Betrieben–Emissionsminderung durch Optimierte Stickstoffkreisläufe und Sensorgestützte Teilflächenspezifische Düngung (Digitally Based Nitrogen Management in Agricultural Farms–Emission Reduction through Optimized Nitrogen Cycles and Sensor Based Site-Specific Fertilization)*; Forschungsbericht an Deutsche Bundesstiftung Umwelt, Technische Universität München: Freising, Germany, 2020. Available online: https://www.dbu.de/projekt_30743/01_db_2848.html (accessed on 2 July 2022).
61. Cao, Q.; Miao, Y.; Feng, G.; Gao, X.; Li, F.; Liu, B.; Yue, S.; Cheng, S.; Ustin, S.L.; Khosla, R. Active canopy sensing of winter wheat nitrogen status: An evaluation of two sensor systems. *Comput. Electron. Agric.* **2015**, *112*, 54–67. [CrossRef]
62. Westermeier, M.; Maidl, F.X. Vergleich von Spektralindizes zur Erfassung der Stickstoffaufnahme bei Winterweizen (*Triticum aestivum* L.). *J. Kulturpfl.* **2019**, *71*, 238–248.

63. John Deere, Active Yield. Available online: https://www.deere.de/assets/docs/region-2/parts-and-service/manuals-and-training/combines/s-series/Active-Yield-DE.pdf (accessed on 2 July 2022).

64. Segarra, J.; Buchaillot, M.L.; Araus, J.L.; Kefauver, S.C. Remote sensing for precision agriculture: Sentinel-2 improved features and applications. *Agronomy* **2020**, *10*, 641. [CrossRef]